**QUANTITATIVE ANALYSIS OF LENTIVIRUS INCORPORATION OF
HETEROLOGOUS VIRAL AND NON-VIRAL PROTEINS
FOR LUNG GENE THERAPY**

A Dissertation
Presented to
The Academic Faculty

By

Cindy Jung

In Partial Fulfillment
of the Requirements for the Degree
Doctor of Philosophy in Biomedical Engineering

Georgia Institute of Technology

December 2007

QUANTITATIVE ANALYSIS OF LENTIVIRUS INCORPORATION OF
HETEROLOGOUS VIRAL AND NON-VIRAL PROTEINS
FOR LUNG GENE THERAPY

Approved by:

Dr. Joseph M. Le Doux, Advisor
Department of Biomedical Engineering
Georgia Institute of Technology and
Emory University

Dr. Richard Compans
Department of Microbiology and Immunology
Emory University School of Medicine

Dr. Andrés J. Garcia
School of Mechanical Engineering
Georgia Institute of Technology

Dr. Nael McCarty
School of Biology
Georgia Institute of Technology

Dr. Cheng Zhu
School of Mechanical Engineering
Georgia Institute of Technology

Date Approved: November 7, 2007

For my parents and my sister

For Chen

ACKNOWLEDGMENTS

As my time in graduate school is drawing to an end, I am filled with mixed emotions: glad to almost be "done" (although is anyone really "done"?), and sad because I'll miss interacting with so many wonderful people on a daily basis. Besides, I still have that one experiment to do that will make my project more complete and significant! But I digress. I have many people to thank and I would like to start off by thanking my thesis advisor, Joe Le Doux. For the past many years, he has guided, supported, and challenged me with his determination and his enthusiasm for science. He was dedicated to teaching me how to critically analyze my data, coherently present it, and concisely and clearly write it up, all while pushing me to independently plan and execute the next series of experiments. I admit it was frustrating at times, however I am grateful to Joe for I feel I am a better researcher because of it.

I would like to thank my committee members, Dr. Compans for his knowledge of all things virology, Dr. McCarty for his perspective on cystic fibrosis and immunology, and Dr. Garcia and Dr. Zhu for their emphasis on application-oriented research and critical analysis. I appreciated all their advice and feedback. I would also like to acknowledge the BME department and the IBB staff.

The most rewarding part of graduate school is all the people you meet as colleagues that develop into great friends. I am grateful for the friendships of Sarah Coleman, Gelsy Torres-Oviedo, Lola Brown, and Manu Platt whose camaraderie helped me through the first years of the BME program. I would especially like to point out the past and present members of the Le Doux Lab who made the rest of the years fly by: Natalia Landázuri and Delfi Krishna for their lab wisdom and spirit, Jamie Chilton for always being there, and Nimisha Gupta, the other half of "Nindy", for being my BFF

inside and out of lab. I won't go into the details, but there were definitely some interesting times with this group of inspirational and free-spirited ladies.

I would like to thank my family who are a constant source of unconditional love and support. I am grateful for my parents for always encouraging me by telling me to "study hard", never asking how much longer it would take to finish, and always being only a phone call or 14 hour car ride away. I am appreciative of my sister for always being willing to help or talk. And I am thankful for Chen's Mom for making the last years of graduate school easier (and healthier) by cooking homemade meals.

Finally, I would like to thank my husband, Chen, for his unfailing love, encouragement, and support. Putting it down in words would not even capture an ounce of what he endures and does for me. Somehow he always has a great attitude and a smile on his face, and none of this would be possible without him.

TABLE OF CONTENTS

LIST OF TABLES

LIST OF FIGURES

FIGURE

SUMMARY

Gene therapy is the delivery of genetic material to cells to produce a therapeutic effect. Retroviruses are one of the most common viral vectors used for gene therapy, especially lung gene therapy. However the lung has many physical and immunological barriers to gene transfer vectors, and currently, too few cells are genetically modified for the effective treatment of lung diseases such as cystic fibrosis. One of the main reasons for low cell transduction is the lack of commonly-used receptors for gene therapy vectors on the apical surface of polarized epithelial cells. The objective of this project was to determine how to incorporate proteins into the lentiviral lipid bilayer in order to develop a recombinant retrovirus that can efficiently deliver genes to polarized cells via their apical membranes.

We created a lentivirus pseudotyped with envelope proteins from human parainfluenza type 3 (HPIV3), which has a natural tropism for the apical surface of polarized lung epithelial cells. Lentivirus particles were able to incorporate HPIV3 glycoproteins, hemagglutinin-neuraminidase (HN) and fusion (F), and viruses were able to transduce polarized cells via the apical surface in a manner consistent with lentiviral-mediated transduction via sialated receptors for HPIV3. However titers were too low for clinical use.

We also determined whether lentiviruses could incorporate non-viral proteins into its lipid bilayer and examined the factors necessary for protein incorporation. We investigated the ability of two glycosylphosphatidylinositol (GPI) anchored proteins, folate receptor (FR-WT) and Tac-CD16 (CD25 or the interleukin-2 receptor alpha chain which has been modified with the GPI anchor motif from CD16) to incorporate into viruses. We found that Tac-CD16 and FR-WT exhibited the classic GPI anchored protein property of associating with lipid rafts, however Tac-CD16 colocalized with Gag

and incorporated into lentiviral particles, while FR-WT did not colocalize with Gag and was not incorporated into virus particles. We found that FR-WT colocalized to less dense rafts and Tac-CD16, Gag, and amphotropic Env were localized to more dense rafts. Treatment of cells with fumonisin B1 (FB1) or methyl-beta-cyclodextrin (MβCD) increased colocalization of FR-WT with Gag in lipid rafts such that FR-WT was incorporated into virus particles. Taken together, these results demonstrated lipid rafts segregate raft proteins, and for a protein to be incorporated into virus particles, it must be colocalized with lentivirus-associated rafts.

We then investigated the cause of low HPIV3 pseudotyped lentivirus titers. We determined transfected cells contained fewer cell-surface HN and F than wild-type infected cells. We codon-optimized HN to increase HN expression and used it to transfect lentivirus producer cells. Cell surface expression of HN, as well as the amount of HN incorporated into virus particles, increased. Virus transduction of cells, including to the apical surface of polarized cells, also increased. Interestingly, even though codon optimization improved the expression levels of HN and virus titers, we found that HPIV3 pseudotyped viruses still contained about 14-fold fewer envelope proteins than lentiviruses pseudotyped with the amphotropic envelope protein. We then hypothesized HN and F incorporation was low because interactions between HN and F with lentiviral Gag were low. We found that HN and F were not as colocalized with Gag or lipid rafts as amphotropic Env and tried to increase passive and active interactions with Gag to increase incorporation levels. To increase active interactions with Gag, we created HN and HIV Env fusion proteins that would actively interact with Gag. We found that colocalization and incorporation increased with the fusion proteins, however titers decreased. To increase passive interactions with Gag, we disrupted the barriers that prevented HN and F from passively interacting with Gag. When producer cells of lentiviruses pseudotyped with HPIV3 (HPIV3 LV) or amphotropic Env (Ampho LV) were

treated with 0.5 mM MβCD for 54 hours after transfection to disturb lipid rafts, titers of HPIV3 LV increased while titers of Ampho LV decreased. When we analyzed the amount of envelope incorporation from MβCD treated producer cells, we found the amount of amphotropic Env in virus particles decreased 3.0-fold while the amount of HN increased 1.4-fold. This data suggested that increasing interactions of HPIV3 envelope proteins with Gag through active and passive interactions enhanced HN and F incorporation into lentiviral particles.

In summary, we analyzed the process of incorporating heterologous viral and non-viral proteins into lentiviruses and determined key factors that allowed for successful and functional protein incorporation into the lentiviral lipid bilayer. We found that proteins can be incorporated into virus particles if they colocalized with lentivirus-associated rafts, and that heterologous viral proteins from HPIV3 can pseudotype lentiviruses for infection of polarized cells. This research is significant because it provides insight into viral assembly and protein incorporation for the generation of pseudotyped lentiviruses for human gene transfer.

CHAPTER 1

BACKGROUND AND OBJECTIVES

1.1 Gene Therapy for Diseases of the Lung

Gene therapy is the delivery of genetic material to cells to produce a therapeutic effect. An excellent example of a pulmonary disease in which gene therapy may prove therapeutic is cystic fibrosis (CF). Affecting over 30,000 individuals in the United States annually, CF is the most common lethal autosomal recessive disease in the Caucasian population [1]. Although many organs in the body are affected, it is in the lung where disease manifestation, such as thick mucus, inflammation, and bacterial infections, is the major cause of morbidity and mortality. The most common cause of cystic fibrosis was identified as mutations in the cystic fibrosis transmembrane conductance regulator (CFTR) gene, which encodes a chloride ion channel [2]. Mutations in CFTR lead to imbalanced ion and water movement across the airway epithelium.

Gene therapy is an attractive option for CF because it is a monogenic disorder and there are currently no satisfactory treatments for it. From the cloning of the CFTR gene [3] to present day, much progress has been made towards effective gene therapy for CF. Proof-of-principle has been demonstrated for CFTR gene transfer *in vitro* and in animal models [4, 5]. Clinical trials in CF patients were first carried out in 1993 [6], however of the 29 trials since then, only one of them has gone on to Phase II [7]. The main conclusions from the clinical trials were that while relatively safe and feasible, too few cells were genetically modified and the effects of gene transfer were only temporary [2]. It was believed that CF gene therapy was an easily attainable goal because the gene was identified and the target could be reached noninvasively. However it is still unsuccessful in *effectively* treating cystic fibrosis patients because of many barriers to

1

gene therapy vectors, which results in too few cells being genetically modified permanently with the normal CFTR gene to have a significant effect on the manifestation of the disease.

Besides CF, the use of gene therapy to attempt to treat other pulmonary diseases is increasing. Examples include other monogenic disorders such as α_1-antitrypsin deficiency, and also more complicated diseases such as chronic obstructive pulmonary disease (COPD), asthma, interstitial lung diseases, and even lung cancer [8]. However similar to CF, gene therapy is only a promising treatment for these diseases because of the numerous barriers facing gene therapy vectors [8].

1.2 Barriers of Lung Gene Therapy

As accessible as it may seem for delivery of gene therapy vectors, the lung has many physical and immunological barriers that inhibit effective transduction of the target cells. Since extensive research has been performed on gene delivery for the treatment of CF, the following paragraphs will highlight the difficulties faced during gene delivery to the CF lung as an example. These barriers, namely identifying and delivering the genetic material to the target cell type, apply not only to CF gene delivery, but generally also to gene delivery in other pulmonary diseases.

The lung is lined with a pseudo-stratified epithelial monolayer composed of many cell types including basal, mucus, serous, ciliated, and intermediate cells [9]. Identifying the target cell type for CF gene therapy has proved difficult due to the heterogeneous and complicated distribution pattern of CFTR in the lungs. While most of the pathology of CF manifests in the distal small airways, it is in ciliated cells located in the superficial epithelium and the difficult-to-access submucosal glands of the proximal airways that has the highest CFTR expression levels [10, 11]. Also, putative progenitor cells should be ideally targeted instead of the epithelial cells, which are terminally differentiated with

a lifespan of 21-120 days [9, 12]. However many distinct populations of lung progenitor cells have been identified [13], and besides residing in difficult-to-access areas, it is unclear which progenitor population to target. There is however encouraging evidence that only 5-10% of the epithelial cells in the lung need to be genetically modified with the normal CFTR for correction of the chloride transport abnormalities [14, 15].

The first obstacle the gene transfer vector will encounter in any lung is the mucus layer (Figure 1.1). In the normal airway, a thin layer of mucus is a natural innate immune barrier designed to trap viruses and bacteria. The act of mucociliary clearance will then clear these foreign objects from the lung. Because of the defective ion channel, the mucus of CF patients is characterized by viscous secretions, which has been shown to severely limit the transport ability of gene transfer vectors to the cells [16]. Pretreatment of the mucus with mucolytic drugs improves transduction efficiencies, however there is still the natural defense of mucociliary clearance to overcome [17]. CF patients also produce sticky sputum, which consists of inflammatory cells, cell debris, mucus, and DNA, all of which has been shown to limit access of viral and nonviral vectors to epithelial cells [18]. Beneath the mucus layer, is the airway surface liquid (ALS), which contains electrolytes, immunoglobulins, cytokines, antimicrobial peptides and proteins, surfactant proteins, proteinase inhibitors, and other epithelial secretions [19]. In the lungs of CF patients, the inflammatory debris in the ALS is markedly increased and has been shown to inhibit gene transfer to the lung [20-23], however it does not seem to have affected retroviral-mediated gene transfer [24]. In addition, the lung has innate immune responses to foreign particles, including alveolar macrophages and neutrophils which act to phagocytose and inactivate viral particles [24, 25], and humoral responses which may affect the choice of gene transfer vector used [26]. Also, gene transfer vectors will have to locally pass through the glycocalyx and extracellular matrix, whose
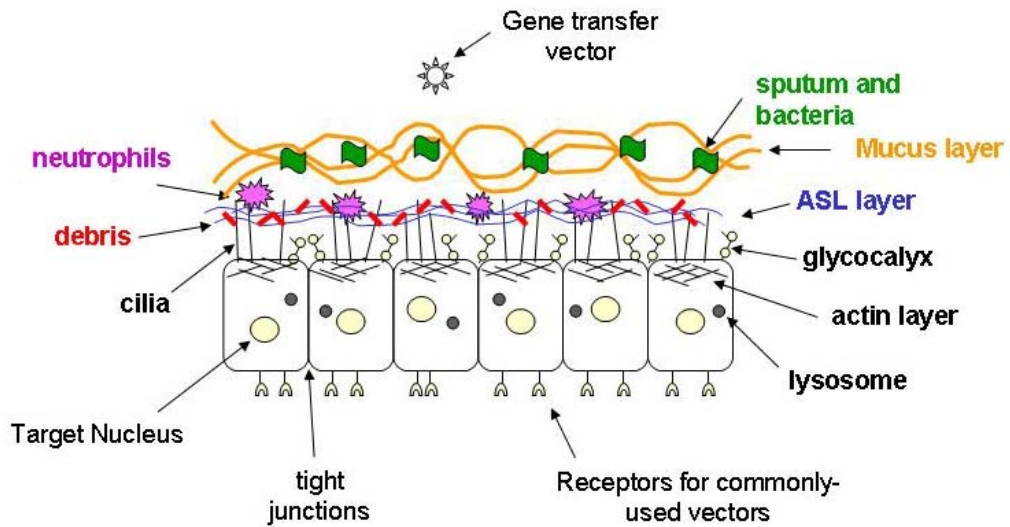
Figure 1.1. Barriers of lung gene therapy. Gene transfer vectors encounter many barriers in the lung such as the mucus layer, airway surface liquid layer, cellular debris, immune cells, bacteria, sputum, and cilia. Once past those barriers, the gene transfer vector must circumvent the glycocalyx, thick actin layer, tight junctions preventing access to common receptors for gene therapy vectors, and lysosmes to reach the target nucleus.

treatment with proteinases *in vitro* has been shown to increase the low viral-mediated gene transfer [27-29].

The epithelial cells themselves present a greater barrier for successful CF gene therapy. The lung is lined with a highly polarized layer of epithelial cells, which have an asymmetric distribution of cell surface proteins. It has been extremely difficult to transfer genes to the apical membrane of polarized epithelial cells even *in vitro* because tight junctions between cells limit the access of commonly-used gene transfer vectors to their cellular receptors, which are preferentially located on the basolateral side [30-32]. Additionally, the low rate of endocytosis from the exposed apical membrane further reduces uptake of gene transfer vectors [31, 32]. Strategies to enhance transduction from the apical surface with viral and nonviral vectors include tight-junction disruption [33-36], UV irradiation [32], and calcium phosphate co-precipitation [37], however their

4

use in CF therapy is questioned since they damage the lung epithelium. Once past the cell membrane, gene transfer vectors will also have to circumvent the complex architecture of the polarized epithelial cell to deliver the gene to the nucleus, navigating around the thick actin layer and evading endosomal breakdown [38].

CF clinical trials have been mainly marked by the low number of cells transduced. In order for effective treatment to occur in any lung gene therapy, the gene therapy vector must be able to get past the body's various physical and immune defense mechanisms. However, overcoming these numerous physical and immune barriers will still leave a major issue required for successful treatment: <u>apical binding and internalization of the vector into the cells for gene delivery.</u>

1.3 <u>Retroviral-mediated Gene Delivery</u>

Retroviruses are one of the most common viral vectors used for gene therapy especially lung gene therapy [7]. Often derived from Moloney murine leukemia virus (MLV), they comprise of two copies of genomic RNA containing the psi or packaging sequence and reverse transcriptase (encoded by the Pol gene). These proteins are surrounded by structural core proteins (encoded by the Gag gene), followed by a lipid bilayer acquired from the producer cell, and envelope glycoproteins (encoded by the Env gene) which protrude out from the lipid bilayer (Figure 1.2). Generally retroviruses attach to the cell surface through nonspecific interactions between proteins on the surface of the cell and on the virus, and not through receptor/Env-dependent binding [39, 40]. However once at the cell surface, the envelope protein of retroviruses can specifically bind to its receptor if present and induce fusion of the lipid bilayers for efficient viral entry. After fusion, the genome of the virus and virus proteins are released into the cell, reverse transcription of the RNA into DNA occurs, and the viral DNA is
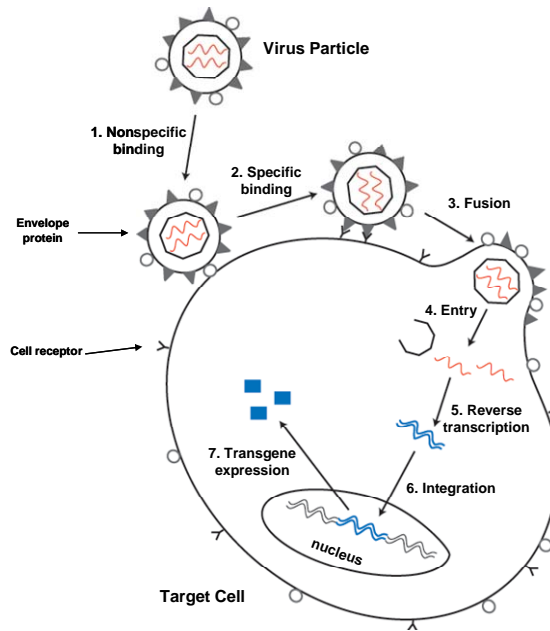
Figure 1.2. Transduction of target cells by recombinant retroviruses. Cells are transduced by incubation with stocks of retroviruses. Retroviruses diffuse to the surface of the cell and bind via nonspecific interactions. The envelope proteins then bind to cell receptors and initiate fusion between the lipid bilayer of the virus and the cell which releases the internal components of the virus into the cytosol. In the cytoplasm, the RNA genome of the virus is reverse transcribed to DNA, the DNA is transported to the nucleus and integrated into the chromosomal DNA of the cell. The therapeutic gene is then expressed.
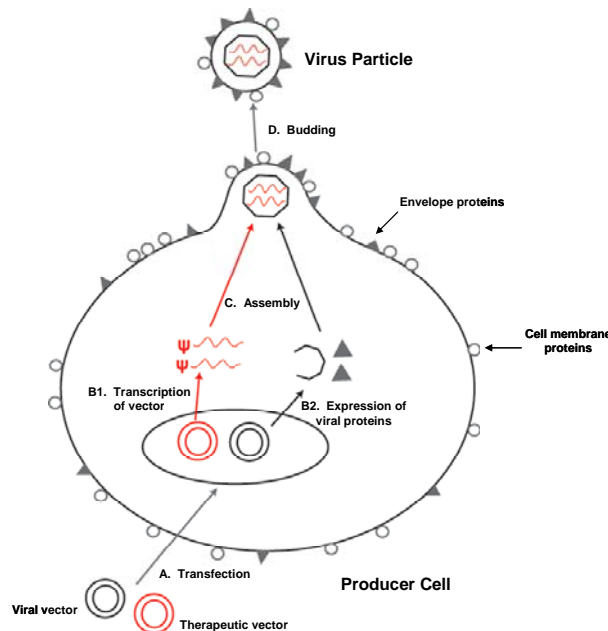
Figure 1.3. Production of recombinant retroviruses. Recombinant retroviruses are produced by transfecting the producer cell with vectors containing the therapeutic gene and the viral gene. The therapeutic gene contains the packaging sequence that allows for efficient incorporation into virus particles. The viral vector encodes for viral proteins such as capsid proteins and envelope proteins. The capsid proteins self-assemble around the RNA genome with the packaging sequence, and bud from the surface of the cell into the cell culture medium. During budding, the virus particle incorporates a lipid bilayer from the cell. This lipid bilayer contains the virus envelope proteins and other cell membrane proteins.

directed to the nucleus where it integrates into the chromosomal DNA of the host cell. During and after integration, the viral DNA is stably expressed and inherited by daughter cells. Recombinant retroviruses are identical to that of wild-type viruses but engineered such that they encode for a therapeutic gene of interest or a reporter gene, and do not contain the viral genes necessary for replication [41].

For the production of recombinant retroviruses, generally cells are transfected with plasmids encoding for the viral genes (Gag, Pol, Env) and the therapeutic vector (Figure 1.3). The producer cells express the viral proteins and transcribe the therapeutic vector, after which the viral proteins recognize the psi-sequence in the therapeutic vector and package it. The viral proteins subsequently assemble into a virus particle which buds from the cell membrane. The media, which contain putative virus particles, is then collected and used to deliver genes to the target cells.

The ability of retroviral vectors to efficiently integrate the gene has led to much interest in their use for lung gene therapy [42]. Besides eliminating the need for re-administration, retroviral vectors also have an adequate packaging capacity for RNA, and envelope proteins which may be less immunogenic than that of other viral gene delivery systems such as adenoviral or AAV vectors [43]. Some limitations however include producing enough particles for clinical trials, the need for target cells to be actively dividing, unlike cells of the lung [42], and also limited receptor number on the apical side of polarized airway epithelial cells [44]. Lentiviral vectors, such as those based on human immunodeficiency virus (HIV), are a subclass of retroviruses that can overcome the need for dividing target cells as they can infect and integrate their genome into non-dividing cells. They also have been shown to transcytose through a polarized monolayer of cells [45], which may be useful for infecting progenitor cells. In addition, lentiviral vectors can also incorporate the envelope proteins of other viruses into their viral lipid bilayer, thereby changing its targeting, in a process known as pseudotyping.

1.4 <u>Viral and Non-Viral Protein Incorporation into Lentiviruses</u>

Pseudotyping.   Pseudotyping lentiviruses is an attractive feature since the envelope proteins are strongly associated with the virus, and viruses can be targeted to abundant receptors on the apical surface of airway cells without modifications of the envelope protein that can reduce virus-cell fusion [46]. Lentiviruses pseudotyped with the envelope protein from Ebola virus were able to infect 30% of mice trachea, including submucosal glands, with long-term and high gene expression [47]. However, safety is a concern and work is being performed to redesign the envelope protein for improved safety characteristics [48]. A more recent study has been performed with a lentivirus pseudotyped with influenza D glycoprotein which resulted in persistent *in vivo* gene expression of polarized airway epithelial mouse cells for over one year, perhaps indicating infection of progenitor cells [49].

The envelope proteins from human parainfluenza virus type 3 (HPIV3) may be a good choice for the pseudotyping of lentiviruses. HPIV3 has been shown to have a natural tropism for airway epithelial cells, efficiently infecting cells via sialic acid-containing receptors that are abundantly expressed on the apical membrane of lung cells [50, 51]. HPIV3 is an enveloped, negative-strand RNA virus which replicates in the cytoplasm of cells. The binding and fusing abilities of HPIV3 have been separated into two envelope proteins, hemagluttinin-neuraminidase (HN) which binds to sialic acid, and fusion (F). The simian immunodeficiency virus has been shown to be pseudotyped with the F and HN envelope proteins from another member of the paramyxovirus family, Sendai virus [52]. This vector was able to transduce cells *in vitro*, however it has not yet been tested *in vivo*.

Non-Viral Proteins. Studies with HIV have shown that viruses can carry many host cell proteins internally and externally on its lipid bilayer. While much is still unknown on how these proteins are incorporated and why, there is growing evidence

8

that viruses may use host cell proteins for enhanced infection [53]. For example, virus-associated cellular adhesion molecule ICAM-1 has been shown to increase HIV infectivity in target T-cells by 5 to 10-fold [54]. Natural insertion of the costimulatory molecules CD80 and CD86 onto the viral lipid bilayer not only increases virus infectivity by facilitating attachment, they can stimulate the NF-κB transcription factor [55]. Besides natural insertion, retroviruses can be engineered to incorporate nonviral proteins for enhanced targeting by overexpression of the protein, however the effects have not been quantified [56]. It has also been shown that it is important to choose targeted receptors on the cell that can efficiently support a productive cell infection pathway [57].

One class of host proteins that lentiviruses can incorporate into their lipid bilayer are glycosylphosphatidylinositol (GPI)-anchored proteins [58, 59]. These proteins are post-translationally modified at the C-terminal with the lipid-anchoring GPI moiety [60]. GPI-anchored proteins are localized to lipid rafts on the cell surface [61], and attachment of a GPI-anchor to a protein can retarget the protein to lipid rafts on the outer plasma membrane [62]. Lipid rafts are regions on the cell surface enriched in cholesterol and sphingomyelin, which allow for tighter packing and resistance to solubilization in detergents at low temperatures [63]. Lentiviruses have been shown to use lipid rafts as a scaffold from which to assemble and bud [64, 65]. Besides host GPI-anchored proteins, lentiviruses have also been shown to incorporate GPI-anchored viral proteins in their viral lipid bilayer [66, 67]. It may be advantageous to incorporate a targeted yet non-fusogenic protein into the viral lipid bilayer with GPI-anchoring for enhanced binding or signaling to target cells.

1.5 <u>Thesis Objectives</u>

The objective of this project is to determine how to incorporate proteins into the lentiviral lipid bilayer in order to develop a recombinant retrovirus that can efficiently

deliver genes to polarized epithelial cells via their apical membranes. To accomplish these objectives, we pursued the following aims:

1. Create and characterize lentiviruses pseudotyped with the human parainfluenza type 3 (HPIV3) envelope proteins, hemagglutinin-neuraminidase (HN) and fusion (F), for infection of polarized cells via the apical surface.

2. Identify the factors necessary for incorporation of proteins into the lentiviral lipid bilayer.

3. Engineer the human parainfluenza envelope proteins, HN and F, such that they are functionally incorporated into lentiviral particles for improved transduction efficiency to polarized cells via the apical surface.

1.6 <u>Organization of the Thesis</u>

In chapter one, we will briefly introduce gene therapy for diseases of the lung and retroviral-mediated gene transfer. A major emphasis will be placed on barriers of lung gene transfer and incorporation of viral and non-viral proteins into lentivirus particles.

In chapter two, we create lentiviruses pseudotyped with the human parainfluenza type 3 envelope proteins, HN and F for infection of polarized cells. We characterize the level of envelope incorporation, determine if the viruses can transduce cells, and also determine whether transduction is consistent with HN and F pseudotyped lentivirus infection.

In chapter three, we investigate the cause of low HPIV3 pseudotyped lentivirus titers. We compare expression levels in transfected cells to wild-type HPIV3 infected cells, and determine whether an increase in HN expression will increase incorporation levels and titer.

In chapter four, we determine whether two GPI anchored proteins are incorporated into lentiviral particles. We also determine whether incorporation is due to

colocalization with lentiviral Gag in lipid rafts and the effect of lipid raft disturbance on virus incorporation.

In chapter five, we investigate whether increasing active or passive interactions of HN with lentiviral Gag increases the amount of envelope incorporation. We also determine whether this leads to an increase in titer.

In chapter six, we summarize our major conclusions and present some suggestions for future work.

1.7 <u>References</u>

1.   Davies, J.C., et al. *Cystic Fibrosis.* ENCYCLOPEDIA OF LIFE SCIENCES 2006 [cited   2006   3-28];   Available   from: http://www.els.net/doi:10.1038/npg.els.0002005.

2.   Griesenbach, U., D.M. Geddes, and E.W. Alton, *Gene therapy for cystic fibrosis: an example for lung gene therapy.* Gene Ther, 2004. **11 Suppl 1**: p. S43-50.

3.   Riordan, J.R., et al., *Identification of the cystic fibrosis gene: cloning and characterization of complementary DNA.* Science, 1989. **245**(4922): p. 1066-73.

4.   Alton, E.W., et al., *Non-invasive liposome-mediated gene delivery can correct the ion transport defect in cystic fibrosis mutant mice.* Nat Genet, 1993. **5**(2): p. 135-42.

5.   Drumm, M.L., et al., *Correction of the cystic fibrosis defect in vitro by retrovirus-mediated gene transfer.* Cell, 1990. **62**(6): p. 1227-33.

6.   Zabner, J., et al., *Adenovirus-mediated gene transfer transiently corrects the chloride transport defect in nasal epithelia of patients with cystic fibrosis.* Cell, 1993. **75**(2): p. 207-16.

7.   *Gene Therapy Clinical Trials Worldwide.* 2006, Wiley.

8.   Kolb, M., et al., *Gene therapy for pulmonary diseases.* Chest, 2006. **130**(3): p. 879-84.

9.   O'Dea, S. and D.J. Harrison, *CFTR gene transfer to lung epithelium--on the trail of a target cell.* Curr Gene Ther, 2002. **2**(2): p. 173-81.

10.   Kalin, N., et al., *DeltaF508 CFTR protein expression in tissues from patients with cystic fibrosis.* J Clin Invest, 1999. **103**(10): p. 1379-89.

11. Engelhardt, J.F., et al., *Submucosal glands are the predominant site of CFTR expression in the human bronchus.* Nat Genet, 1992. **2**(3): p. 240-8.

12. Warburton, D., et al., *Commitment and differentiation of lung cell lineages.* Biochem Cell Biol, 1998. **76**(6): p. 971-95.

13. Bishop, A.E., *Pulmonary epithelial stem cells.* Cell Prolif, 2004. **37**(1): p. 89-96.

14. Dorin, J.R., et al., *A demonstration using mouse models that successful gene therapy for cystic fibrosis requires only partial gene correction.* Gene Ther, 1996. **3**(9): p. 797-801.

15. Johnson, L.G., et al., *Efficiency of gene transfer for restoration of normal airway epithelial function in cystic fibrosis.* Nat Genet, 1992. **2**(1): p. 21-5.

16. Driskell, R.A. and J.F. Engelhardt, *Current status of gene therapy for inherited lung diseases.* Annu Rev Physiol, 2003. **65**: p. 585-612.

17. Ferrari, S., D.M. Geddes, and E.W. Alton, *Barriers to and new approaches for gene therapy and gene delivery in cystic fibrosis.* Adv Drug Deliv Rev, 2002. **54**(11): p. 1373-93.

18. Kitson, C., et al., *The extra- and intracellular barriers to lipid and adenovirus-mediated pulmonary gene transfer in native sheep airway epithelium.* Gene Ther, 1999. **6**(4): p. 534-46.

19. Reynolds, H.Y., *Integrated host defense against infections*, in *The lung: scientific foundations*, R.G. Crystal, et al., Editors. 1997, Lippincott-Raven Publishers: Philadelphia. p. 2353-2365.

20. van Heeckeren, A., T. Ferkol, and M. Tosi, *Effects of bronchopulmonary inflammation induced by pseudomonas aeruginosa on adenovirus-mediated gene transfer to airway epithelial cells in mice.* Gene Ther, 1998. **5**(3): p. 345-51.

21. Zhang, H.G., et al., *Inhibition of tumor necrosis factor alpha decreases inflammation and prolongs adenovirus gene expression in lung and liver.* Hum Gene Ther, 1998. **9**(13): p. 1875-84.

22. Duncan, J.E., J.A. Whitsett, and A.D. Horowitz, *Pulmonary surfactant inhibits cationic liposome-mediated gene delivery to respiratory epithelial cells in vitro.* Hum Gene Ther, 1997. **8**(4): p. 431-8.

23. Zsengeller, Z.K., et al., *Keratinocyte growth factor stimulates transduction of the respiratory epithelium by retroviral vectors.* Hum Gene Ther, 1999. **10**(3): p. 341-53.

24. McCray, P.B., Jr., et al., *Alveolar macrophages inhibit retrovirus-mediated gene transfer to airway epithelia.* Hum Gene Ther, 1997. **8**(9): p. 1087-93.

25.	Worgall, S., et al., *Role of alveolar macrophages in rapid elimination of adenovirus vectors administered to the epithelial surface of the respiratory tract.* Hum Gene Ther, 1997. **8**(14): p. 1675-84.

26.	Kennedy, M.J., *Current status of gene therapy for cystic fibrosis pulmonary disease.* Am J Respir Med, 2002. **1**(5): p. 349-60.

27.	Bals, R., et al., *Transduction of well-differentiated airway epithelium by recombinant adeno-associated virus is limited by vector entry.* J Virol, 1999. **73**(7): p. 6085-8.

28.	Batra, R.K., et al., *Retroviral gene transfer is inhibited by chondroitin sulfate proteoglycans/glycosaminoglycans in malignant pleural effusions.* J Biol Chem, 1997. **272**(18): p. 11736-43.

29.	Pickles, R.J., et al., *Retargeting the coxsackievirus and adenovirus receptor to the apical surface of polarized epithelial cells reveals the glycocalyx as a barrier to adenovirus-mediated gene transfer.* J Virol, 2000. **74**(13): p. 6050-7.

30.	Walters, R.W., et al., *Basolateral localization of fiber receptors limits adenovirus infection from the apical surface of airway epithelia.* J Biol Chem, 1999. **274**(15): p. 10219-26.

31.	Pickles, R.J., et al., *Limited entry of adenovirus vectors into well-differentiated airway epithelium is responsible for inefficient gene transfer.* J Virol, 1998. **72**(7): p. 6014-23.

32.	Duan, D., et al., *Polarity influences the efficiency of recombinant adenoassociated virus infection in differentiated airway epithelia.* Hum Gene Ther, 1998. **9**(18): p. 2761-76.

33.	Chu, Q., et al., *EGTA enhancement of adenovirus-mediated gene transfer to mouse tracheal epithelium in vivo.* Hum Gene Ther, 2001. **12**(5): p. 455-67.

34.	Duan, D., et al., *Endosomal processing limits gene transfer to polarized airway epithelia by adeno-associated virus.* J Clin Invest, 2000. **105**(11): p. 1573-87.

35.	Wang, G., et al., *Increasing epithelial junction permeability enhances gene transfer to airway epithelia In vivo.* Am J Respir Cell Mol Biol, 2000. **22**(2): p. 129-38.

36.	Chu, Q., et al., *Binding and uptake of cationic lipid:pDNA complexes by polarized airway epithelial cells.* Hum Gene Ther, 1999. **10**(1): p. 25-36.

37.	Walters, R.W., et al., *Incorporation of adeno-associated virus in a calcium phosphate coprecipitate improves gene transfer to airway epithelia in vitro and in vivo.* J Virol, 2000. **74**(1): p. 535-40.

38.	Zabner, J., et al., *Cellular and molecular barriers to gene transfer by a cationic lipid.* J Biol Chem, 1995. **270**(32): p. 18997-9007.

39.   Lei, P., B. Bajaj, and S.T. Andreadis, *Retrovirus-associated heparan sulfate mediates immobilization and gene transfer on recombinant fibronectin.* J Virol, 2002. **76**(17): p. 8722-8.

40.   Guibinga, G.H., et al., *Cell surface heparan sulfate is a receptor for attachment of envelope protein-free retrovirus-like particles and VSV-G pseudotyped MLV-derived retrovirus vectors to target cells.* Mol Ther, 2002. **5**(5 Pt 1): p. 538-46.

41.   Cone, R.D. and R.C. Mulligan, *High-efficiency gene transfer into mammalian cells: generation of helper-free recombinant retrovirus with broad mammalian host range.* Proc Natl Acad Sci U S A, 1984. **81**(20): p. 6349-53.

42.   Olsen, J.C., et al., *Correction of the apical membrane chloride permeability defect in polarized cystic fibrosis airway epithelia following retroviral-mediated gene transfer.* Hum Gene Ther, 1992. **3**(3): p. 253-66.

43.   McCormack, J.E., et al., *Anti-vector immunoglobulin induced by retroviral vectors.* Hum Gene Ther, 1997. **8**(10): p. 1263-73.

44.   Wang, G., et al., *Influence of cell polarity on retrovirus-mediated gene transfer to differentiated human airway epithelia.* J Virol, 1998. **72**(12): p. 9818-26.

45.   Hocini, H., et al., *Active and selective transcytosis of cell-free human immunodeficiency virus through a tight polarized monolayer of human endometrial cells.* J Virol, 2001. **75**(11): p. 5370-4.

46.   Zhao, Y., et al., *Identification of the block in targeted retroviral-mediated gene transfer.* Proc Natl Acad Sci U S A, 1999. **96**(7): p. 4005-10.

47.   Kobinger, G.P., et al., *Filovirus-pseudotyped lentiviral vector can efficiently and stably transduce airway epithelia in vivo.* Nat Biotechnol, 2001. **19**(3): p. 225-30.

48.   Medina, M.F., et al., *Lentiviral vectors pseudotyped with minimal filovirus envelopes increased gene transfer in murine lung.* Mol Ther, 2003. **8**(5): p. 777-89.

49.   Sinn, P.L., et al., *Persistent gene expression in mouse nasal epithelia following feline immunodeficiency virus-based vector gene transfer.* J Virol, 2005. **79**(20): p. 12818-27.

50.   Ferrari, S., et al., *A defective nontransmissible recombinant Sendai virus mediates efficient gene transfer to airway epithelium in vivo.* Gene Ther, 2004. **11**(22): p. 1659-64.

51.   Zhang, L., et al., *Infection of ciliated cells by human parainfluenza virus type 3 in an in vitro model of human airway epithelium.* J Virol, 2005. **79**(2): p. 1113-24.

52.   Kobayashi, M., et al., *Pseudotyped lentivirus vectors derived from simian immunodeficiency virus SIVagm with envelope glycoproteins from paramyxovirus.* J Virol, 2003. **77**(4): p. 2607-14.

53.   Cantin, R., S. Methot, and M.J. Tremblay, *Plunder and stowaways: incorporation of cellular proteins by enveloped viruses.* J Virol, 2005. **79**(11): p. 6577-87.

54.   Fortin, J.F., et al., *Host-derived ICAM-1 glycoproteins incorporated on human immunodeficiency virus type 1 are biologically active and enhance viral infectivity.* J Virol, 1997. **71**(5): p. 3588-96.

55.   Giguere, J.F., et al., *Insertion of host-derived costimulatory molecules CD80 (B7.1) and CD86 (B7.2) into human immunodeficiency virus type 1 affects the virus life cycle.* J Virol, 2004. **78**(12): p. 6222-32.

56.   Chandrashekran, A., et al., *Growth factor displayed on the surface of retroviral particles without manipulation of envelope proteins is biologically active and can enhance transduction.* Journal of Gene Medicine, 2004. **6**: p. 1189-1196.

57.   Krishna, D., J. Raykin, and J.M. Le Doux, *Targeted receptor trafficking affects the efficiency of retrovirus transduction.* Biotechnol Prog, 2005. **21**(1): p. 263-73.

58.   Frank, I., et al., *Acquisition of host cell-surface-derived molecules by HIV-1.* Aids, 1996. **10**(14): p. 1611-20.

59.   Pickl, W.F., F.X. Pimentel-Muinos, and B. Seed, *Lipid rafts and pseudotyping.* J Virol, 2001. **75**(15): p. 7175-83.

60.   Ikezawa, H., *Glycosylphosphatidylinositol (GPI)-anchored proteins.* Biol Pharm Bull, 2002. **25**(4): p. 409-17.

61.   Brown, D.A. and J.K. Rose, *Sorting of GPI-anchored proteins to glycolipid-enriched membrane subdomains during transport to the apical cell surface.* Cell, 1992. **68**(3): p. 533-44.

62.   Brown, O., et al., *Subcellular post-transcriptional targeting: delivery of an intracellular protein to the extracellular leaflet of the plasma membrane using a glycosyl-phosphatidylinositol (GPI) membrane anchor in neurons and polarised epithelial cells.* Gene Ther, 2000. **7**(22): p. 1947-53.

63.   Simons, K. and W.L. Vaz, *Model systems, lipid rafts, and cell membranes.* Annu Rev Biophys Biomol Struct, 2004. **33**: p. 269-95.

64.   Chazal, N. and D. Gerlier, *Virus entry, assembly, budding, and membrane rafts.* Microbiol Mol Biol Rev, 2003. **67**(2): p. 226-37, table of contents.

65.   Nguyen, D.H. and J.E. Hildreth, *Evidence for budding of human immunodeficiency virus type 1 selectively from glycolipid-enriched membrane lipid rafts.* J Virol, 2000. **74**(7): p. 3264-72.

66.   Ragheb, J.A. and W.F. Anderson, *Uncoupled expression of Moloney murine leukemia virus envelope polypeptides SU and TM: a functional analysis of the role of TM domains in viral entry.* J Virol, 1994. **68**(5): p. 3207-19.

67.   Salzwedel, K., et al., *Expression and characterization of glycophospholipid-anchored human immunodeficiency virus type 1 envelope glycoproteins.* J Virol, 1993. **67**(9): p. 5279-88.

CHAPTER 2

**LENTIVIRAL VECTORS PSEUDOTYPED WITH ENVELOPE GLYCOPROTEINS
DERIVED FROM HUMAN PARAINFLUENZA VIRUS TYPE 3[1]**

2.1 <u>Abstract</u>

We describe the generation of lentiviruses pseudotyped with human parainfluenza type 3 envelope (HPIV3) glycoproteins. Lentivirus particles, expressed in 293T/17 cells, incorporate HPIV3 hemagglutinin-neuraminidase (HN) and fusion (F) proteins into their lipid bilayers and are able to transduce human kidney epithelial cells and polarized MDCK, HBE, and A549 cells. Neuraminidase, AZT, and anti-HPIV3 antisera block transduction, which is consistent with lentiviral-mediated transduction via sialated receptors for HPIV3. Our findings show that HPIV3 pseudotyped lentiviruses can be formed and may have a number of useful properties for human gene transfer.

2.2 <u>Introduction</u>

Lentiviruses have been increasingly considered as a potential gene transfer vector for human gene therapy, primarily because they are able to stably modify cells that are not dividing [1]. Stable modification is important for the treatment of chronic and inherited disease [2]. The ability to modify cells that are not dividing is also advantageous for *in vivo* gene transfer since most cells in the body are quiescent or replicate slowly [3]. The type of cell that a lentivirus is able to genetically modify is largely dictated by the interaction between the envelope protein of the virus and its cellular receptor [4]. Lentiviruses that harbor the envelope protein of the wild-type virus are only able to transfer genes to cells that express CD4 and are therefore of limited use

---

[1] Modified from Biotechnol Prog 2004 Nov-Dec;20(6):1810-6.

17

for human gene therapy. To overcome this limitation, lentiviruses have been pseudotyped with a number of different viral envelope proteins to enable them to transduce a wider range of cell types [5-8]. The most commonly used lentiviruses are pseudotyped with the rhabdoviral G protein of the vesicular stomatitis virus (VSV-G) [9-11]. VSV-G pseudotyped lentiviruses can be produced with high titers, concentrated several hundred-fold by ultracentrifugation with minimal loss of virus activity, and are able to transfer genes to a wide range of cells types.

Unfortunately, VSV-G pseudotyped viruses are not able to transfer genes to all cell types of interest for human gene therapy. For example, they are unable to efficiently transduce airway epithelial cells via their apical surface, the target of interest for many gene therapies of the lung, including cystic fibrosis [12]. Moreover, the cytotoxicity of VSV-G complicates the development of stable VSV-G pseudotyped virus producer cell lines and may limit the total dose of virus that can be applied to cells to transduce them [11]. VSV-G pseudotyped viruses are also not suitable for therapies that need gene delivery to be restricted to one cell type (i.e., for targeted gene delivery).

One strategy to overcome some of these shortcomings is to determine if other envelope proteins are able to form pseudotypes with lentiviruses. Human parainfluenza type 3 (HPIV3), a paramyxovirus, is of interest because it is able to infect polarized lung epithelial cells via their apical surface, a property that would be valuable for gene transfer to the lung [13]. In addition, HPIV3 segregates the two main functions of viral envelope proteins, binding and fusion, into two glycoproteins, the hemagglutinin-neuraminidase (HN) and fusion (F) proteins, a characteristic that could be useful for the development of targeted viruses. The HN protein provides HPIV3 with the ability to bind to a cell surface sialated receptor for the virus. The F glycoprotein, in conjunction with HN, induces the lipid bilayer of the virus to fuse with the plasma membrane of the host

18

cell. In this study, we determined if human parainfluenza type 3 (HPIV3) proteins could be used to pseudotype lentiviruses.

2.3 Materials and Methods

Chemicals and antibodies. Poly-L-Lysine and 3′-Azido-3′-deoxythymidine (AZT) were purchased from Sigma (St. Louis, MO). Complete mini protease inhibitor cocktail tablets and neuraminidase (*Clostridium perfringens*) were purchased from Roche Diagnostics (Indianapolis, IN). Dulbecco's phosphate-buffered saline (DPBS) with and without calcium and magnesium were purchased from Mediatech (Herndon, VA). 5-Bromo-4-chloro-3-indolyl-β-D-galactopyranoside (X-Gal) was purchased from Denville Scientific (Metuchen, NJ). Mouse ascites monoclonal antibody c110 against HPIV3-F was generously provided by B.R. Murphy, Respiratory Viruses Section, NIAID, NIH (Bethesda, MD). Guinea pig anti-serum against HPIV3 (strain 47885) was obtained through the NIAID Reference Reagent Repository (Bethesda, MD). Monoclonal rabbit antibodies specific for HPIV3-HN were described previously [14]. Cy3-conjugated donkey anti-mouse IgG (H+L), Cy2-conjugated donkey anti-guinea pig IgG (H+L), and normal donkey serum were purchased from Jackson Immunoresearch Laboratories, Inc. (West Grove, PA).

Plasmids. For construction of a HPIV3-F and HPIV3-HN expression plasmid, the entire coding sequence of HPIV3-F (GenBank accession no. M14892) and HPIV3-HN (GenBank accession no. 403376) were PCR amplified and cloned into the *Cla I* and *Sph I* sites of pCAGGS.MCS [15]. The ligation sites of the plasmid were verified by DNA sequencing.

Cell culture. 293T/17 cells (human embryonic kidney epithelial), MDCK cells (Madin-Darby canine kidney epithelial; ATCC CCL-34), and HeLa cells (human cervical

19

kidney) were maintained in Dulbecco's modified essential medium (DMEM) supplemented with 10% heat-inactivated fetal bovine serum, 100 U/mL of penicillin, and 100 μg/mL streptomycin (HyClone Laboratories; Logan, UT).

Immunofluorescence microscopy.   293T/17 cells, seeded the previous day in 12-well plates coated with poly-L-lysine (2 x 10^6 cells per well), were infected with wild type HPIV3 at a multiplicity of infection (MOI) of 10 or transfected with 2 ug each of both HPIV3-F and HN glycoproteins using Lipofectamine 2000 (Invitrogen; Carlsbad, CA) according to the manufacturer's instructions. The cells were incubated for 24 hours at 37°C before plating 5 x 10^5 cells on coverslips (#1.5 12 mm, Fisher Scientific; Suwanee, GA). Twenty-four hours later, cells were fixed for 10 minutes in 2% paraformaldehyde in phosphate buffered saline (PBS) at 25°C, washed in PBS and 5% donkey sera (PBS/serum), and incubated in primary antibody in PBS/serum for one hour at 25°C. After washing three times (PBS), cells were incubated with labeled secondary antibody in PBS/serum for one hour at 25°C before washing three times in PBS and once in double distilled water. Cells were mounted onto glass slides with gelvatol [16] and samples examined under a microscope (Olympus IX50; Melville, NY) through a 10x lens.

Virus Production.   Human parainfluenza virus type 3 (strain Wash/57/47885) was obtained from the National Institute of Allergy and Infectious Disease (Bethesda, MD) and propagated on monolayers of HeLa cells. Lentiviruses pseudotyped with the amphotropic or human parainfluenza virus type 3 envelope proteins were produced by using Lipofectamine 2000 to co-transfect 293T cells with 8 μg of the packaging construct pCMVΔR8.91 (kind gift of Scott S. Case), 8 μg of lentivirus vector pTY-EFnlacZ or pTY-eGFP (AIDS Research and Reference Reagent Program, Bethesda, MD), and 8 μg of the amphotropic envelope protein expression plasmid pFB4070ASALF (a kind gift of Stephen Russell) or 8 μg each of pCAGGS-hPIV3-F and pCAGGS-hPIV3-HN. Viral

20

supernatants were collected every 12 hours from 36-60 hours after transfection, filtered sterilized (0.45 μm), and frozen (-80^{0}C) for later use.

Transduction. Target cells were seeded in poly-L-lysine coated 12-well plates (1 x 10^5 per well) and incubated at 37°C. The next day, viral supernatant dilutions were incubated with cells for 48 hours, and then the cells fixed and stained for β-galactosidase activity with X-Gal and the number of *lacZ*+ colony forming units (CFU) per ml counted [17]. To determine the effect of neuraminidase or AZT on transduction, cells were pretreated for 90 minutes with neuraminidase (0 to 2 U/mL) or AZT (2.5 μM), incubated with virus brought to the same concentration of these reagents, then fixed and stained for β-galactosidase activity. To examine the ability of the viruses to transduce polarized cells, MDCK cells were seeded 4 days prior to transduction in 0.4 μm tissue culture treated Transwell polyester supports (1 x 10^5 cells per insert) (Costar-Corning; Corning, NY), and then incubated at 37°C until polarized as evidenced by a step jump in their transepithelial resistance (>200 Ω*cm^2) [18] as measured with a voltohmmeter (World Precision Instruments; Sarasota, FL). Viral supernatants, concentrated 10-fold by ultrafiltration with Macrosep centrifugal concentrators (300-kDa molecular mass cutoff; Pall Gelman Laboratory; Ann Arbor, MI) with 8 μg/mL of Polybrene, were applied to the apical (100 μL) or basolateral (50 μL) surfaces of the polarized cells for one hour. Two days later, the cells were fixed and stained for β-galactosidase activity. As a control, cells were depolarized by incubation with EDTA (6 mM) in Hepes (10 mM) buffer, and then transduced with concentrated viral supernatants to determine the effect of depolarization on infection.

Metabolic labeling and immunoprecipitation. Thirty-six hours after transfection, cells were incubated with methionine and cysteine-free DMEM for 15 min at 37°C. Cells were then labeled for 18 hours at 37°C with 500 μCi of [^{35}S]methionine-

cysteine protein labeling mix (Perkin Elmer Life Sciences; Wellesley, MA). Cells were lysed at 4°C for 10 minutes with RIPA buffer (50 mM Tris-HCl [pH 7.6], 150 mM NaCl, 0.5% Triton X-100, 0.5% sodium deoxycholate, 0.1% SDS, and protease inhibitors), centrifuged for 10 min at 20,800 × g to pellet the nuclei, HPIV envelope proteins isolated from the supernatants with guinea pig anti-serum against HPIV3 pre-bound to protein-A sepharose beads, and then analyzed by SDS-PAGE as described below. Virus samples were obtained by ultracentrifugation of viral supernatants (4 mL) in a SW55Ti Beckman rotor (110,000 × g, 2 h, 4°C) through a 20% sucrose cushion. For separation and purification of viral vector by continuous density gradient centrifugation, viral supernatant (2 mL) were centrifuged in a Beckman SW41Ti rotor (150,000 × g, 16 h, 4°C) through a 20%-60% continuous sucrose density gradient prepared with a SG series gradient maker (Hoefer Scientific Instruments; San Francisco, CA). Eight fractions (1.25 mL) were collected and the density of each fraction determined as mass/volume and reported in g/mL. Fractions were diluted with 10.75 mL Dulbecco's PBS without calcium and magnesium, and then the viruses centrifuged a second time in a Beckman SW41Ti Rotor (150,000 × g, 2 h and 4°C). Virus pellets were resuspended in RIPA buffer (50 μL) for 30 minutes at 25°C. Samples were separated by size by SDS-PAGE (4-15%), and then the gel dried (72°C for 45 minutes) and visualized by autoradiography (BioMax MR film; Amersham; Piscataway, NJ).

Data analysis. Data are summarized as the mean +/- the standard deviation for at least triplicate samples. Statistical analysis was performed using one-way analysis of variance for repeated measurements of the same variable. The Tukey multiple comparison test was used to conduct pairwise comparisons between means. Differences at $P < 0.05$ were considered statistically significant.

2.4 Results

We constructed expression plasmids for human parainfluenza virus type 3 hemagglutinin-neuraminidase (pCAGGS-HPIV3-HN) and fusion (pCAGGS-HPIV3-F) proteins. To investigate the expression of these envelope glycoproteins, we transfected 293T/17 cells with the plasmids, radiolabeled the cells with [^{35}S]methionine-cysteine protein labeling mix, then immunoprecipitated lysates of the cells with a mouse monoclonal antibody against HPIV3-F and rabbit monoclonal antibody against HPIV3-HN. The samples were separated by size by SDS-PAGE and visualized by autoradiography. The envelope glycoproteins HPIV3-F (about 50 kDa) and HPIV3-HN (about 70 kDa) glycoproteins were easily detected, confirming their expression in transfected 293T/17 cells (Figure 2.1). Expression of these proteins on the surfaces of the cells, expected to be a prerequisite for their incorporation into the lentiviral vectors, was confirmed by immunostaining (Figure 2.2).

To determine if lentivirus vectors are able to form transduction competent pseudotypes with HPIV3-HN and F glycoproteins, we transfected 293T/17 cells with expression vectors that encoded HPIV3-F (pCAGGS-HPIV3-F), HPIV3-HN (pCAGGS-HPIV3-HN), HIV-1 *gag*, *pol*, *rev*, and *tat* (pCMVΔR8.91), and a lentiviral vector that encoded *lacZ* (pTYEFnlacZ). Twenty-four hours later the medium was replaced and the cells cultured an additional 12 hours. Some syncitium formation was observed, indicating that the envelope proteins were biologically active and capable of inducing cell-cell fusion (data not shown). The medium, which contained putative lentivirus-HPIV3 (HPIV3/LV) pseudotyped viruses, was used to transduce 293T/17 and MDCK cells. Low but measurable titers were observed (Table 2.1). Significantly higher titers were observed when the cells were transduced with lentiviruses pseudotyped with the amphotropic envelope protein Ampho/LV (Table 2.1), which confirmed that the cell lines

23
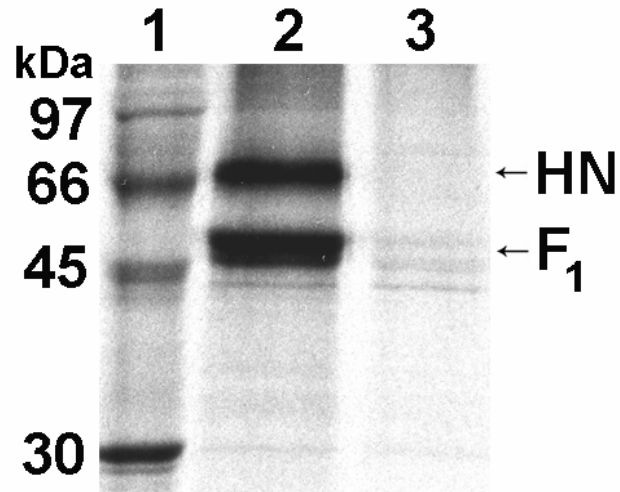
Figure 2.1. Expression of HPIV3-HN and F in 293T/17 cells. Lysates of metabolically labeled 293T/17 cells transfected with pCAGGS-HPIV3-HN and pCAGGS-HPIV3-F were immunoprecipitated with a mouse monoclonal antibody against HPIV3-F and a rabbit monoclonal antibody against HPIV3-HN. The expected bands for HPIV3-HN and HPIV3-F are indicated by the arrows. Lane 1, molecular weight markers; lane 2, lysates of 293T/17 cells transfected with pCAGGS-HPIV3-HN and pCAGGS-HPIV3-F; lane 3, lysates of mock transfected 293T/17 cells.
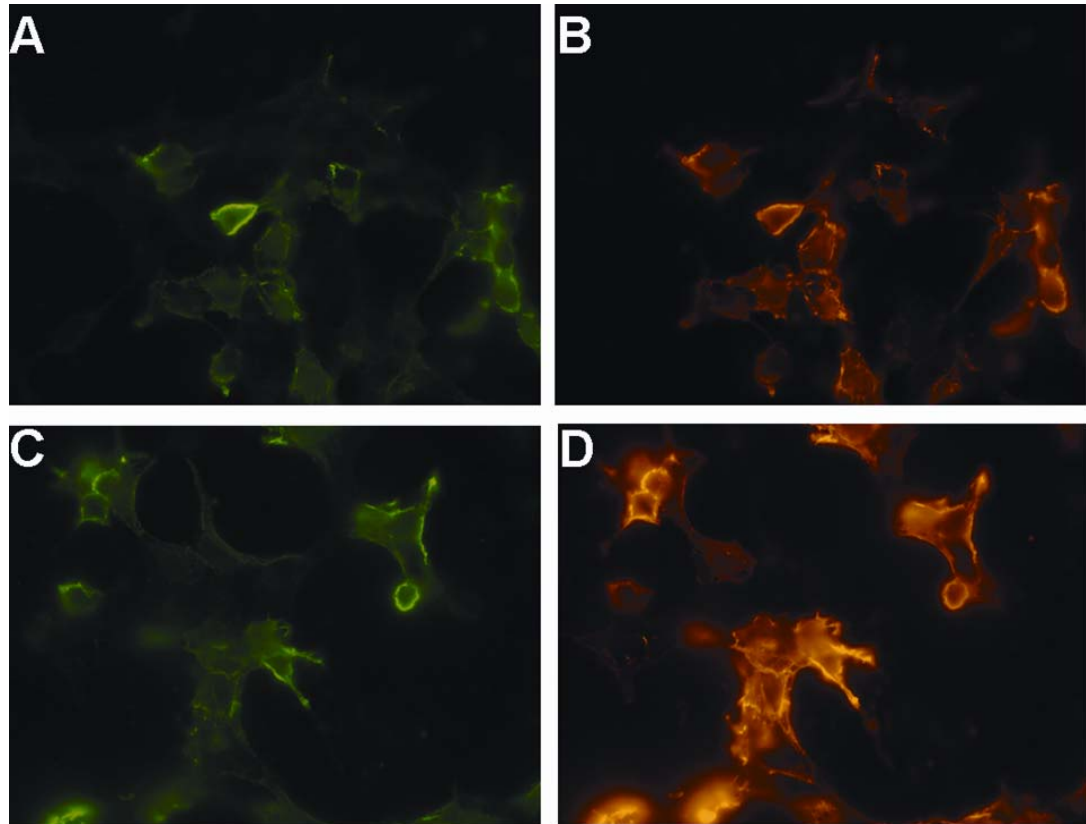
Figure 2.2. HPIV3-HN and F surface expression in 293T/17 cells. Cells were transfected with both pCAGGS-HPIV3-F and pCAGGS-HPIV3-HN, then 48h later fixed, but not permeabilized, and immunostained with HPIV3-specific guinea pig polyclonal antibody and anti-guinea pig Cy2-conjugated donkey secondary antibody (A) or mouse ascites against HPIV3-F and anti-mouse Cy3-conjugated donkey secondary antibody (B). As a positive control, wild-type HPIV3 infected cells were fixed and immunostained for HPIV3 (C) and HPIV3-F (D) using the same antibodies. Cells were viewed by epifluorescence microscopy (10X).

we tested were not refractory to lentivirus transduction and that our virus production methods were sufficient to yield high titer virus stocks.

We conducted additional experiments to determine if the titers we measured were the result of bonafide lentiviral-mediated transduction events. We found that lentiviruses pseudotyped with only one (HN or F) or none (bald) of the HPIV3 envelope proteins were unable to transduce cells, and that transduction was almost completely blocked by treatment of cells with AZT (2.5 μM) thirty minutes prior to and during infection (Table 2.1). Elimination of sialic acid from the surfaces of the cells by treating them with neuraminidase before and during infection reduced virus titers in a dose-dependent manner (Figure 2.3). Titers were reduced more than 98% when cell-surface sialic acids were cleaved by incubating the cells with *C. perfringens* neuraminidase (2 U/mL, 37°C) ninety minutes prior to, and during, transduction (Table 2.1). As expected, the titers of amphotropic pseudotyped lentiviruses, which do not need to interact with cell-surface sialic acids to infect cells, were not reduced by neuraminidase treatment of the cells. In addition, incubation of cells with antisera against HPIV inhibited transduction by HPIV3 pseudotyped lentiviruses but, as expected, had no effect on transduction by amphotrophic pseudotyped lentiviruses (Figure 2.4). These data confirmed that the titers we observed were the result of lentivirus transduction, and were not caused by pseudotransduction or other non-viral mediated events. Our data also showed that the lentiviruses were pseudotyped with HPIV3 envelope proteins (i.e., HPIV3/LV viruses) transduced cells through interactions between the HPIV3-HN and F proteins and a sialated cell-surface receptor.

Given the low titers of the HPIV3/LV virus stocks, we considered it a possibility that the virus particles were not physically associated with the HPIV3 envelope proteins,

26

TABLE 2.1. Titers of lentiviruses pseudotyped with human parainfluenza type 3 (HPIV3) envelope proteins HN and F

Target Cells	HPIV3 pseudotyped lentivirus			Amphotropic pseudotyped lentivirus			HN only, F only, or no Env pseudotyped lentivirus
	Control[a]	AZT[b] (2.5 µM)	Neuraminidase[c] (2.0 U/mL)	Control[a]	AZT[b] (2.5 µM)	Neuraminidase[c] (2.0 U/mL)	Control[a]
293T/17	$3.98\ (\pm 0.85) \times 10^2$	ND	$1.00\ (\pm 0.82) \times 10^0$	$1.62\ (\pm 0.17) \times 10^6$	$1.00\ (\pm 0.82) \times 10^4$	$1.94\ (\pm 0.24) \times 10^6$	ND
MDCK	$9.07\ (\pm 1.01) \times 10^1$	ND	ND	$6.78\ (\pm 0.86) \times 10^4$	ND	$6.98\ (\pm 0.87) \times 10^4$	ND

ND: no colony forming units detected

[a] Serial dilutions of lentivirus stocks, encoding for the *lacZ* transgene, were used to transduce cells seeded the previous day (1.0×10^5 cells/well) in poly-L-lysine coated twelve-well plates. The transduced cells were incubated for 2 days at 37°C until confluent, fixed and stained for *lacZ* activity with X-Gal, colonies of *lacZ*^{+} cells counted, and the titer (CFU/mL) calculated.
[b] Cells were incubated with 2.5 µM 3'-Azido-3'-deoxythymidine (AZT) thirty minutes prior to and during the virus titer experiment.
[c] Cells were incubated with 2.0 U/mL *C.perfringens* neuraminidase at 37°C ninety minutes prior to and during the virus titer experiment.

27
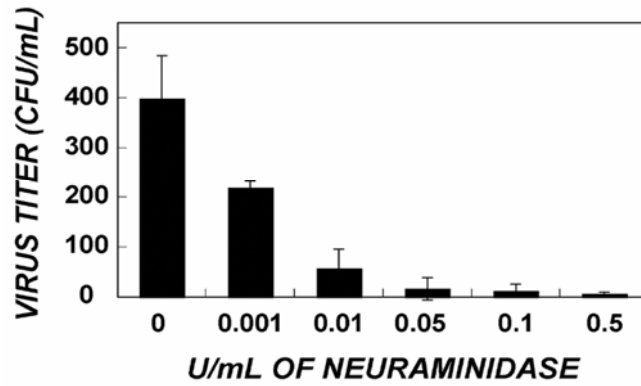
Figure 2.3. Dose-response curve of pseudotype transduction in the presence of neuraminidase. 293T cells were incubated with varying amounts of neuraminidase at 37 ^{0}C ninety minutes prior to and during the virus titer experiment. Transduced cells were incubated for 2 days at 37 ^{0}C until confluent, fixed and stained for *lacZ* activity with X-gal, colonies of lacZ$^+$ cells counted, and the titer (CFU/mL) calculated.

Figure 2.4. The effect of HPIV3 specific antisera on transduction. 293T cells were incubated at 37 ^{0}C without (-) or with (+) a 1:300 dilution of anti-HPIV3 guinea pig polyclonal antibody during transduction. Transduced cells were incubated for 2 days at 37 ^{0}C until confluent, fixed and stained for *lacZ* activity with X-gal, colonies of lacZ$^+$ cells counted, and the titer (CFU/mL) calculated as previously described. * significantly different from control ($p < 0.05$) by Tukey multiple comparison test.

and that the transduction events we had observed were the result of the complementation of envelope negative viruses with membrane vesicles (i.e., not associated with a lentivirus core) containing HPIV3 envelope proteins. As a first step towards determining if HPIV3-HN proteins were associated with the lentivirus particles, we measured the hemagglutination (HA) titer of a stock of HPIV3/LV pseudotyped viruses by incubating serial dilutions of the viruses with equal volumes of guinea pig red blood cells for 1 hour at 4°C. The HA titer of the HPIV3/LV pseudotyped virus stocks was 16 HA units/mL. As controls we measured the HA titer of a stock of wild type HPIV3 virus (512 HA units/mL), of envelope-negative lentiviruses (<4 HA units/mL), and of culture media from cells that expressed the HPIV3 envelope proteins HN and F but no lentivirus proteins (<4 HA units/mL). Agglutination was reversed and HA titers reduced to undetectable levels when the hemagglutination microtiter plates were warmed to 37°C for one hour, which confirmed that that the pseudotyped lentiviruses contained neuraminidase activity. These data support the conclusion that lentivirus vectors are able to incorporate enzymatically active HPIV3-HN proteins.

To determine if lentivirus vectors are able to incorporate both HPIV3-HN and HPIV3-F proteins, we transfected 293T/17 cells with pCAGGS-HPIV3-F, pCAGGS-HPIV3-HN, pCMVΔR8.91, and pTYEFnlacZ, then thirty-six hours later metabolically labeled the cells with [^{35}S]methionine-cysteine protein labeling mix. Cell culture supernatant was harvested and the radiolabeled virus particles partially purified by ultracentrifugation through a 20% sucrose cushion, resuspended in lysis buffer, separated by size by SDS-PAGE, then the gel dried and visualized by autoradiography. As controls, supernatant was harvested from 293T/17 cells that had not been transfected, or had been transfected to express lentivirus proteins only (i.e., envelope negative viruses), lentivirus proteins and HPIV3-F only, or lentivirus proteins and HPIV3-

HN only, or had been infected with wild-type HPIV3 virus. We found that both HPIV3-HN and HPIV3-F were present in lysates of HPIV3/LV pseudotypes (Figure 2.5A), but to a lesser extent than wild-type HPIV3. In cells that expressed only HPIV3-F (Figure 2.5A, lane 4), both the inactive precursor (F_0) and its activated proteolytic cleavage product (F_1) were visible, demonstrating that the protein is properly processed in 293T/17 cells. Interestingly, more envelope protein was detected in virus lysates when only HPIV3-HN or HPIV3-F was expressed in the virus producer cells than when both proteins were expressed.

We considered it a possibility, although unlikely, that the HPIV3 envelope proteins that we had detected in the previous experiment were present in the supernatants of virus producer cells, not as integral components of intact pseudotyped lentiviruses, but instead as part of non-viral lipid complexes that co-purified with the lentiviruses. To verify that the HPIV3-HN and F proteins were in fact physically associated with lentivirus particles and not part of non-viral lipid complexes that co-purify with lentiviruses, we purified radiolabeled virus supernatants by ultracentrifugation through a 20%-60% sucrose density gradient. Fractions were collected, pelleted by ultracentrifugation, resuspended in lysis buffer, separated by size by SDS-PAGE, then the gel dried and visualized by autoradiography. We found that HPIV3-HN and HPIV3-F proteins migrated to the same fractions as the lentivirus capsid (CA) and matrix (MA) proteins (Figure 2.5B). Taken together, our results indicate that HPIV3 envelope proteins are released into the medium when expressed in cells that are producing lentivirus particles, and that the released lentiviruses are able to incorporate HPIV3-HN and F envelope proteins within their lipid bilayers to form pseudotyped viruses that are capable of transducing cells.
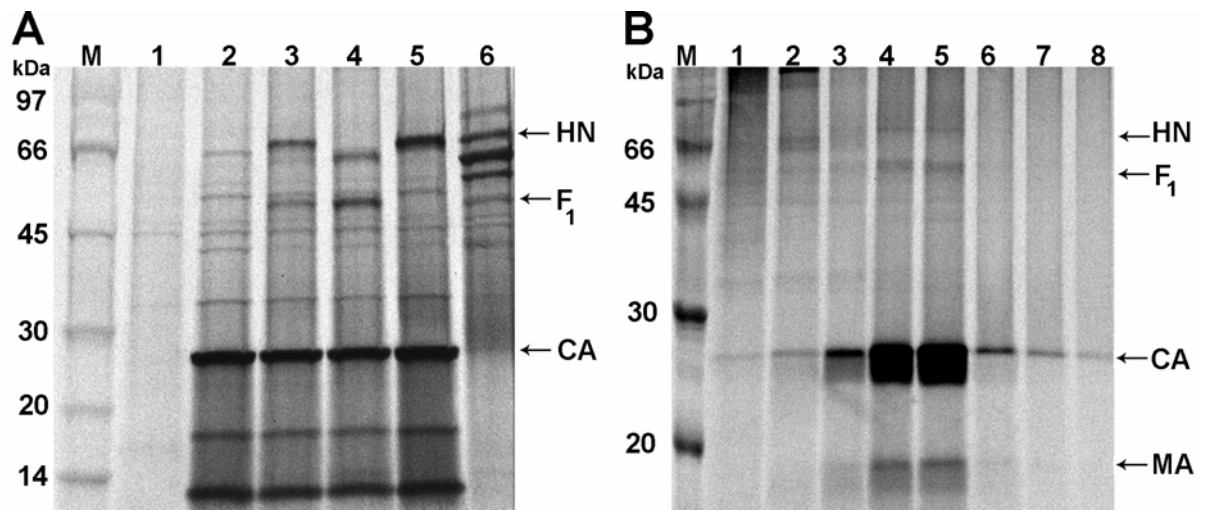
Figure 2.5. HPIV3-HN and F incorporation into lentivirus particles. (A) Supernatants from metabolically labeled 293T/17 producer cells were partially purified by ultracentrifugation through a 20% sucrose cushion, resuspended in lysis buffer, separated by size by SDS-PAGE electrophoresis, then the gel dried and visualized by autoradiography. Supernatants from 293T/17 cells producing lentiviruses pseudotyped with both HPIV3 envelope proteins (lane 3), with HPIV3-F only (lane 4) or with HPIV3-HN only (lane 5), are shown. The expected bands for HPIV3-HN, F1, and lentivirus capsid (CA) proteins are indicated by the arrows. Supernatants from mock transfected 293T/17 cells (lane 1) served as a negative control for HPIV3-HN and F protein expression. Supernatants from 293T/17 cells infected with wild type HPIV3 (lane 6) served as a positive control for HPIV3-HN and F protein expression. 293T/17 cells producing non-enveloped lentiviruses (lane 2) served as a positive control for lentivirus protein expression. Molecular weight markers are in lane M. (B) Supernatants from metabolically labeled 293T/17 cells producing lentiviruses pseudotyped with both HPIV3 envelope proteins were purified by ultracentrifugation through a continuous sucrose gradient (20% to 60%), eight fractions collected, and the density of each fraction measured. Each fraction was pelleted by ultracentrifugation, resuspended in lysis buffer, separated by size by SDS-PAGE electrophoresis, then the gel dried and visualized by autoradiography. The expected bands for HPIV3 envelope proteins (HN and F1) were detected in the same fractions (4 and 5) that contained lentiviral capsid (CA) and matrix (MA) proteins. Molecular weight markers are in lane M. The density of fractions 1 through 8 were 1.109, 1.133, 1.154, 1.172, 1.191, 1.220, 1.237 and 1.241 g/mL.

Concentration of the parainfluenza pseudotyped viruses would be advantageous for increasing titer. We tested the ability of HPIV3/LV to be concentrated either with a centrifugal concentrator or with cationic and anionic polymers [17]. We found that HPIV3/LV viruses can be concentrated 10-fold with a 7-fold increase in viral titer (Figure 2.6). We also investigated the possibility that virus titers could be increased by incubation of the producer cells with 0.05 U/mL of neuraminidase to inhibit interactions between sialidated glycoproteins and HPIV3 glycoproteins that could hinder the release of HPIV3 pseudotyped lentiviral particles [19]. After pelleting viruses with the cationic and anionic polymers and resuspending to the original amount with media, we found that the addition of neuraminidase to virus producer cells has no effect on titer (Figure 2.7A). We also attempted to increase titers by incubation of producer cells with 10 mM sodium butyrate which has been shown to activate expression of the packaging construct [20], however treatment had no effect on titers (Figure 2.7B).

To assess whether the HPIV3 pseudotyped lentivirus exhibited the tropism of parainfluenza on polarized cells, 10-fold concentrated HPIV3/LV was applied to the apical or basolateral surface of polarized MDCK cells in the presence of polybrene. Amphotrophic pseudotyped lentiviruses, which preferentially transduce polarized cells via their basolateral membranes, were also applied as a control. We confirmed that the cells were polarized and that tight junctions were intact during transduction by verifying that the transepithelial resistance was high (> 200 $\Omega*cm^2$) before and after transduction.

Lentiviruses pseudotyped with the HPIV3 glycoproteins were able to transduce polarized cells with equal efficiency from the apical and basolateral surface (Figure 2.8). As expected, lentiviruses pseudotyped with amphotrophic envelope protein preferentially infected cells when applied to the basolateral side of polarized cells. When polarization was disrupted by treatment of cells with a calcium chelator (EDTA), amphotropic lentivirus-mediated gene transfer increased several-fold to double the level seen during

32
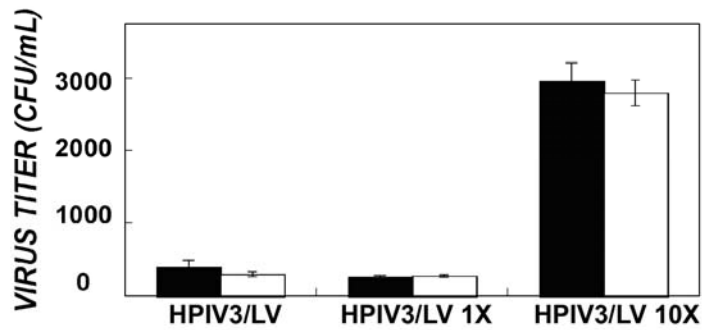
Figure 2.6. Concentration of HPIV3 lentiviral pseudotypes increases titer. HPIV3/LV virus was concentrated either with a centrifugal concentrator (open bars) or cationic and anionic polymers (closed bars) and diluted in fresh media. 293T cells were then transduced and incubated for 2 days at 37 ^{0}C until confluent, fixed and stained for *lacZ* activity with X-gal, colonies of *lacZ*$^+$ cells counted, and the titer (CFU/mL) calculated.
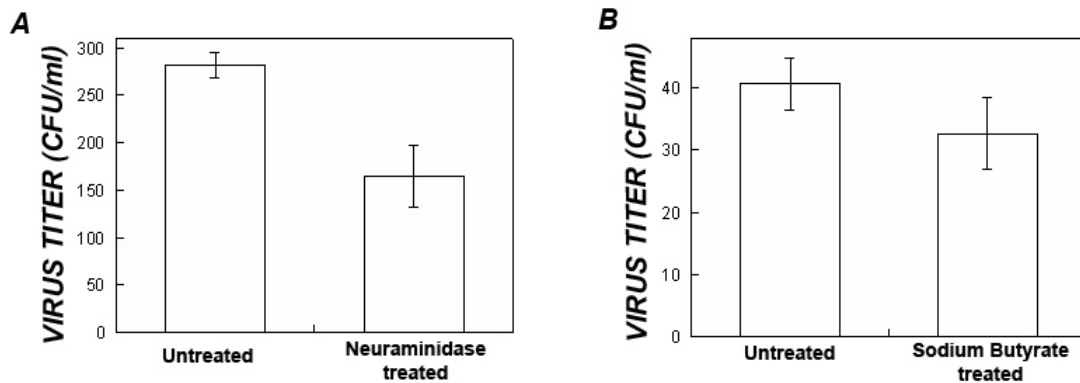
Figure 2.7. Treatment of HPIV3/LV producer cells does not enhance titers. HPIV3/LV producer cells were incubated with 0.05 U/mL neuraminidase or 10 mM sodium butyrate 24 hours after transfection for 24 hours before viruses were harvested. HPIV3/LV virus was then pelleted with cationic and anionic polymers and diluted in fresh media. 293T cells were then transduced and incubated for 2 days at 37 ^{0}C until confluent, fixed and stained for *lacZ* activity with X-gal, colonies of *lacZ*$^+$ cells counted, and the titer (CFU/mL) calculated.
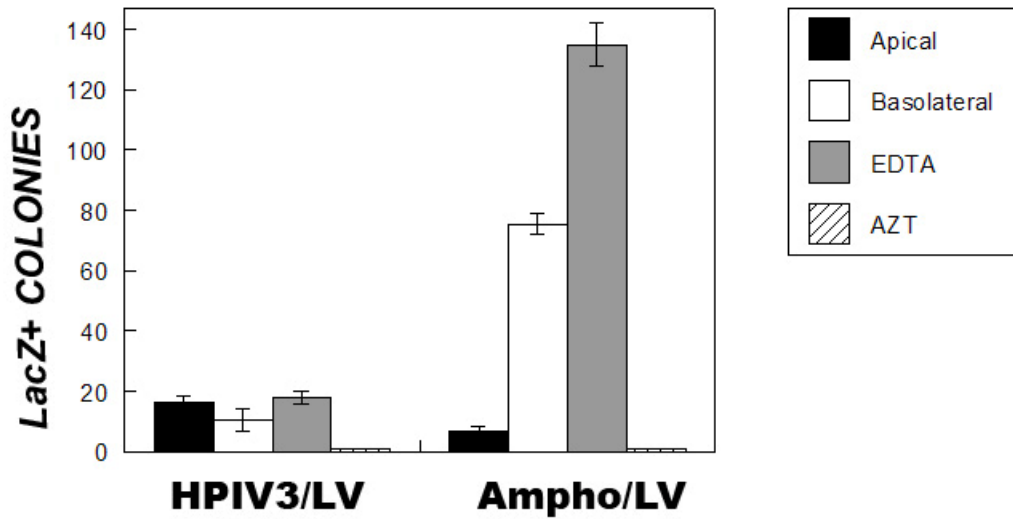
Figure 2.8. Transduction of polarized MDCK cells by HPIV3/LV and Ampho/LV. Polarized MDCK cells as measured by a transepithelial resistance > 200 Ω were transduced apically (closed bars) with 100 μL of 10X HPIV3/LV or 1X Ampho/LV, or 50 μL basolaterally (open bars) by inversion of the Transwell. Cells were transduced for 1 h in the presence of 8 μg/mL polybrene. As a control, cells were depolarized with 6 mM EDTA in HEPES (10 mM) for 30 min prior to and during apical transduction (grey bars), or incubated with 2.5 μM AZT thirty minutes prior to and during the experiment (hatched bars). Cells were incubated for 2 d at 37 ^{0}C until confluent, fixed and stained for *lacZ* activity with X-gal, and the number of *lacZ$^+$* colonies counted.

basolateral infection of polarized cells [21]. As a control, when 2.5 μM AZT was added during the transduction of polarized and unpolarized cells, the titers of both HPIV3/LV and Ampho/LV were abolished.

Though titers of HPIV3 pseudotyped lentiviruses are several orders of magnitude less than amphotropic pseudotyped lentiviruses, HPIV3 pseudotyped eGFP-containing lentiviruses were able to transduce polarized lung cells with similar efficiency as amphotropic pseudotyped lentiviruses from the apical side (Figure 2.9).
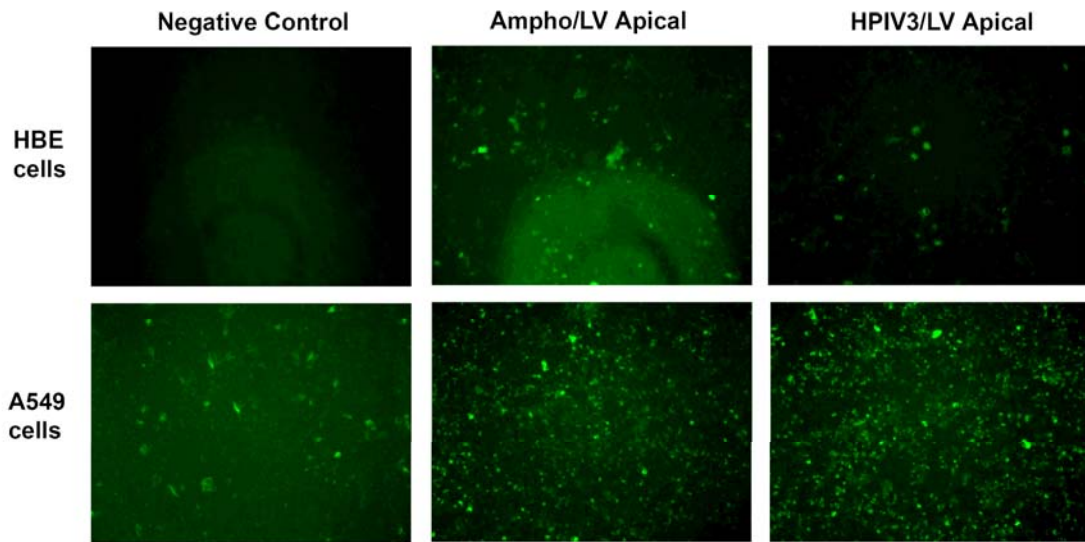
Figure 2.9. Transduction of polarized HBE or A549 cells by HPIV3/LV and Ampho/LV. Polarized HBE cells as measured by a transepithelial resistance > 600 Ω were transduced apically with 100 μL of polymer-pelleted 2X HPIV3/LV or 2X Ampho/LV carrying the eGFP gene. Cells were transduced for 2 d and viewed by epifluorescent microscopy at 10X. Polarized A549 as measured by a transepithelial resistance > 120 Ω were transduced apically with 100 μL of HPIV3/LV or Ampho/LV carrying the eGFP gene for 1.5 h and cultured for 2 d before viewed by epifluorescent microscopy at 10X.

2.5 Discussion

We have demonstrated that HPIV3 HN and F proteins are incorporated into lentivirus particles to form infectious viruses. The titers of the HPIV3 pseudotyped lentiviruses are low, possibly because the viruses contain too few envelope proteins to efficiently infect cells [22]. A number of approaches can be envisioned to increase the level of envelope protein incorporation. One approach might be to increase the number of transiently transfected cells that express all of the genes necessary to produce a transduction competent virus by reducing the number of plasmids needed to transfect the virus producer cells, such as by developing a cell line that stably expresses HPIV3-F and the retroviral vector. Another approach might be to genetically modify the envelope proteins to increase their level of incorporation. This approach has been successfully used to increase the level of incorporation of heterologous envelope proteins by truncation of their cytoplasmic domains, fusion with the cytoplasmic domains of retroviral or lentiviral envelope proteins, or through the use of more sophisticated modifications designed to relieve steric hindrance or alter envelope protein folding [23-26].

Alternatively, it is possible that HPIV3/LV viruses inefficiently infect cells because of a defect in the interactions between HN and F when they are within the context of a pseudotyped lentivirus particle. Although the exact mechanism is not known, membrane fusion mediated by HPIV3-F glycoproteins, which are in the form of a trimer, strictly requires the presence of homotypic HN glycoproteins, which are in the form of a tetramer [13, 27]. Presumably, upon binding to its cell surface receptor, the HN glycoproteins undergo a conformational change that allows them to interact with neighboring F glycoproteins, inducing them to initiate fusion between the virus and cell [28-30]. Perturbations in the structure or stoichiometry of the HN-F complexes, perhaps due to their association with heterologous lentivirus capsid proteins, might reduce the efficiency with which virus fusion is induced after receptor binding.

36

Previous successes with improving the infectivity of other pseudotyped viruses suggest that it may be possible to substantially improve the titers of HPIV3/LV pseudotyped viruses. For example, the titer of an African green monkey simian immunodeficiency virus (SIVagm) pseudotyped with Sendai virus envelope proteins was increased several-fold by truncation of the cytoplasmic domain of the Sendai virus F protein, and by addition of the cytoplasmic tail of the SIVagm envelope protein to the N-terminus of the Sendai virus HN protein [23]. Similar approaches have increased the titers of a number of other pseudotyped retroviruses and lentiviruses [24, 31-34].

High titer HPIV3/LV viruses may have a number of useful properties as gene transfer vectors. As we have shown, lentiviruses pseudotyped with HPIV3 envelope proteins adopt the tropism of wild-type HPIV3 viruses, which may enable them to transduce a number of different cell types that express the sialated HPIV3 receptor, including polarized lung epithelial cells via their apical membrane. HPIV3/LV viruses are also likely to be more resistant to inactivation during purification and concentration steps then are viruses pseudotyped with retroviral envelope proteins. Unlike retrovirus envelope proteins that are weakly associated with the virus particle via non-covalent bonds, HPIV3-HN and F are both transmembrane proteins. We also speculate that because HPIV3/LV pseudotyped viruses have two envelope proteins, one that mediates binding (HN), and one that mediates fusion (F), it may be possible to genetically engineer the virus to bind to a specific, targeted cell type without adversely affecting its fusogenicity.

In summary, we have shown that lentiviruses can be pseudotyped with HPIV3 envelope proteins to exhibit the tropism of HPIV3. HPIV3/LV viruses may have a number of advantages as gene transfer vectors, including the ability to transfer genes to cells that are susceptible to infection by wild-type HPIV3, and could prove useful as a

model experimental system for studying the factors that control the incorporation and function of heterologous envelope proteins in lentivirus particles.

2.6 <u>References</u>

1. Pfeifer, A. and I.M. Verma, *Gene therapy: promises and problems.* Annu Rev Genomics Hum Genet, 2001. **2**: p. 177-211.

2. Mulligan, R.C., *The basic science of gene therapy.* Science, 1993. **260**(5110): p. 926-32.

3. Thomas, C.E., A. Ehrhardt, and M.A. Kay, *Progress and problems with the use of viral vectors for gene therapy.* Nat Rev Genet, 2003. **4**(5): p. 346-58.

4. Clapham, P.R. and A. McKnight, *Cell surface receptors, virus entry and tropism of primate lentiviruses.* J Gen Virol, 2002. **83**(Pt 8): p. 1809-29.

5. Reiser, J., et al., *Transduction of nondividing cells using pseudotyped defective high-titer HIV type 1 particles.* Proc Natl Acad Sci U S A, 1996. **93**(26): p. 15266-71.

6. Beyer, W.R., et al., *Oncoretrovirus and lentivirus vectors pseudotyped with lymphocytic choriomeningitis virus glycoprotein: generation, concentration, and broad host range.* J Virol, 2002. **76**(3): p. 1488-95.

7. Stitz, J., et al., *Lentiviral vectors pseudotyped with envelope glycoproteins derived from gibbon ape leukemia virus and murine leukemia virus 10A1.* Virology, 2000. **273**(1): p. 16-20.

8. Sinn, P.L., et al., *Lentivirus vectors pseudotyped with filoviral envelope glycoproteins transduce airway epithelia from the apical surface independently of folate receptor alpha.* J Virol, 2003. **77**(10): p. 5902-10.

9. Emi, N., T. Friedmann, and J.K. Yee, *Pseudotype formation of murine leukemia virus with the G protein of vesicular stomatitis virus.* J Virol, 1991. **65**(3): p. 1202-7.

10. Arai, T., et al., *A new system for stringent, high-titer vesicular stomatitis virus G protein-pseudotyped retrovirus vector induction by introduction of Cre recombinase into stable prepackaging cell lines.* J Virol, 1998. **72**(2): p. 1115-21.

11. Yang, Y., et al., *Inducible, high-level production of infectious murine leukemia retroviral vector particles pseudotyped with vesicular stomatitis virus G envelope protein.* Hum Gene Ther, 1995. **6**(9): p. 1203-13.

12. Johnson, L.G., et al., *Pseudotyped human lentiviral vector-mediated gene transfer to airway epithelia in vivo.* Gene Ther, 2000. **7**(7): p. 568-74.

13. Collins, P.L., R.M. Chanock, and K. McIntosh, *Parainfluenza viruses*, in *Fields Virology*, B.N. Fields, et al., Editors. 1996, Lippincott-Raven Publishers: Philadelphia. p. 1205-1243.

14. Ray, R. and R.W. Compans, *Monoclonal antibodies reveal extensive antigenic differences between the hemagglutinin-neuraminidase glycoproteins of human and bovine parainfluenza 3 viruses.* Virology, 1986. **148**: p. 232-36.

15. Niwa, H., K. Yamamura, and J. Miyazaki, *Efficient selection for high-expression transfectants with a novel eukaryotic vector.* Gene, 1991. **108**(2): p. 193-99.

16. Smith, R.F., *Microscopy and Photomicrography.* 2nd ed. 1994, Boca Raton: CRC Press. 162.

17. Le Doux, J.M., et al., *Complexation of retrovirus with cationic and anionic polymers increases the efficiency of gene transfer.* Human Gene Therapy, 2001. **12**: p. 1611-21.

18. Rothen-Rutishauser, B., et al., *MDCK cell cultures as an epithelial in vitro model: cytoskeleton and tight junctions as indicators for the definition of age-related stages by confocal microscopy.* Pharmaceutical Research, 1998. **15**(7): p. 964-71.

19. Bosch, V., et al., *Inhibition of release of lentivirus particles with incorporated human influenza virus haemagglutinin by binding to sialic acid-containing cellular receptors.* J Gen Virol, 2001. **82**(Pt 10): p. 2485-94.

20. Gasmi, M., et al., *Requirements for efficient production and transduction of human immunodeficiency virus type 1-based vectors.* J Virol, 1999. **73**(3): p. 1828-34.

21. Wang, G., et al., *Increasing epithelial junction permeability enhances gene transfer to airway epithelia In vivo.* Am J Respir Cell Mol Biol, 2000. **22**(2): p. 129-38.

22. Bachrach, E., et al., *Efficient cell infection by Moloney murine leukemia virus-derived particles requires minimal amounts of envelope glycoprotein.* J Virol, 2000. **74**(18): p. 8480-6.

23. Kobayashi, M., et al., *Pseudotyped lentivirus vectors derived from simian immunodeficiency virus SIVagm with envelope glycoproteins from paramyxovirus.* J Virol, 2003. **77**(4): p. 2607-14.

24. Mammano, F., et al., *Truncation of the human immunodeficiency virus type 1 envelope glycoprotein allows efficient pseudotyping of Moloney murine leukemia virus particles and gene transfer into CD4+ cells.* J Virol, 1997. **71**(4): p. 3341-5.

25. Spiegel, M., et al., *Pseudotype formation of Moloney murine leukemia virus with Sendai virus glycoprotein F.* J Virol, 1998. **72**(6): p. 5296-302.

26. Tailor, C.S., et al., *Mutation of amino acids within the gibbon ape leukemia virus (GALV) receptor differentially affects feline leukemia virus subgroup B, simian sarcoma-associated virus, and GALV infections.* J Virol, 1993. **67**(11): p. 6737-41.

27. Yao, Q., X. Hu, and R.W. Compans, *Association of the parainfluenza virus fusion and hemagglutinin-neuraminidase glycoproteins on cell surfaces.* J Virol, 1997. **71**(1): p. 650-6.

28. Tong, S. and R.W. Compans, *Alternative mechanisms of interaction between homotypic and heterotypic parainfluenza virus HN and F proteins.* J Gen Virol, 1999. **80 (Pt 1)**: p. 107-15.

29. Heminway, B.R., Y. Yu, and M.S. Galinski, *Paramyxovirus mediated cell fusion requires co-expression of both the fusion and hemagglutinin-neuraminidase glycoproteins.* Virus Res, 1994. **31**(1): p. 1-16.

30. Porotto, M., et al., *Triggering of human parainfluenza virus 3 fusion protein (F) by the hemagglutinin-neuraminidase (HN) protein: an HN mutation diminishes the rate of F activation and fusion.* J Virol, 2003. **77**(6): p. 3647-54.

31. Kowolik, C.M. and J.K. Yee, *Preferential transduction of human hepatocytes with lentiviral vectors pseudotyped by Sendai virus F protein.* Mol Ther, 2002. **5**(6): p. 762-9.

32. Christodoulopoulos, I. and P.M. Cannon, *Sequences in the cytoplasmic tail of the gibbon ape leukemia virus envelope protein that prevent its incorporation into lentivirus vectors.* J Virol, 2001. **75**(9): p. 4129-38.

33. Hohne, M., et al., *Truncation of the human immunodeficiency virus-type-2 envelope glycoprotein allows efficient pseudotyping of murine leukemia virus retroviral vector particles.* Virology, 1999. **261**(1): p. 70-8.

34. Stitz, J., et al., *MLV-derived retroviral vectors selective for CD4-expressing cells and resistant to neutralization by sera from HIV-infected patients.* Virology, 2000. **267**(2): p. 229-36.

CHAPTER 3

LENTIVIRUSES INEFFICIENTLY INCORPORATE HUMAN PARAINFLUENZA TYPE 3 ENVELOPE PROTEINS[2]

3.1 Abstract

We have previously shown that the envelope glycoproteins of human parainfluenza type 3 (HPIV3), F and HN, are able to pseudotype lentiviruses, but the titers of these viruses are too low for use in clinical gene transfer. In this study we investigated the cause of these low titers. We compared the mRNA and protein expression levels of HN and F in transfected cells and in cells infected with wild-type HPIV3. Transfected cells contained similar levels of HN and F cytosolic mRNA, but fewer cell-surface HN and F proteins (3.8 and 1.3-fold less, respectively), than cells infected with wild-type HPIV3. To increase expression of HN in transfected cells, we codon-optimized HN and used it to transfect lentivirus producer cells. Cell surface expression of HN, as well as the amount of HN incorporated into virus particles, increased 2 to 3-fold. Virus titers increased 1.2 to 6.4-fold, and the transduction efficiency of polarized MDCK cells via their apical surfaces increased 1.4-fold. Interestingly, even though codon optimization improved the expression levels of HN and virus titers, we found that HPIV3 pseudotyped viruses contained about 14-fold fewer envelope proteins than lentiviruses pseudotyped with the amphotropic envelope protein. Taken together, our findings suggest that titers are low, not because virus producer cells express levels of HPIV3 envelope proteins that are too low, but because too few of these proteins are incorporated by the lentiviruses for them to be able to efficiently transduce cells.

3.2 <u>Introduction</u>

Recombinant retroviruses are used in gene therapy clinical trials because they can permanently integrate a therapeutic gene into the DNA of target cells, resulting, in principle, in a long-term cure [1, 2]. Lentiviral vectors, such as those based on human immunodeficiency virus (HIV), are a subclass of retroviruses that can infect and integrate their genome into non-dividing cells [3]. Retroviral-mediated gene transfer can be used to treat inherited genetic disorders, complex genetic disorders, and infectious diseases, and has numerous applications in tissue engineering. Unfortunately, the current generation of recombinant retroviruses have some limitations that restrict their usefulness for *in vivo* applications [4, 5]. For example, it is difficult to control the tropism of retroviruses; that is, the types of cells that retroviruses can, and cannot, transduce.

Retroviral tropism is largely determined by the interaction between envelope proteins that protrude from the surface of the virus and receptors for the virus on the surface of the cell [6, 7]. Frequently, retroviruses that are being studied for use in human gene therapy have had their wild-type envelope protein replaced with one from another virus to form a pseudotyped virus (i.e., a virus composed of proteins from more than one virus). The most commonly-used envelope proteins for pseudotyping retroviruses are the amphotropic and VSVG envelope proteins [7, 8]. These proteins are favored primarily because they enable the viruses to transduce a wide range of human cell types.

Unfortunately this lack of cell-type specificity may reduce the usefulness of VSVG or amphotropic envelope proteins for viral-mediated gene therapy *in vivo*, where it is often important to transduce a specific targeted cell type and no others. In addition, VSVG and amphotropic pseudotyped retroviruses do not efficiently transduce some clinically relevant cell types such as polarized epithelial cells of the lung via their apical

surfaces, which are important targets for cystic fibrosis and other lung gene therapies [9-11]. To overcome this problem, researchers have attempted to pseudotype lentiviruses with envelope proteins derived from a number of lung-tropic viruses, including influenza, respiratory syncytial virus, influenza D, Ross River virus, and Jaagsiekte sheep retrovirus [12-16]. Unfortunately, lentiviruses pseudotyped with these proteins either do not transduce polarized airway cells via their apical surfaces, or do so with efficiencies that are too low to be useful for clinical gene transfer.

Some promising envelope proteins have been genetically modified to improve their ability to pseudotype lentiviruses. Kobayashi et al. successfully genetically modified both Sendai virus envelope proteins F and HN to pseudotype SIV-derived lentiviruses (SIVagm) [17]. These viruses transduced polarized rat tracheal epithelial cells *in vitro*, but their ability to efficiently transduce cells *in vivo* has not yet been tested. Medina et al. modified the Zaire strain of the Ebola virus glycoprotein (EboZ) to improve its safety and gene transfer efficiency by deleting toxic sequences [18]. Lentiviruses pseudotyped with these engineered Zaire EboZ envelope proteins transduced up to 52% of polarized mouse airway epithelial cells *in vivo* after direct tracheal injection [18].

As part of this important continuing effort to identify and develop alternative lentivirus pseudotypes for the purposes of human gene therapy, we have begun to investigate the ability of human parainfluenza virus type 3 (HPIV3) envelope proteins to pseudotype lentiviruses. We expect HPIV3 pseudotyped lentiviruses to be useful for gene delivery to the lung because wild-type HPIV3 infection begins with interactions between the envelope proteins (hemagluttinin-neuraminidase (HN) and fusion (F)) of the virus and cell-surface sialic-acid containing receptors that are abundantly expressed on the apical membranes of lung cells [19, 20]. Importantly, HPIV3 infections do not generate long-term immunity in infected patients. This suggests that it may be possible to administer HPIV3 pseudotyped viruses to a patient as often as necessary to achieve

the desired therapeutic outcome, which would be a distinct advantage over most other viral vectors [21, 22].

We have previously shown that human parainfluenza virus type 3 envelope proteins F and HN are able to pseudotype lentiviruses, and that these viruses infect polarized cells via their apical surfaces, albeit with titers too low to be useful for clinical gene transfer [23]. In this study, we tested the hypothesis that titers are low because too few particles are released by the virus producer cells, cellular expression of the HPIV3 envelope proteins (HN and F) is low, or too few HPIV3 envelope proteins are incorporated by the lentiviruses. The implications of our findings for the generation of pseudotyped lentiviruses that are useful for clinical gene transfer are discussed.

3.2 Materials and Methods

Chemicals and antibodies. Poly-L-lysine, 1,5-Dimethyl-1,5-diazaundecamethylene polymethobromide (Polybrene), o-phenylenediamine dihydrochloride (OPD), and 5-Bromo-4-chloro-3-indolyl-β-D-galactopyranoside (X-Gal) were purchased from Sigma Chemical (St. Louis, MO). Complete mini protease inhibitor cocktail tablets were purchased from Roche Diagnostics (Indianapolis, IN). Coomassie Plus-200 protein assay reagent was purchased from Pierce (Rockford, IL). Mouse ascites monoclonal antibody 215 against HPIV3-F and mouse ascites monoclonal antibody 66/4 against HPIV3-HN were generously provided by Judy Beeler (WHO Programme for Vaccine Development Reagent Bank for Respiratory Syncytial Virus and Parainfluenza Type 3). HIV-1 p24 gag mouse ascites monoclonal antibody #24-3 was obtained through the AIDS Research and Reference Reagent Program, Division of AIDS, NIAID, NIH: HIV-1 p24 gag monoclonal from Dr. Michael H. Malim. Mouse ascites monoclonal antibody c110 against HPIV3-F was generously provided by B.R. Murphy, Respiratory Viruses Section, NIAID, NIH (Bethesda, MD). Guinea pig

antiserum against HPIV3 (strain 47885) was obtained through the NIAID Reference Reagent Repository (Bethesda, MD). Mouse anti-gp70 antibodies were purified from the supernatant of the 83A25 hybridoma cell line [24] following standard procedures [25]. Cy2-conjugated donkey anti-guinea pig IgG (H+L), Cy2-conjugated donkey anti-mouse IgG (H+L), horseradish peroxidase (HRP)-conjugated donkey anti-mouse IgG (H+L), and normal donkey serum were purchased from Jackson Immunoresearch Laboratories, Inc. (West Grove, PA).

Cell culture. 293T/17 cells and HeLa cells were maintained in Dulbecco's modified essential medium (DMEM) supplemented with 10% heat inactivated fetal bovine serum (FBS), 100 U/mL of penicillin, and 100 μg/mL streptomycin (HyClone Laboratories; Logan, UT). Vero cells and MDCK cells were maintained in Minimum essential medium (Eagle) supplemented with 10% fetal bovine serum, 100 U/mL of penicillin, and 100 μg/mL streptomycin. Plates coated with poly-L-lysine were incubated for 5 min in the 0.01% solution (150-300 kDa), washed once with deionized water, and dried.

Virus production.   Human parainfluenza virus type 3 (strain Wash/57/47885), obtained from the National Institute of Allergy and Infectious Disease (Bethesda, MD), was propagated on monolayers of HeLa cells.   Lentiviruses pseudotyped with the amphotropic or human parainfluenza virus type 3 envelope proteins were produced by transfecting 293T/17 cells, seeded (1×10^7 per well) the previous day on poly-L-lysine coated plates with Lipofectamine 2000 (Invitrogen; Carlsbad, CA) and 6 μg of the packaging construct pCMVΔR8.91 [26], 6 μg of the lentivirus vector pTYEFnlacZ or pTYEFeGFP (AIDS Research and Reference Reagent Program; Bethesda, MD), and 6 μg of the amphotropic envelope protein expression plasmid pFB4070ASALF [27] or 6 μg each of the HPIV3 F and HN envelope expression plasmids (i.e., pCAGGS-hPIV3-F and pCAGGS-hPIV3-HN, respectively).   Viral supernatants were collected every 12 h from

48 to 60 h after transfection, filter sterilized (0.45 μm), and frozen (-80°C) for later use. For some experiments, an expression vector encoding codon-optimized HPIV3-HN was used to generate pseudotyped lentiviruses. Codon-optimization of HPIV3-HN was performed by GENEART, Inc (Toronto, Canada). The cDNA was subcloned into the *Cla I* and *Sph I* sites of the pCAGGS.MCS expression vector [28] and the structure of the ligation sites was verified by DNA sequencing.

Metabolic labeling and immunoprecipitation. To detect proteins in virus stocks and producer cells, cells were transfected as above, or infected with wild-type HPIV3 at an MOI of 1 for twenty-four hours, and then incubated with methionine and cysteine-free DMEM for 15 min at 37°C. Cells were then radiolabeled for 16 h at 37°C with 450 μCi of [35S]methionine-cysteine protein labeling mix (GE Healthcare; Piscataway, NJ). Cells were lysed at 4°C for 10 min with RIPA buffer (50 mM Tris- HCl [pH 7.6], 150 mM NaCl, 0.5% Triton X-100, 0.5% sodium deoxycholate, 0.1% SDS, and protease inhibitors) and centrifuged for 10 min at 20,800 x g to pellet the nuclei. Virus samples were obtained by ultracentrifugation of the viral supernatants in a SW41Ti Beckman rotor (150,000 x g, 2 h, 4°C) through a 20% sucrose cushion after which the pellets were resuspended in RIPA buffer for 30 min at 25°C. Cell lysates or virus samples were immunoprecipitated with guinea pig anti-serum against HPIV3, mouse monoclonal antibody against gp70 (83A25), mouse monoclonal antibody against F (c110), or mouse monoclonal antibody against HN (66/4) prebound to protein-A sepharose beads (Pierce). Equal amounts per sample of p24 (Retro-Tek HIV-1 p24 Antigen ELISA Kit; ZeptoMetrix; Buffalo, NY) or total protein were loaded, the proteins were separated by size by SDS-PAGE (4-15%), and then the gel dried (72°C for 45 min) and visualized by autoradiography (Bio-Max MR film; Amersham; Piscataway, NJ). To quantitatively compare the amount of protein that was visualized as bands on the film, we used ImageJ to measure the band area and intensity and compared the product of

46

the two values (we assumed the amphotropic and HPIV3 envelope proteins were labeled to a similar extent since the fraction of their residues that are cysteines or methionines are about the same (20 residues out of 548 in F, 25 residues out of 572 in HN, and 33 residues out of 654 in amphotropic env)). We also compared the amount of radioactivity that was in the bands. We cut out the bands from the gels as slices, brought their volume to 3 mL with Ecoscint A scintillation cocktail (National Diagnostics), and used a scintillation counter (Tricarb 2900TR; Perkin Elmer) to quantify the amount of ^{35}S in the samples.

Immunoblotting. To detect p24 in virus samples, equal amounts of protein from each sample were combined 1:2 (v/v) with sample buffer containing 5% β-mercaptoethanol (both from Bio-Rad; Hercules, CA), vortexed, boiled for 5 min, separated by size by SDS-PAGE (4-20% Tris-HCl gel, Bio-Rad), and transferred to a PVDF membrane (0.2 μm, Bio-Rad). To probe for p24 in the membrane, mouse anti-p24 (24-3) was diluted 1:5000 in blocking buffer (5% nonfat milk in PBS with 0.1% Tween 20) and bound IgG was detected by incubation with HRP-conjugated donkey anti-mouse (diluted 1:100,000 in blocking buffer), and detected with a chemiluminescent detection system (Super Signal West Femto kit; Pierce).

Cell-based ELISA. We used cell-based ELISAs to quantitatively compare the amount of F and HN expressed on the surfaces of the HeLa cells. We plated 20,000 HeLa cells per well and transfected them with Polyfect (Qiagen; Valencia, CA) and either 0.2 µg of pCAGGS-hPIV3-HN alone, 0.2 µg of pCAGGS-hPIV3-HN and 0.2 µg pCAGGS-hPIV3-F, 0.2 µg codon optimized HN (pCAGGS-CO-HPIV3-HN) alone, 0.2 µg pCAGGS-CO-HPIV3-HN and 0.2 µg pCAGGS-hPIV3-F, or infected them with wild-type HPIV3 at an MOI of 1. The next day the cells were washed once with PBS (100 µL/well), fixed for 10 min with 4% paraformaldehye (100 µL/well), and blocked for 15 min with PBS/sera (100 µL/well). Next, the cells were incubated with anti-F (215) or anti-HN

47

(66/4) antibodies (diluted 1:800 in PBS/sera, 100 µL per well) for 1 h at room temperature. Cells were then washed four times with PBS (100 µL/well) and incubated with HRP-conjugated donkey anti-mouse secondary antibody (diluted 1:500 in PBS/sera) for 1 h at room temperature. Following four additional washes with PBS the wells were developed for 10 min with OPD solution (100 µL/well) (10 mg OPD, 10µL H_2O_2 in 25 mL of substrate buffer (24 mM citric acid·monohydrate, 51 mM $Na_2HPO_4·7H_2O$, pH 5.0)). The reaction was stopped with 8 N sulfuric acid (50 µL/well), the optical density at 490 nm (OD490) was measured using an absorbance plate reader (Versamax; Molecular Devices; Sunnyvale, CA), and the nonspecific background at 650 nm (OD650) was subtracted. Values for each point are the average of at least triplicate wells.

Flow cytometry. To quantitatively measure F and HN surface expression on 293T cells, approximately $2x10^6$ cells were seeded on poly-L-lysine coated 6-well plates and transfected with Lipofectamine 2000 using 1 µg of each plasmid (F only, HN only, or HPIV3/LV which included plasmids for HN, F, Gag-Pol, and lacZ) or infected with wild-type HPIV3 at an MOI of 1. The next day, cells were washed with PBS, released with versene (PBS, 5 mM EDTA), and incubated with a 1:500 dilution of anti-F (c110) or anti-HN (guinea pig antisera) in DMEM at 4°C for 1 hour. Next, the cells were washed three times with DMEM and once with PBS and then incubated with donkey anti-mouse or guinea pig Cy2-conjugated secondary antibody diluted 1:500 in PBS at 4°C for 1 hour and then the cells were washed as before in PBS and resuspended in 500 µL of PBS/10% FBS. An average of 50,000 cells were counted per sample with the LSR II flow cytometer (Becton Dickinson) and the data analyzed with a FACS DiVa (BD Biosciences; Palo Alto, CA).

RNA isolation and quantitative real-time PCR. Total, cytoplasmic, and nuclear RNA was extracted from cells using an RNeasy Mini Kit and Qiashredder (Qiagen) and

48

the concentration of nucleic acid in the samples was determined by measuring their absorbance at 260 nm. We transfected 293T/17 cells ($2x10^6$) with 4 µg HPIV3-HN, 1 µg each of HPIV3-F, HN, β-galactosidase, and Gag-Pol, or infected them with wild-type HPIV3 at an MOI of 1. Two days later, total RNA or cytoplasmic and nuclear RNA fractions were isolated from cell lysates and 1 µg of RNA was reverse transcribed using OligoDT primers with the Superscript First-Strand Synthesis for RT-PCR kit (Invitrogen). The resulting DNA (1 µL) was then amplified by polymerase chain reaction (PCR) using Platinum Pfx DNA polymerase and reagents (Invitrogen) and HN or F-specific primers, after which the amplicons were separated by size by agarose gel electrophresis on a 1% agarose gel. The sequences of the HN primers were PCR-HN-Forward (5' TACCAATCACGGGAAAGATGC 3') and PCR-HN-Reverse (5' TGGAATCTCTGTTTTGAACAACATAGG 3'). The sequences of the F primers were PCR-F-Forward (5' TGCTAATTATTACAACCATGATTATGGC 3') and PCR-F-Reverse (5' ACATATGGTTTATCATTTTGATCCACTCG 3'). For quantitative real-time PCR, 1 µl of each cDNA reaction was analyzed in triplicate for the amplification of HPIV3-HN and GAPDH. Amplification conditions were performed with an ABI Prism sequence detection system in the presence of SYBR green (ABI) and relative standard curve analysis was performed on the samples as outlined in ABI user bulletin 2 (Relative quantitation of gene expression: ABI PRISM 7700 sequence detection system: user bulletin 2: Rev B). The pairs of primers we used were qPCR-HN-forward (5' CAAAAATAAGGTTAATGCCGGG 3') and qPCR-HN-reverse (5' AGGACGGAGTTCTAACACAGCC 3'), or the intron-spanning qPCR-GAPDH-forward (5' TGAAGGTCGGAGTCAACGG 3') and q-PCR-GAPDH-reverse (5' AGAGTTAAAAGCAGCCCTGGTG 3').

Transduction. Target cells were seeded in poly-L-lysine coated 12-well plates ($1x10^5$ cells per well) and incubated at 37°C. The next day, viral supernatant dilutions

were incubated with cells for 48 h, after which the cells were fixed and stained for β-galactosidase activity with X-Gal, and the number of *lacZ*+ colony-forming units (CFU) per milliliter was counted. To examine the ability of the viruses to transduce polarized cells, MDCK cells were seeded on tissue culture treated Transwell polyester supports (4 x 10^4 cells per insert) (Costar-Corning; Corning, NY) and then incubated at 37°C until polarized as evidenced by a step jump in their transepithelial resistance (>600 Ω^*cm^2) as measured with a voltohmmeter (World Precision Instruments; Sarasota, FL). Supernatants of viruses that encoded green fluorescent protein (GFP) (100 µL) were mixed with 8 µg/mL of Polybrene and then applied to the apical or basolateral surfaces of the polarized cells for 2 h. The cells were washed twice with DMEM, cultured for two days, and then analyzed by flow cytometry for GFP expression. As a control, cells were incubated with EDTA (6mM) in Hepes (10 mM) for 30 min to depolarize them, and then transduced with viral supernatants to determine the effect of depolarization on infection. To measure the titer of wild-type HPIV3, a standard plaque assay was performed. Briefly, serial dilutions of the viruses were prepared and incubated on confluent monolayers of cells for 1 h at 37°C. The cells were then overlaid with a solution of 1% agar (Fisher Scientific; Fairlawn, NJ) in DMEM supplemented with 4% FBS. The cells were incubated at 37°C for 3 days, and then stained with 1 mL of 0.05% neutral red (Fisher) in PBS for 1 hour and washed twice in PBS, after which the number of visible plaque-forming units (PFU) per milliliter were counted.

Statistics. Data are summarized as the mean ± the standard deviation for at least triplicate samples. Statistical analysis was performed using one-way analysis of variance for repeated measurements of the same variable.   The Tukey multiple comparison test was used to conduct pairwise comparisons between means. Differences at *p* < 0.05 were considered statistically significant.

3.4 <u>Results</u>

   We have previously shown that lentiviruses form low titer pseudotypes with HPIV3-F and HPIV3-HN [23]. We reasoned that titers were low because the virus producer cells released too few particles, cellular expression of the HPIV3 envelope proteins (HN and F) was low, or too few HPIV3 envelope proteins were incorporated by the lentiviruses. To determine if fewer particles were released by HPIV3-lentivirus producer cells, we compared the amount of virus capsid protein present in high titer stocks of amphotropic lentivirus to the amount present in stocks of HPIV3 pseudotyped lentivirus. We transfected 1×10^7 293T/17 cells in a 10cm dish with plasmids encoding for β-galactosidase, lentiviral Gag-Pol, and either HPIV3-F and HPIV3-HN, or the MuLV amphotropic envelope (Env) protein. Two days later the virus-laden supernatants were harvested, filter sterilized, pelleted by ultracentrifugation through a 20% sucrose cushion, and then analyzed by Western blot for the presence of lentiviral p24 (Figure 3.1). Similar amounts of p24 were detected in both amphotropic pseudotyped lentiviruses and HPIV3 pseudotyped lentiviruses, which suggests that insufficient release of the particles from the virus producer cells is not the cause for the low titer of HPIV3 pseudotyped lentiviruses.

   We also wondered if titers could be low because the HPIV3-lentivirus particles decayed at a faster rate than amphotropic lentivirus particles. We produced HPIV3 or amphotropic pseudotyped lentivirus as above, harvested, filter sterilized, and then incubated the viral supernatant for 0, 8, 19, or 27 hours at 37^0C before transducing cells in a diluted titer assay (Figure 3.2). HPIV3-lentivirus particles decay at a similar rate to amphotropic-lentivirus particles ($t_{1/2}$ = 15.7 ± 1.6 hours compared to $t_{1/2}$ = 15.2 ± 1.0 hours, respectively).

Figure 3.1. HPIV3-pseudotyped lentiviral stocks contain similar numbers of virus particles as amphotropic Env-pseudotyped lentiviral stocks. 293T/17 cells (1×10^7) were transfected with 6 µg each of plasmids encoding β-galactosidase, lentiviral Gag-Pol, and either HPIV3-F and HPIV3-HN, or MuLV amphotropic envelope (Env) protein. Supernatants containing amphotropic lentiviruses (Lane 2) or HPIV3-pseudotyped lentiviruses (Lane 3) were concentrated 18-fold by ultracentrifugation through a 20% sucrose cushion. The pellet was analyzed by Western blot using p24 mouse ascites monoclonal antibody (#24-3) and HRP-conjugated anti-mouse secondary antibody. The data is representative of three separate experiments.
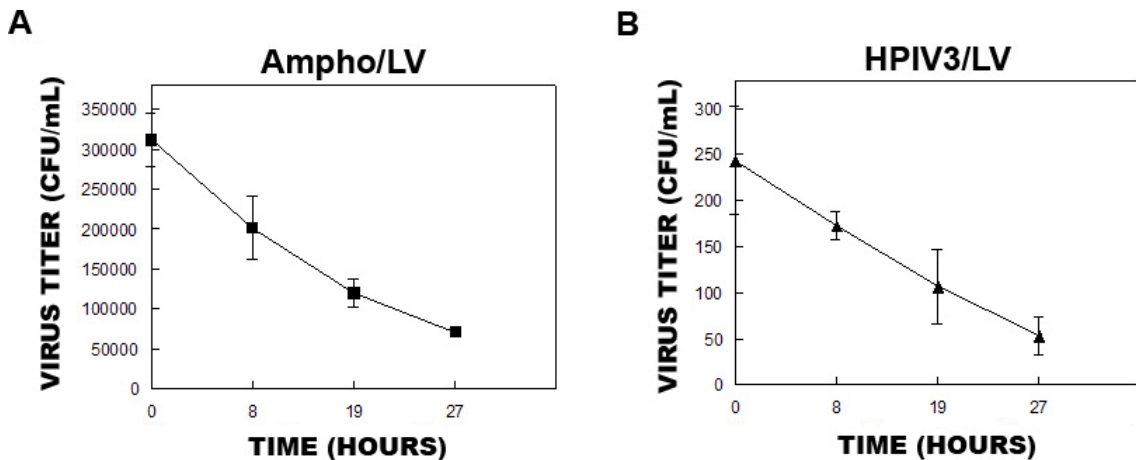
Figure 3.2. HPIV3-pseudotyped lentiviral stocks decay at a similar rate to amphotropic Env-pseudotyped lentiviral stocks. 293T/17 cells (1×10^7) were transfected with 6 µg each of plasmids encoding β-galactosidase, lentiviral Gag-Pol, and either HPIV3-F and HPIV3-HN, or MuLV amphotropic envelope (Env) protein. Supernatants containing amphotropic lentiviruses (A) or HPIV3-pseudotyped lentiviruses (B) were decayed for 0, 8, 19, or 27 hours at 37^0C and used to transduce cells. Transduced cells were incubated for 2 days at 37 ^{0}C until confluent, fixed and stained for *lacZ* activity with X-gal, colonies of lacZ$^+$ cells counted, and the titer (CFU/mL) calculated.

Next, we examined the possibility that titers were low due to inadequate expression of F and HN in producer cells. First we compared HPIV3 F and HN expression levels in cells transfected to produce HPIV3 pseudotyped lentivirus to expression levels in cells infected with wild-type HPIV3. We plated HeLa cells in a 96-well dish and the following day, transfected cells with plasmids for either F or HN, both F and HN, or infected cells with wild-type HPIV3 at an MOI of 1. Two days later, we used a cell-based ELISA to quantify the expression levels of F and HN. Cells were immunostained with a mouse monoclonal antibody against HPIV3-F (215) or HN (66/4), and a HRP-conjugated secondary antibody, after which the cells were developed with a solution of o-phenylenediamine dihydrochloride (OPD) and the optical density of each well measured (Figure 3.3). Expression of F in transfected cells was 1.6-fold lower than in wild-type infected cells when the cells were transfected to express F only, and slightly higher – 1.3-fold lower than in wild-type infected cells – when the cells were co-transfected to express both F and HN. HN expression in transfected cells was 3.8-fold lower than in wild-type infected cells, whether or not the cells expressed HN only or both HN and F. We also used flow cytometry to compare F and HN expression in transfected and infected cells. Cells were plated in a 6-well dish, transfected or infected as described above, immunostained with a mouse monoclonal antibody against HPIV3-F (c110) or a guinea pig polyclonal antibody against HN, and then the percentage of cells that expressed the envelope proteins quantified (Table 3.1). The percentage of transfected cells that expressed F and HN was 1.4 and 1.7-fold lower, respectively, than that of wild-type infected cells. These results show that the expression of F to some extent, and HN to a greater extent, is lower in virus producer cells than in cells infected with wild-type HPIV3.
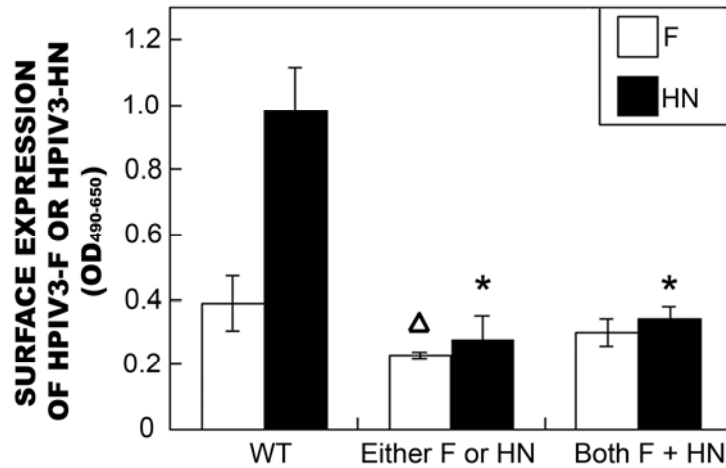
Figure 3.3. The expression levels of cell-surface HPIV3-F and HN is lower in transfected cells than in cells infected with wild-type HPIV3. Hela cells (20,000) were transfected with expression plasmids for HPIV3-F (0.2 μg) and/or HPIV3-HN (0.2 μg), or infected with wild-type (WT) HPIV3 at an MOI of 1. Two days later, cells were washed, fixed (2% paraformaldehyde), blocked (PBS/sera), and then sequentially stained with mouse monoclonal specific for HPIV3-F (215) or HN (66/4) and an HRP-conjugated anti-mouse secondary antibody. Stained cells were developed with a solution of OPD, the optical density at 490 nm was measured using an absorbance plate reader, and the nonspecific background at 650nm was subtracted. Values for each point are the average of at least triplicate wells. Statistically significant differences (p<0.05) from the expression levels of F and HN in cells infected with wild-type HPIV3 are denoted with Δ and *, respectively.

Table 3.1. The percentage of cells that express HPIV3-F and HN in transfected and wild-type infected cells.

Treatment	HPIV3-F (%)[a,b]	HPIV3-HN (%)[a,c]
Untreated	0.37 ± 0.15	0.50 ± 0.21
Transfected with F	61 ± 11	N/A
Transfected with HN	N/A	51 ± 15
Transfected with F, HN, Gag-Pol, LacZ	67 ± 10	30 ± 1.5
Infected with wild-type HPIV3	88 ± 13	85 ± 11

Flow cytometric analysis was used to determine the percentage of 293T cells that expressed HPIV3 F or HN when transfected with expression plasmids for F alone, HN alone, F, HN, Gag-Pol, and LacZ, or infected with wild-type HPIV3. [a]Percentages represent the mean of experimental values +/- one standard deviation. [b]HPIV3-F (%); percentage of cells expressing HPIV3-F. [c]HPIV3-HN (%); percentage of cells expressing HPIV3-HN. N/A=not applicable.

54

Since HN expression was the most limiting, we decided to examine more closely the causes for its low level of expression in transfected cells. First we wondered if HN mRNA was inappropriately spliced in transfected cells due to the presence of cryptic splice sites within its sequence. We considered this a possibility since transfection of virus producer cells with an expression plasmid for HN alters the lifecycle of the HN mRNA from one that has evolved to operate entirely within the cytoplasm in infected cells to one in which it is formed and processed within the nucleus in transfected cells. To test for this possibility, total RNA was isolated from 293T/17 cells that had been transfected with the HPIV3-HN expression vector or from cells infected with wild-type HPIV3, reverse-transcribed, amplified by PCR using primers that span the entire HN sequence, and then the amplicons separated by size by gel electrophoresis (Figure 3.4A). The molecular weights of the amplicons were the same which indicated that the HN mRNA had not been aberrantly spliced. Similarly, Figure 3.4A also shows F is not aberrantly spliced.

We also assessed whether HN mRNA in transfected cells was efficiently exported from the nucleus. Cytoplasmic and nuclear RNA were isolated from fractionated cells, reverse transcribed, and then amplified by real-time PCR (Figure 3.4B). No significant differences ($p < 0.05$) in HN mRNA levels were detected, regardless of whether the cells were infected with wild-type HPIV3, transfected with only the expression plasmid for HN, or multiply transfected to express HN, Gag-Pol, and the lentiviral transgene β-galactosidase. A small amount of HN RNA was detected in the nuclear fraction of wild-type HPIV3 infected cells due to limitations with the experimental procedure which did not completely prevent contamination of the nuclear fraction with cytoplasmic mRNA. These results suggest that HN mRNA is efficiently exported from the nucleus to the cytoplasm in transfected cells.

A

HPIV3-HN   HPIV3-F

	1	2	3	4	5	6	7	8	9	10	11	12	13	14	15
HN/F	+	-	+	+	-	+	P		P	+	-	+	+	-	+
RT	+	+	+	-	-	-				+	+	+	-	-	-

B
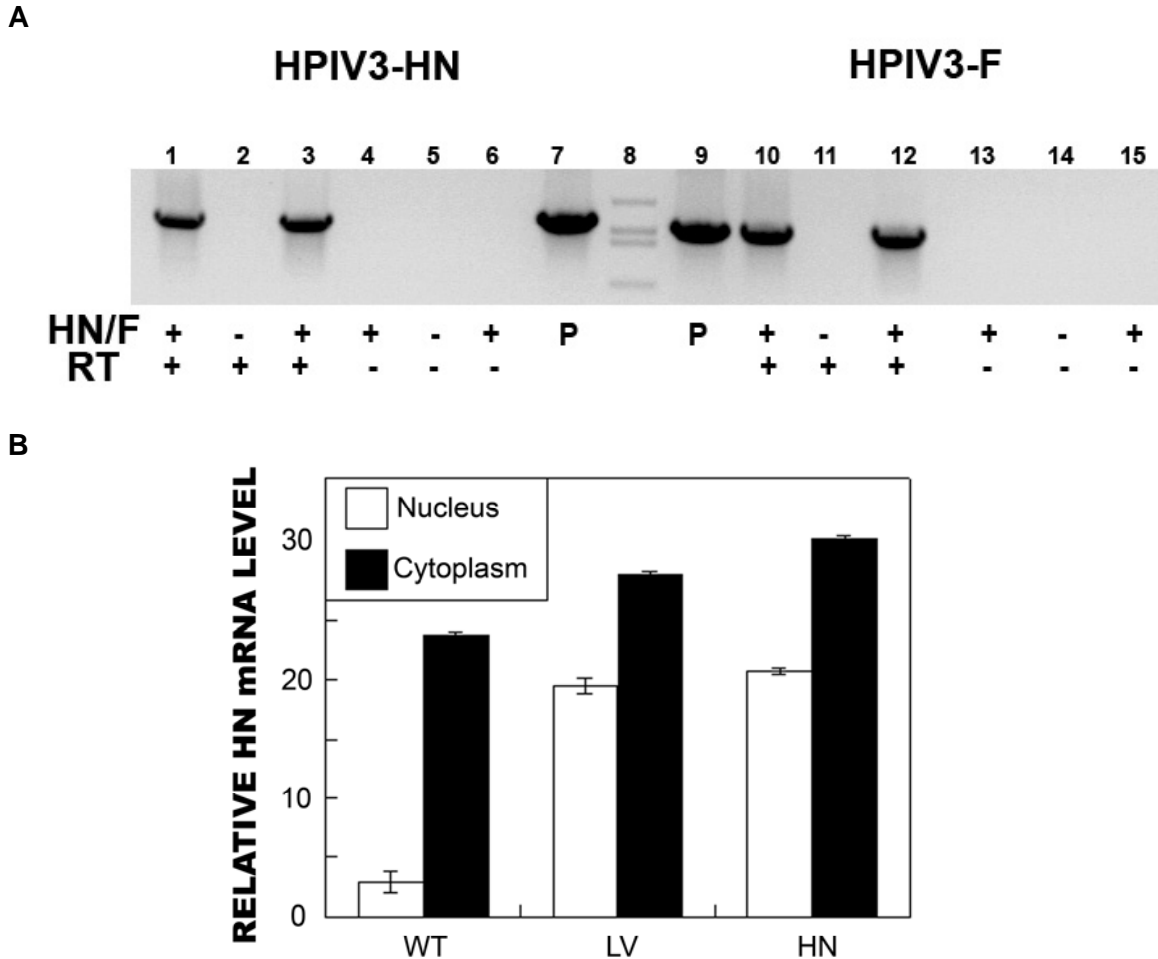
Figure 3.4. HN and F RNA is not aberrantly spliced and HN is efficiently exported from the nucleus to the cytoplasm. (A) 293T/17 cells (2×10^6) were transfected with an expression plasmid for HPIV3-HN (4 μg) (lanes 1 and 4), HPIV3-F (4 μg) (lanes 10 and 13), or infected with wild-type HPIV3 at an MOI of 1 (lanes 3, 6, 12, 15). Two days later, total RNA was isolated from lysates of the cells and 1 μg was reverse-transcribed using OligodT primers. The resulting DNA was then amplified by polymerase chain reaction (PCR) using HN-specific primers (Lanes 1-7) or F-specific primers (Lanes 9-15), after which the amplicons were separated by size by agarose gel electrophresis on a 1% agarose gel. The positive control was the HPIV3-HN or F plasmid DNA that was used to transfect the cells (Lane 7 for HN and 9 for F), and the negative controls were samples from untreated cells (lanes 2 and 5 for HN and lanes 11 and 14 for F) and samples that were PCR-amplified without first being reverse transcribed (lanes 4-6, 13-15). (B) 293T/17 cells (2×10^6) were transfected with 1 μg of an expression plasmid for HPIV3-HN (HN), 1 μg each of expression plasmids for HPIV3-F, HPIV3-HN, β-galactosidase, and lentiviral Gag-Pol (LV), or infected with wild-type HPIV3 (WT) at an MOI of 1. Two days later, RNA from the cytoplasmic and nuclear fractions were isolated using the RNeasy kit per the manufacturer's instructions. Portions (1 μg) of the cytoplasmic and nuclear RNA fractions were reverse-transcribed using OligodT primers and then quantified by real-time PCR using HN-specific or GAPDH-specific primers. Bars show the mean level ± standard deviation of HN RNA normalized to GAPDH control from triplicates of three experiments.

Since our data suggested that HN expression was not low due to aberrant mRNA splicing or export to the cytoplasm, we next considered the possibility that translation was impaired due to suboptimal codon usage or the presence of mRNA structures or negative regulatory sequences that inhibit translation. We codon optimized the HN sequence to improve codon usage and to eliminate any inhibitory structures or sequences that might have been present, and then constructed an expression plasmid for the codon-optimized HN. To examine the effect of codon-optimization on HN expression, we transfected HeLa cells with the just the expression plasmid for the codon-optimized HPIV3-HN, or we co-transfected the cells with expression plasmids for both the codon optimized HN and wild-type F. In parallel, cells were transfected with an expression plasmid for wild-type HN, or co-transfected with expression plasmids for both wild-type HN and F. Two days later, we quantified the expression levels of HN and F by cell-based ELISA. We found that HN expression was more than two-fold higher when codon-optimized HN was used to transfect cells, but, interestingly, these increases were only observed in cells that were co-transfected with codon-optimized HN and wild-type F (Figure 3.5A). Cells that were singly transfected with codon-optimized HN did not express significantly higher levels of cell-surface HN than cells transfected with wild-type HPIV3-HN or co-transfected with wild-type HPIV3 HN and F. Surprisingly, F expression, which also increases in the presence of HN (1.6-fold), more than doubled (2.1-fold) in the presence of codon-optimized HN (Figure 3.5B).

To determine if codon optimization increased envelope incorporation into lentiviral particles, we transfected 293T/17 cells with expression plasmids that encoded HPIV3-F, lentiviral Gag-Pol, the lentiviral vector encoding the β-galactosidase transgene, and codon optimized or non-codon optimized HPIV3-HN. The next day we metabolically labeled the cells with [35S] methionine-cysteine protein labeling mix for 16 hours, immunoprecipitated HPIV3-HN from lysates of the cells and from the virus supernatant

57

A
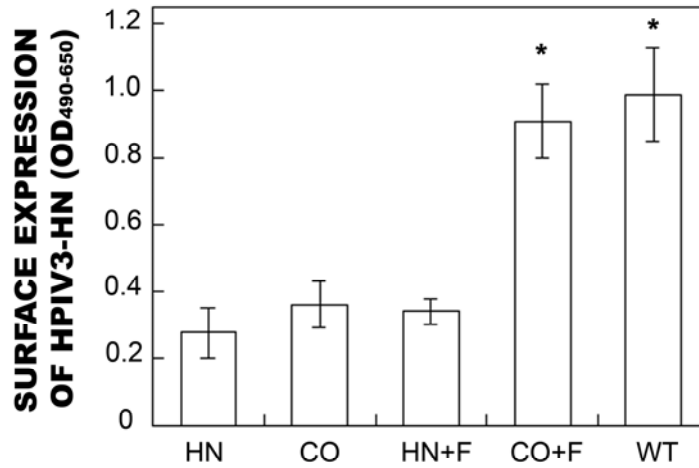
B
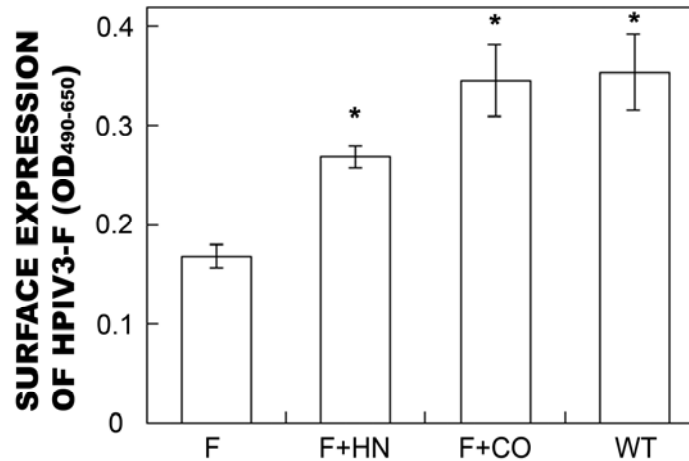
Figure 3.5. Cells transfected with codon-optimized HPIV3-HN express higher levels of HPIV3 envelope proteins. (A) Hela cells (20,000) were singly transfected (0.2 μg each) with an expression plasmid for wild-type HPIV3-HN (HN) or codon optimized HPIV3-HN (CO), or doubly transfected with wild-type HPIV3-F and wild-type HPIV3-HN (HN+F) or codon-optimized HPIV3-HN (CO+F), or infected with wild-type (WT) HPIV3 virus at an MOI of 1. (B) Hela cells (20,000) were singly transfected (0.2 μg each) with an expression plasmid for wild-type HPIV3-F (F) or doubly transfected with wild-type HPIV3-F and wild-type HPIV3-HN (F+HN) or codon-optimized HPIV3-HN (F+CO), or infected with wild-type (WT) HPIV3 virus at an MOI of 1. Two days later, the cells were washed, fixed (2% paraformaldehyde), blocked (PBS/sera), and sequentially immunostained with a mouse monoclonal antibody against (A) HPIV3-HN (66/4) or (B) HPIV3-F (215), and an HRP-conjugated anti-mouse secondary antibody. The stained cells were developed with a solution of OPD, the optical density at 490 nm was measured using an absorbance plate reader, and the nonspecific background at 650nm was subtracted. Values for each point are the mean of at least triplicate wells. Statistically significant differences ($p<0.05$) from cells singly transfected with an expression plasmid for wild-type HN or F are denoted with an asterisk.

that had been previously concentrated 10-fold, separated the immunoprecipitated proteins by gel electrophoresis, dried the gel, and visualized the labeled proteins by autoradiography (Figure 3.6A). We found that codon optimization increased the amount of HN incorporated into lentiviral particles, as well as increased expression in producer cells.   To quantify the amount of HN in each sample, we excised the bands that contained HN from the gel and measured their radioactivity with a scintillation counter. We found that lentivirus particles produced using codon optimized HN contained 2.2-fold more HN than particles produced with the original expression plasmid, and virus producer cells transfected with codon optimized HN expressed 1.7-fold more HN than cells transfected with the original expression plasmid.

We next determined whether codon optimization of HPIV3-HN increased titers of pseudotyped lentiviruses. Titers of the viruses made with the codon optimized HN were 1.2 to 6.4-fold higher than those made with the original HN, but were still more than 100-fold lower than lentiviruses pseudotyped with the amphotropic envelope protein (Table 3.2). These findings prompted us to determine if the HPIV3-pseudotyped lentiviruses contained fewer envelope proteins per virus particle than the amphotropic-pseudotyped viruses. We transfected 293T/17 cells with plasmids encoding β-galactosidase, Gag-Pol, and the amphotropic envelope protein only, HPIV3-F only, codon optimized HPIV3-HN only, HPIV3-F and codon optimized HPIV3-HN, or no envelope protein. Next, we metabolically labeled the cells for 16 hours, concentrated the supernatant by ultracentrifugation through a 20% sucrose cushion, separated the proteins by size using SDS-PAGE, and then visualized the gel by autoradiography.   Using image analysis software (ImageJ), we found that amphotropic-pseudotyped lentiviruses contained 14-fold more envelope proteins (Figure 3.6B, lane 3) than lentiviruses pseudotyped with HPIV3 F and codon-optimized HN (Figure 3.6B, lane 6) even though ample amounts of

Table 3.2. Lentivirus titers.

Target Cells	HN+F LV (cfu/mL)[a]	CO-HN+F LV (cfu/mL)[a]	Ampho LV (cfu/mL)[a]	WT HPIV3 (pfu/mL)[b]
293T	$3.5\ (\pm 0.43)\times 10^2$	$2.3\ (\pm 0.12)\times 10^3$	$2.4\ (\pm 0.29)\times 10^5$	$2.9\ (\pm 0.21)\times 10^5$
Hela	$1.1\ (\pm 0.14)\times 10^2$	$2.0\ (\pm 0.10)\times 10^2$	$8.2\ (\pm 0.87)\times 10^3$	$3.5\ (\pm 0.29)\times 10^5$
MDCK	$9.3\ (\pm 0.15)\times 10^1$	$4.3\ (\pm 1.2)\times 10^2$	$5.4\ (\pm 1.0)\times 10^4$	$2.6\ (\pm .05)\times 10^4$
Vero	$5.2\ (\pm 0.03)\times 10^1$	$3.3\ (\pm 0.87)\times 10^2$	$6.5\ (\pm 1.1)\times 10^2$	$1.2\ (\pm 0.10)\times 10^6$
A549	$2.0\ (\pm 0.15)\times 10^2$	$1.9\ (\pm 0.50)\times 10^3$	$7.0\ (\pm 1.7)\times 10^3$	$4.8\ (\pm 0.35)\times 10^5$
3T3	$4.6\ (\pm 1.1)\times 10^0$	$5.3\ (\pm 1.2)\times 10^0$	$2.5\ (\pm 0.09)\times 10^5$	$8.5\ (\pm 0.29)\times 10^2$

Lentiviruses pseudotyped with wild-type HN and F (HN+F LV), codon optimized HN and wild-type F (CO-HN+F LV), or amphotropic Env (Ampho LV), and wild-type HPIV3 (WT HPIV3) were used to transduce target cells. Titer of [a]lentiviral pseudotypes (cfu/mL) and [b]wild-type HPIV3 (pfu/mL) represent the mean of experimental values +/- one standard deviation.
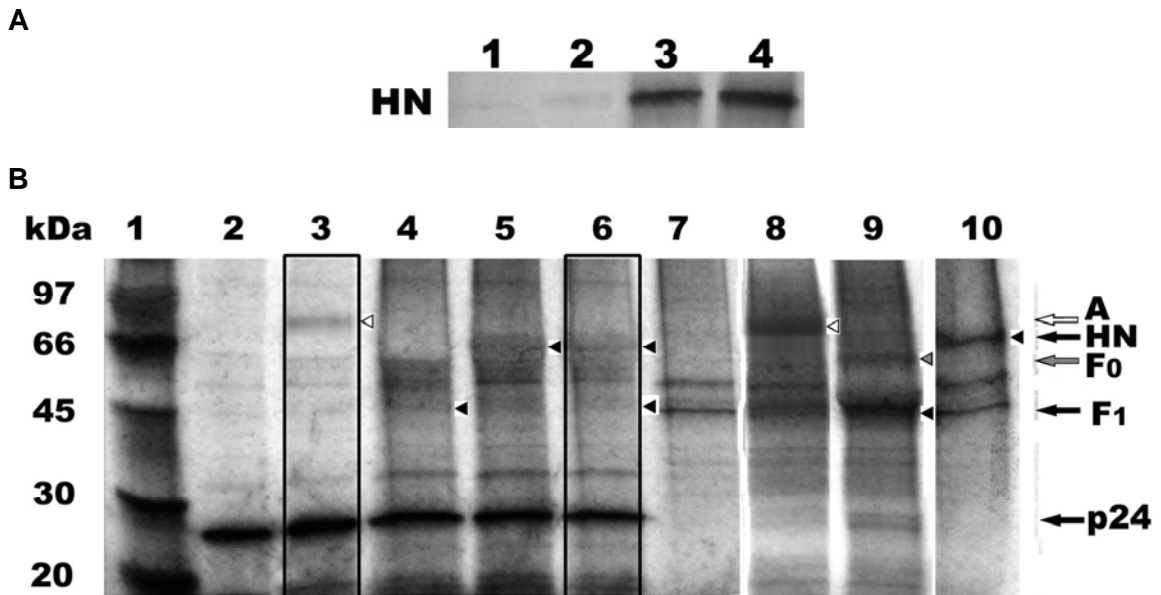
Figure 3.6. The number of envelope proteins incorporated by HPIV3/LV is higher when they are generated by virus producer cells transfected with codon-optimized HN than when they are generated by virus producer cells transfected with non codon-optimized HN, but several-fold lower than in amphotropic lentiviruses. 293T/17 cells (1×10^7) were transfected with expression plasmids (6 μg each) for β-galactosidase, HIV-1 Gag-Pol, and (A) HPIV3-F, and either HPIV3-HN (lanes 1 and 3) or codon-optimized HPIV3-HN (lanes 2 and 4), or (B) the amphotropic envelope protein only (lanes 3 and 8), HPIV3-F only (lane 4), codon-optimized HPIV3-HN only (lane 5), or both HPIV3-F and codon-optimized HPIV3-HN (lanes 6, 9, 10), or no envelope protein as a negative control (lanes 2 and 7). The next day, the cells were serum-starved for 15 minutes, metabolically-labeled with 450 μCi [35S] methionine and cysteine for 12-16 hours, after which the cells were lysed and the culture medium supernatants collected, ultracentrifuged through a 20% sucrose cushion, and then resuspended in PBS to (A) 10-fold or (B) 100-fold their original concentration. (A) The cell culture supernatants (lanes 1 and 2) and cell lysates (lanes 3 and 4) were immunoprecipitated with a guinea pig polyclonal antibody against HPIV3-HN. (B) The cell lysates were immunoprecipitated with anti-gp70 (83A25; lane 8), anti-HPIV3-F (c110; lane 9), or anti-HPIV3-HN (66/4; lane 10) monoclonal antibodies. The amount of virus in the cell culture supernatants (lanes 2-6) was quantified by an ELISA for p24 and used to ensure equal loading of the samples. All of the samples were resuspended in lysis buffer, separated by size by SDS-PAGE, and then the gel dried and visualized by autoradiography.

HN and F were expressed (Figure 3.6B, lanes 9 and 10). These results suggest that lentiviruses inefficiently incorporate HN and F envelope proteins.

Finally, we wanted to determine if lentiviruses produced using the expression plasmid for codon optimized HN infected polarized epithelial cells more efficiently than lentiviruses produced using the expression plasmid for wild-type HN. MDCK cells were plated in tissue culture-treated Transwell polyester supports and transduced them from the apical or basolateral surface with lentiviruses that were pseudotyped with HPIV3-F and HPIV3-HN or HPIV3-CO-HN, or with the amphotropic envelope protein as a control. Two days later we used flow cytometry for GFP expression to quantify the number of transduced cells (Figure 3.7). We found that lentiviruses produced by cells transfected with codon optimized HN transduced 1.4-fold more polarized MDCK cells than lentiviruses produced by cells transfected with wild-type HN. Codon optimized HN-containing pseudotyped lentivirus also transduced 1.9-fold more cells than amphotropic pseudotyped lentivirus, even though their titer on dividing non-polarized MDCK cells was 100-fold lower. This is consistent with previous observations that amphotropic pseudotyped lentiviruses preferentially transduce polarized cells via their basolateral surface [29], whereas HPIV3 preferentially transduces polarized cells via their apical surfaces [30]. We also examined the effect of depolarization of the cells on transduction by incubating the cells with medium that contained EDTA. Consistent with other studies, we found that amphotropic lentivirus transduction increased 3-fold when the cells were depolarized [29, 31].

Interestingly, depolarization of the cells reduced HPIV3-lentivirus transduction by 1.3-fold. Perhaps this is because the cellular receptors for HPIV3, which are predominantly expressed in the apical membrane of polarized MDCK cells [32], redistribute throughout the entire plasma membrane when the cells are depolarized,
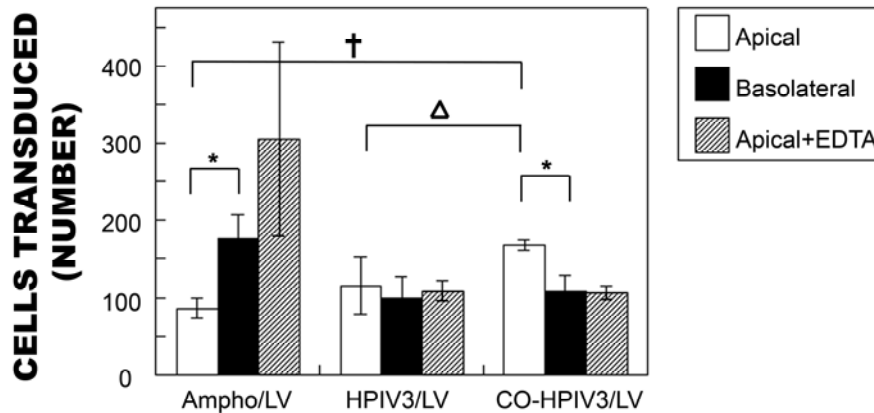
Figure 3.7. HPIV3 pseudotyped lentiviruses produced by cells transfected with codon-optimized HN transduce polarized MDCK cells more efficiently than amphotropic lentiviruses or HPIV3 pseudotyped lentiviruses produced by cells transfected with non codon-optimized HN. eGFP encoding lentiviruses (100 μL) pseudotyped with the amphotropic Env, HPIV3 F + codon-optimized HPIV3 HN, or HPIV3 F + non-codon-optimized HPIV3 HN were brought to 8 μg/mL Polybrene and applied to the apical (white bars) or basolateral (black bars) surfaces of polarized MDCK cells. As a control, cells were depolarized with 6 mM EDTA in HEPES (10 mM) for 30 min prior to and during apical transduction (grey bars). Two hours later, the cells were washed with medium to remove any unbound viruses, and cultured for 2 days at 37^0C, after which flow cytometry was used to determine the number of cells that expressed eGFP. Values are from three different experiments. Statistically significant differences ($p<0.05$) in transduction efficiencies when the cells were transduced 1) via their apical and basolateral surfaces, 2) with viruses pseudotyped with non codon-optimized or codon-optimized HN, and 3) with viruses pseudotyped with the amphotropic Env or with codon optimized HN are denoted with *, Δ, and † respectively.

Table 3.3. Number of polarized HBE cells transduced by virus.

Virus	Apical	Basolateral	Apical + EDTA
None	117	1121	107
Ampho/LV	142	3847	1055
CO-HPIV3/LV	161	4393	174
HPIV3/LV	107	1753	174

Flow cytometric analysis was used to determine the number of polarized HBE cells that were transduced with pseudotyped lentiviruses. eGFP encoding lentiviruses (100 μL) pseudotyped with the amphotropic Env, HPIV3 F + codon-optimized HPIV3 HN, or HPIV3 F + non-codon-optimized HPIV3 HN were brought to 8 μg/mL Polybrene and applied to the apical or basolateral surfaces of polarized HBE cells. As a control, cells were depolarized with 6 mM EDTA in HEPES (10 mM) for 30 min prior to and during apical transduction. Four hours later, the cells were washed with medium to remove any unbound viruses, and cultured for 2 days at 37^0C, after which flow cytometry was used to determine the number of cells that expressed eGFP. Values are a representative of three different experiments.

reducing the concentration of receptors that are available for HPIV3-lentivirus transduction.

We also wanted to determine if lentiviruses produced using the expression plasmid for codon optimized HN infected polarized lung cells more efficiently than lentiviruses produced using the expression plasmid for wild-type HN. HBE cells were plated in tissue culture-treated Transwell polyester supports and transduced from the apical or basolateral surface with lentiviruses that were pseudotyped with HPIV3-F and HPIV3-HN or HPIV3-CO-HN, or with the amphotropic envelope protein as a control. Two days later we used flow cytometry for GFP expression to quantify the number of transduced cells (Table 3.3). We found that lentiviruses produced by cells transfected with codon optimized HN transduced 1.5-fold more polarized HBE cells from the apical surface than lentiviruses produced by cells transfected with wild-type HN. Codon

optimized HN-containing pseudotyped lentivirus also transduced 1.1-fold more cells apically than amphotropic pseudotyped lentivirus.

3.5 Discussion

We have previously shown that it is possible to pseudotype lentiviruses with HPIV3 envelope proteins and that these viruses are able to transduce polarized cells via their apical surfaces, but the titers of these viruses are too low to be useful for clinical gene transfer. We hypothesized that titers were low because the virus producer cells released too few particles, cellular expression of the HPIV3 envelope proteins (HN and F) was low, or too few HPIV3 envelope proteins were incorporated by the lentiviruses. To test this hypothesis, we compared the amount of virus capsid protein in stocks of HPIV3 pseudotyped viruses and high titer amphotropic lentiviruses. We also examined the expression levels of HN and F mRNA in the nucleus and cytoplasm of transfected virus producer cells, and compared them to expression levels in cells infected with replication competent wild-type HPIV3. Finally, we metabolically labeled cells that were producing HPIV3 and amphotropic pseudotyped lentiviruses, and compared the numbers of envelope proteins that were incorporated into the two types of viruses. We found that stocks of HPIV3 pseudotyped viruses contained similar numbers of viruses as stocks of high titer amphotropic lentiviruses. We also found that transfected virus producer cells expressed similar levels of HN and F mRNA as cells infected with wild-type HPIV3, but fewer cell-surface HN and F proteins (3.8 and 1.3-fold less, respectively). Fortunately, codon-optimization of HPIV3 HN increased expression more than 2-fold in cells co-transfected with HPIV3 F and HN. Most significant, we found that even when virus producer cells were transfected with codon-optimized HPIV3 HN, HPIV3 pseudotyped lentiviruses incorporated nearly 14-fold fewer envelope proteins than amphotropic pseudotyped lentiviruses. Lysates of the two sets of producer cells

contained similar amounts of HPIV3 and amphotropic envelope proteins, which, coupled with our mRNA expression data, suggest that the number of envelope proteins in HPIV3-pseudotyped viruses is low not because these proteins are poorly expressed, but because they are not efficiently incorporated by lentivirus particles.

Our observation that titers increased more than 6-fold when the number of HPIV3 HN per particle increased about 2-fold is consistent with our conclusion that these viruses contain a low number of envelope proteins (Env). This is because previous work has shown that increasing the number of Env per retrovirus raises titers, but only when the number of Env per particle is below a relatively small threshold number, above which further increases do not improve titers [33-37]. This suggests that the number of Env per HPIV3 pseudotyped virus is below the threshold number, and that titers can be significantly improved with further increases in the number of HPIV3 Env per particle.

One straightforward strategy to increase the number of Env per particle is to enhance their expression in virus producer cells. In this study, we increased HPIV3 HN expression by codon-optimizing its sequence. Interestingly, codon-optimization increased HPIV3 HN expression only in cells that also expressed HPIV3 F. Also, the cell-surface expression of HPIV3 F was higher in cells that co-expressed codon-optimized HPIV3 HN than in cells that co-expressed wild-type HPIV3 HN. These observations suggest that HPIV3 F and HN may interact within the cell such that an increase in the expression level of one may promote higher levels of cell-surface expression of the other. Previous work supports the possibility that HPIV F and HN interact intracellularly. For example, Hu et al showed that the HPIV type 2 and 3 F proteins do not cause fusion unless they are co-expressed with HN from the same type of human parainfluenza virus [38]. Furthermore, Tong et al found that mutant forms of HPIV F proteins, engineered to contain a C-terminal signal for retention in the endoplasmic reticulum, inhibited cell fusion by blocking the transport of HPIV2 HN to the

66

cell surface (when HPIV2 F-KDEL was used) or by reducing its steady-state intracellular expression (when HPIV3 F-KDEL was used) [39].

These studies suggest that HPIV3 F and HN interact intracellularly, but we can only speculate how, in virus producer cells, an increase in the expression of one of these proteins would result in an increase in the cell-surface expression of the other. Perhaps F and HN influence each other's intracellular trafficking dynamics such that, when the expression of either protein is increased, a higher proportion of the proteins are part of a heterodimer of the two proteins, which may increase the likelihood that they will localize to, or be retained at, the cell surface. Previous work with other proteins has shown that protein-protein interactions and heterodimerization can significantly affect their subcellular trafficking and localization. For example, the feline herpesvirus glycoprotein E must form a heterodimer with glycoprotein I to be efficiently transported out of the endoplasmic reticulum (ER) [40]. Similarly, the alphavirus E1 protein must form a complex with p62, the precursor of the E2 protein, to efficiently translocate from the ER [41]. Sandrin et al showed murine leukemia virus core proteins interact with envelope glycoproteins, causing them to relocalize to late endosomes [42]. Protein-protein interactions appear to significantly alter the trafficking and subcellular localization of non-viral proteins as well. For example, certain G-protein coupled receptors (GPCR) require heterodimerization for proper surface expression, and their trafficking and internalization is sometimes dramatically altered when they associate with other GPCR subtypes [43, 44]. We do not know if processes similar to these affect HPIV3 F and HN trafficking. Additional work is needed to characterize the intracellular trafficking itineraries of HPIV3 F and HN in virus producer cells, and to determine to what extent they interact with each other, and how these interactions affect their subcellular localization and incorporation into virus particles.

We found that codon-optimized HPIV3 HN is expressed in virus producer cells to similar levels as wild-type HPIV3 HN is expressed in cells infected by replication competent HPIV3. Nevertheless, HPIV3 pseudotyped viruses contain about 14-fold fewer Env than high-titer amphotropic pseudotyped viruses. This suggests that the major factor limiting the titer of HPIV3 pseudotyped viruses is not the expression levels of the HPIV3 Env, but the low efficiency with which they are incorporated by lentiviruses. Recent work has shown that whether or not a protein is incorporated into a lentivirus particle is primarily dictated by whether or not the protein is colocalized with the virus when it buds from the cell [42, 45, 46]. Most proteins that are incorporated by lentiviruses are incorporated through a passive process in which they fortuitously localize to the same site within the cell that lentiviruses bud from [47-49]. We do not know if HPIV3 Env colocalize with budding lentiviruses, but previous work suggests that HPIV3 Env and lentiviruses do not share a common intracellular trafficking pathway. For example, in polarized cells HN and F are preferentially trafficked towards the apical surface from which HPIV3 buds [50], whereas lentivirus capsid proteins (i.e., Gag) are preferentially directed to the basolateral surface from which lentiviruses bud [51]. In nonpolarized cells, recent work suggests that lentiviruses bud from intracellular compartments such as multivesicular bodies and recycling endosomes [52-55] while the same has not been shown for HPIV3 and other paramyxoviruses.

Alternatively, some proteins are incorporated into lentiviruses by an active process that involves specific interactions between the lentivirus protein capsid proteins and the cytoplasmic tails of envelope glycoproteins [45, 56-58]. For example, the HIV-1 glycoprotein gp41 contains an alpha helical motif that appears to interact with and stabilize lattice-like holes in the lipid bilayer that are formed by the oligomerization of HIV-1 matrix proteins during virus assembly and budding [59-61]. Interestingly, even some viral envelope proteins that are not derived from HIV-1, such as MuLV and RD114,

appear to be actively recruited to the sites of lentivirus assembly [45]. These retroviral envelope proteins are normally distributed primarily within the ER, but were found to relocate to the late endosomes in cells that expressed the lentiviral accessory protein Nef. Given that HPIV3 is a different family of virus than HIV-1, and given that HPIV3 HN is a type II protein whereas HIV-1 Env is a type I protein, it is unlikely that HPIV3 Env, and HPIV3 HN in particular, contain amino acid motifs that actively interact with lentivirus proteins.

One strategy to significantly increase the titers of HPIV3 pseudotyped viruses may be to modify their Env to passively or actively colocalize with budding lentiviruses. Some approaches have already been employed to promote the active or passive colocalization of other glycoproteins with lentiviral proteins. For example, Kowolik et al showed that appending the cytoplasmic tail of HIV-1 Env to the Sendai virus F protein increases it incorporation into lentivirus particles, presumably by inducing the F protein to actively interact with lentivirus proteins [62]. Similarly, Kobayashi et al. [17] successfully pseudotyped SIV particles with Sendai virus HN and F envelope proteins by truncating the cytoplasmic tail of F and by appending the cytoplasmic tail of SIV Env to HN. Unfortunately, the mechanism by which these alterations led to improved pseudotype formation was not investigated, although presumably these modifications increased the passive incorporation of F and the active incorporation of HN.

These studies suggest that it may be possible to significantly improve the titers of HPIV3 pseudotyed viruses by modifying their cytoplasmic tails to include amino acid motifs that cause them to colocalize to sites of lentivirus budding. It is important to note that colocalization is necessary, but not always sufficient, for proteins to be incorporated by lentiviruses. In some cases, proteins appear to be actively excluded from lentivirus particles, even though they colocalize with them [47, 48, 63, 64]. Steric hindrance between the cytoplasmic tail of these proteins and the capsids of the budding virus

particles is one likely mechanism by which proteins are actively excluded from lentiviruses [65]. Although we can not rule out the possibility that HPIV3 Env are actively excluded from lentiviruses, it seems unlikely that steric hindrance plays a role since both HPIV3 HN and F have short cytoplasmic domains (31 and 23 amino acids, respectively [66, 67]), and envelope proteins with naturally short cytoplasmic tails such as MuLV Env, and envelope proteins from HIV-2 and SIV with long cytoplasmic tails that have been truncated, have been shown to be efficiently incorporated into lentiviral particles [68, 69].

In conclusion, our results suggest that the titers of HPIV3 pseudotyped lentiviruses are low because HPIV3 envelope proteins are not efficiently incorporated by lentivirus particles. Future work should focus on characterizing the intracellular trafficking itineraries of HN and F, determining to what extent HN and F interact within the cells and thereby influence each others subcellular localization and expression, and engineering HN and F to be more efficiently incorporated by lentiviruses by promoting their passive or active colocalization at intracellular sites of lentivirus budding.

3.6 <u>References</u>

1.   Anderson, W.F., *Human gene therapy.* Nature, 1998. 392(6679 Suppl): p. 25-30.

2.   Sinn, P.L., S.L. Sauter, and P.B. McCray, Jr., *Gene therapy progress and prospects: development of improved lentiviral and retroviral vectors--design, biosafety, and production.* Gene Ther, 2005. 12(14): p. 1089-98.

3.   Naldini, L., et al., *In vivo gene delivery and stable transduction of nondividing cells by a lentiviral vector.* Science, 1996. 272(5259): p. 263-7.

4.   Lavillette, D., S.J. Russell, and F.L. Cosset, *Retargeting gene delivery using surface-engineered retroviral vector particles.* Curr Opin Biotechnol, 2001. 12(5): p. 461-6.

5.   Yi, Y., S.H. Hahm, and K.H. Lee, *Retroviral gene therapy: safety issues and possible solutions.* Curr Gene Ther, 2005. 5(1): p. 25-35.

6.   De Larco, J.E., U.R. Rapp, and G.J. Todaro, *Cell surface receptors for ecotropic MuLV: detection and tissue distributions of free receptors in vivo.* Int J Cancer, 1978. 21(3): p. 356-60.

7.   Kavanaugh, M.P., et al., *Cell-surface receptors for gibbon ape leukemia virus and amphotropic murine retrovirus are inducible sodium-dependent phosphate symporters.* Proc Natl Acad Sci U S A, 1994. 91(15): p. 7071-5.

8.   Chen, S.T., et al., *Generation of packaging cell lines for pseudotyped retroviral vectors of the G protein of vesicular stomatitis virus by using a modified tetracycline inducible system.* Proc Natl Acad Sci U S A, 1996. 93(19): p. 10057-62.

9.   Johnson, L.G., et al., *Pseudotyped human lentiviral vector-mediated gene transfer to airway epithelia in vivo.* Gene Ther, 2000. 7(7): p. 568-74.

10.   Wang, G., P.L. Sinn, and P.B. McCray, Jr., *Development of retroviral vectors for gene transfer to airway epithelia.* Curr Opin Mol Ther, 2000. 2(5): p. 497-506.

11.   Copreni, E., et al., *Lentivirus-mediated gene transfer to the respiratory epithelium: a promising approach to gene therapy of cystic fibrosis.* Gene Ther, 2004. 11 Suppl 1: p. S67-75.

12.   Kobinger, G.P., et al., *Filovirus-pseudotyped lentiviral vector can efficiently and stably transduce airway epithelia in vivo.* Nat Biotechnol, 2001. 19(3): p. 225-30.

13.   Sinn, P.L., et al., *Persistent gene expression in mouse nasal epithelia following feline immunodeficiency virus-based vector gene transfer.* J Virol, 2005. 79(20): p. 12818-27.

14.   Kang, Y., et al., *In vivo gene transfer using a nonprimate lentiviral vector pseudotyped with Ross River Virus glycoproteins.* J Virol, 2002. 76(18): p. 9378-88.

15.   Sinn, P.L., et al., *Gene transfer to respiratory epithelia with lentivirus pseudotyped with Jaagsiekte sheep retrovirus envelope glycoprotein.* Hum Gene Ther, 2005. 16(4): p. 479-88.

16.   Liu, S.L., C.L. Halbert, and A.D. Miller, *Jaagsiekte sheep retrovirus envelope efficiently pseudotypes human immunodeficiency virus type 1-based lentiviral vectors.* J Virol, 2004. 78(5): p. 2642-7.

17.   Kobayashi, M., et al., *Pseudotyped lentivirus vectors derived from simian immunodeficiency virus SIVagm with envelope glycoproteins from paramyxovirus.* J Virol, 2003. 77(4): p. 2607-14.

18.   Medina, M.F., et al., *Lentiviral vectors pseudotyped with minimal filovirus envelopes increased gene transfer in murine lung.* Mol Ther, 2003. 8(5): p. 777-89.

19.   Ferrari, S., et al., *A defective nontransmissible recombinant Sendai virus mediates efficient gene transfer to airway epithelium in vivo.* Gene Ther, 2004. 11(22): p. 1659-64.

20. Zhang, L., et al., *Infection of ciliated cells by human parainfluenza virus type 3 in an in vitro model of human airway epithelium.* J Virol, 2005. 79(2): p. 1113-24.

21. Radosevich, M. and S.J. Ono, *MHC class II gene expression is not induced in HPIV3-infected respiratory epithelial cells.* Immunol Res, 2004. 30(2): p. 125-38.

22. Chanock, R.M., B.R. Murphy, and P.L. Collins, *Parainfluenza viruses*, in *Fields Virology, 4th ed.*, D.M. Knipe, et al., Editors. 2001, Lippincott-Raven Publishers: Philadelphia.

23. Jung, C., et al., *Lentiviral vectors pseudotyped with envelope glycoproteins derived from human parainfluenza virus type 3.* Biotechnol Prog, 2004. 20(6): p. 1810-6.

24. Evans, L.H., et al., *A neutralizable epitope common to the envelope glycoproteins of ecotropic, polytropic, xenotropic, and amphotropic murine leukemia viruses.* J Virol, 1990. 64(12): p. 6176-83.

25. Harlow, E. and D. Lane, *Storing and Purifying Antibodies*, in *Antibodies: A Laboratory Manual*. 1988, Cold Spring Harbor Laboratory Press: Cold Spring Harbor. p. 288-303.

26. Zufferey, R., et al., *Multiply attenuated lentiviral vector achieves efficient gene delivery in vivo.* Nat Biotechnol, 1997. 15(9): p. 871-5.

27. Cosset, F.L., et al., *High-titer packaging cells producing recombinant retroviruses resistant to human serum.* J Virol, 1995. 69(12): p. 7430-6.

28. Niwa, H., K. Yamamura, and J. Miyazaki, *Efficient selection for high-expression transfectants with a novel eukaryotic vector.* Gene, 1991. 108(2): p. 193-99.

29. Wang, G., et al., *Influence of cell polarity on retrovirus-mediated gene transfer to differentiated human airway epithelia.* J Virol, 1998. 72(12): p. 9818-26.

30. Collins, P.L., R.M. Chanock, and K. McIntosh, *Parainfluenza viruses*, in *Fields Virology*, B.N. Fields, et al., Editors. 1996, Lippincott-Raven Publishers: Philadelphia. p. 1205-1243.

31. Wang, G., et al., *Increasing epithelial junction permeability enhances gene transfer to airway epithelia In vivo.* Am J Respir Cell Mol Biol, 2000. 22(2): p. 129-38.

32. Ulloa, F. and F.X. Real, *Differential distribution of sialic acid in alpha2,3 and alpha2,6 linkages in the apical membrane of cultured epithelial cells and tissues.* J Histochem Cytochem, 2001. 49(4): p. 501-10.

33. Sinn, P.L., et al., *Inclusion of Jaagsiekte sheep retrovirus proviral elements markedly increases lentivirus vector pseudotyping efficiency.* Mol Ther, 2005. 11(3): p. 460-9.

34.   Yuste, E., et al., *Virion envelope content, infectivity, and neutralization sensitivity of simian immunodeficiency virus.* J Virol, 2005. 79(19): p. 12455-63.

35.   Logan, A.C., et al., *Factors influencing the titer and infectivity of lentiviral vectors.* Hum Gene Ther, 2004. 15(10): p. 976-88.

36.   Bachrach, E., et al., *Effects of virion surface gp120 density on infection by HIV-1 and viral production by infected cells.* Virology, 2005. 332(1): p. 418-29.

37.   Yuste, E., et al., *Modulation of Env content in virions of simian immunodeficiency virus: correlation with cell surface expression and virion infectivity.* J Virol, 2004. 78(13): p. 6775-85.

38.   Hu, X.L., R. Ray, and R.W. Compans, *Functional interactions between the fusion protein and hemagglutinin-neuraminidase of human parainfluenza viruses.* J Virol, 1992. 66(3): p. 1528-34.

39.   Tong, S. and R.W. Compans, *Alternative mechanisms of interaction between homotypic and heterotypic parainfluenza virus HN and F proteins.* J Gen Virol, 1999. 80 (Pt 1): p. 107-15.

40.   Mijnes, J.D., et al., *Biosynthesis of glycoproteins E and I of feline herpesvirus: gE-gI interaction is required for intracellular transport.* J Virol, 1996. 70(8): p. 5466-75.

41.   Andersson, H., et al., *Oligomerization-dependent folding of the membrane fusion protein of Semliki Forest virus.* J Virol, 1997. 71(12): p. 9654-63.

42.   Sandrin, V., et al., *Intracellular trafficking of Gag and Env proteins and their interactions modulate pseudotyping of retroviruses.* J Virol, 2004. 78(13): p. 7153-64.

43.   Barki-Harrington, L., *Oligomerisation of angiotensin receptors: novel aspects in disease and drug therapy.* J Renin Angiotensin Aldosterone Syst, 2004. 5(2): p. 49-52.

44.   Prinster, S.C., C. Hague, and R.A. Hall, *Heterodimerization of g protein-coupled receptors: specificity and functional significance.* Pharmacol Rev, 2005. 57(3): p. 289-98.

45.   Sandrin, V. and F.L. Cosset, *Intracellular versus cell surface assembly of retroviral pseudotypes is determined by the cellular localization of the viral glycoprotein, its capacity to interact with Gag, and the expression of the Nef protein.* J Biol Chem, 2006. 281(1): p. 528-42.

46.   Pickl, W.F., F.X. Pimentel-Muinos, and B. Seed, *Lipid rafts and pseudotyping.* J Virol, 2001. 75(15): p. 7175-83.

47.   Hammarstedt, M. and H. Garoff, *Passive and active inclusion of host proteins in human immunodeficiency virus type 1 gag particles during budding at the plasma membrane.* J Virol, 2004. 78(11): p. 5686-97.

48.   Cantin, R., S. Methot, and M.J. Tremblay, *Plunder and stowaways: incorporation of cellular proteins by enveloped viruses.* J Virol, 2005. 79(11): p. 6577-87.

49.   Kolegraff, K., P. Bostik, and A.A. Ansari, *Characterization and role of lentivirus-associated host proteins.* Exp Biol Med (Maywood), 2006. 231(3): p. 252-63.

50.   Bose, S., A. Malur, and A.K. Banerjee, *Polarity of human parainfluenza virus type 3 infection in polarized human lung epithelial A549 cells: role of microfilament and microtubule.* J Virol, 2001. 75(4): p. 1984-9.

51.   Owens, R.J., et al., *Human immunodeficiency virus envelope protein determines the site of virus release in polarized epithelial cells.* Proc Natl Acad Sci U S A, 1991. 88(9): p. 3987-91.

52.   Orenstein, J.M., et al., *Cytoplasmic assembly and accumulation of human immunodeficiency virus types 1 and 2 in recombinant human colony-stimulating factor-1-treated human monocytes: an ultrastructural study.* J Virol, 1988. 62(8): p. 2578-86.

53.   Nguyen, D.G., et al., *Evidence that HIV budding in primary macrophages occurs through the exosome release pathway.* J Biol Chem, 2003. 278(52): p. 52347-54.

54.   Pelchen-Matthews, A., B. Kramer, and M. Marsh, *Infectious HIV-1 assembles in late endosomes in primary macrophages.* J Cell Biol, 2003. 162(3): p. 443-55.

55.   Nydegger, S., et al., *HIV-1 egress is gated through late endosomal membranes.* Traffic, 2003. 4(12): p. 902-10.

56.   Cosson, P., *Direct interaction between the envelope and matrix proteins of HIV-1.* Embo J, 1996. 15(21): p. 5783-8.

57.   Freed, E.O. and M.A. Martin, *Domains of the human immunodeficiency virus type 1 matrix and gp41 cytoplasmic tail required for envelope incorporation into virions.* J Virol, 1996. 70(1): p. 341-51.

58.   Yu, X., et al., *The matrix protein of human immunodeficiency virus type 1 is required for incorporation of viral envelope protein into mature virions.* J Virol, 1992. 66(8): p. 4966-71.

59.   Piller, S.C., et al., *Mutational analysis of conserved domains within the cytoplasmic tail of gp41 from human immunodeficiency virus type 1: effects on glycoprotein incorporation and infectivity.* J Virol, 2000. 74(24): p. 11717-23.

60.   Hourioux, C., et al., *Identification of the glycoprotein 41(TM) cytoplasmic tail domains of human immunodeficiency virus type 1 that interact with Pr55Gag particles.* AIDS Res Hum Retroviruses, 2000. 16(12): p. 1141-7.

61.   Murakami, T. and E.O. Freed, *Genetic evidence for an interaction between human immunodeficiency virus type 1 matrix and alpha-helix 2 of the gp41 cytoplasmic tail.* J Virol, 2000. 74(8): p. 3548-54.

62.   Kowolik, C.M. and J.K. Yee, *Preferential transduction of human hepatocytes with lentiviral vectors pseudotyped by Sendai virus F protein.* Mol Ther, 2002. 5(6): p. 762-9.

63.   Christodoulopoulos, I. and P.M. Cannon, *Sequences in the cytoplasmic tail of the gibbon ape leukemia virus envelope protein that prevent its incorporation into lentivirus vectors.* J Virol, 2001. 75(9): p. 4129-38.

64.   Lallos, L.B., et al., *Exclusion of HIV coreceptors CXCR4, CCR5, and CCR3 from the HIV envelope.* AIDS Res Hum Retroviruses, 1999. 15(10): p. 895-7.

65.   Henriksson, P., et al., *Incorporation of wild-type and C-terminally truncated human epidermal growth factor receptor into human immunodeficiency virus-like particles: insight into the processes governing glycoprotein incorporation into retroviral particles.* J Virol, 1999. 73(11): p. 9294-302.

66.   Elango, N., et al., *Human parainfluenza type 3 virus hemagglutinin-neuraminidase glycoprotein: nucleotide sequence of mRNA and limited amino acid sequence of the purified protein.* J Virol, 1986. 57(2): p. 481-9.

67.   Spriggs, M.K., et al., *Fusion glycoprotein of human parainfluenza virus type 3: nucleotide sequence of the gene, direct identification of the cleavage-activation site, and comparison with other paramyxoviruses.* Virology, 1986. 152(1): p. 241-51.

68.   Freed, E.O. and M.A. Martin, *Virion incorporation of envelope glycoproteins with long but not short cytoplasmic tails is blocked by specific, single amino acid substitutions in the human immunodeficiency virus type 1 matrix.* J Virol, 1995. 69(3): p. 1984-9.

69.   Zingler, K. and D.R. Littman, *Truncation of the cytoplasmic domain of the simian immunodeficiency virus envelope glycoprotein increases env incorporation into particles and fusogenicity and infectivity.* J Virol, 1993. 67(5): p. 2824-31.

CHAPTER 4

PROTEIN COLOCALIZATION WITH LENTIVIRUS-ASSOCIATED RAFTS ENABLE INCORPORATION INTO LENTIVIRAL PARTICLES

4.1 <u>Abstract</u>

Lipid rafts have been shown to be important for proper lentivirus assembly and budding. We hypothesized that lipid rafts compartmentalize host cell raft proteins, and protein incorporation into the lentiviral lipid bilayer is dependent upon colocalization with lentivirus-associated rafts. To test this hypothesis, we studied the ability of two glycosylphosphatidylinositol (GPI) anchored proteins, folate receptor (FR-WT) and Tac-CD16 (the interleukin-2 receptor alpha chain fused with the cytoplasmic domain of the GPI-anchored CD16 protein) to associate with viral proteins, Gag and amphotropic Env, in lipid rafts and lentivirus particles. We examined the distribution of the GPI anchored proteins and virus proteins in whole cells, lipid rafts, and viral supernatant. We found that Tac-CD16 and FR-WT exhibited the classic GPI anchored protein property of associating with lipid rafts, however Tac-CD16 colocalized with Gag and incorporated into lentiviral particles, while FR-WT did not colocalize with Gag and was not incorporated into virus particles. In raft fractions separated by a linear sucrose gradient, FR-WT generally colocalized to less dense rafts while Gag and Env were localized to more dense rafts. Tac-CD16 was also located to less dense rafts, but had a wider distribution in the linear gradient than FR-WT. Most significantly, we found that when we treated producer cells with fumonisin B1 (FB1) or methyl-beta-cyclodextrin (MβCD), the amount of colocalization between FR-WT and Gag increased, FR-WT had a wider distribution in the linear raft gradient, and FR-WT was incorporated 2.9 to 11.6-fold more into lentiviral particles, respectively. In contrast, the raft distribution of Tac-CD16 in a

linear gradient decreased and the amount of Tac-CD16 in virus particles decreased 2.4-fold with MβCD treatment. Taken together, these results demonstrated lipid rafts segregate raft proteins, and for a protein to be incorporated into virus particles, it must be colocalized with lentivirus-associated rafts.

4.2 Introduction

Lipid rafts are structured cell membrane subdomains enriched in cholesterol, sphingolipids, and glycosphingolipids [1]. Also known as detergent resistant membranes or detergent insoluble glycolipid enriched membrane domains, rafts are defined biochemically as membrane regions that are insoluble in cold nonionic detergent and are often isolated by flotation through a sucrose gradient [2, 3]. Lipid rafts are dynamic and enriched with glycosylphosphatidylinositol (GPI) anchored proteins [4], doubly acylated proteins [5], and palmitoylated transmembrane proteins [6]. Though the existence of lipid rafts is somewhat controversial in literature [7, 8], their association with particular membrane proteins strongly suggests that lipid rafts have physiological functions such as serving as exclusive platforms for protein and lipid signaling and sorting [9, 10]. Signaling examples include IgE [11], T-cell receptor [12], and integrin signaling [13], and sorting examples include trafficking of proteins through the endoplasmic reticulum [10], Golgi complex [14], vesicles [15], and cell membrane [16]. Rafts have also been implicated as assembly and budding sites for enveloped viruses [17] and proteins from viruses such as human immunodeficiency virus type 1 (HIV-1) [18], influenza [19], Ebola [20], and measles [21] have been shown to associate with rafts.

Much evidence for rafts as sites of HIV assembly exists. The lipid composition of HIV, distinct from that of the host cell, is enriched in cholesterol and sphingolipids [22]. Gag proteins are localized to punctate regions in the plasma membrane instead of being evenly distributed [23]. The matrix protein from Gag, and gp41, the transmembrane

portion of the envelope protein, are both targeted to lipid rafts in the membrane [24, 25]. Assembly and budding is driven by the oligomerization of Gag [26], and depletion of cholesterol from the cell membrane not only causes raft deformities, HIV budding and infectivity is reduced [27-29].

Generally, when HIV buds from the host cell, it incorporates host cell raft molecules such as GM1, and GPI anchored proteins such as Thy-1 and CD59, and does not incorporate host cell proteins excluded from rafts such as CD45 [30, 31]. The ability of HIV to incorporate non-HIV proteins into its lipid bilayer is often exploited for the generation of pseudotyped viruses for targeted gene therapy [32], the generation of decorated viruses in order to enhance virus transduction [33, 34], or the generation of viruses to stimulate the immune system for vaccines [35, 36]. For example, lentiviruses have been pseudotyped with envelope proteins from VSV-G and amphotropic murine leukemia virus [37, 38] and have incorporated proteins such as cell adhesion molecules [34, 39, 40] and cytokines [41, 42]. However it is often challenging to modify the virus surface with a specific protein. In the case of targeting lentiviruses to polarized lung epithelial cells, envelope proteins from influenza, respiratory syncytial virus, baculovirus, and Sendai virus have failed to form pseudotypes with lentiviruses [43]. A clear understanding of how proteins are incorporated into lentiviruses would not only enable a better understanding of lentiviral assembly, it would facilitate the surface modification of lentiviral particles.

There is increasing evidence pointing to distinct and separate populations of lipid rafts [44, 45]. In this study, we tested the hypothesis that lipid rafts compartmentalize host cell raft proteins, and protein incorporation into the lentiviral lipid bilayer is dependent upon colocalization with lentivirus-associated rafts. The implications of our findings for understanding the assembly of lentivirus particles and the generation of surface-modified lentiviruses useful for therapeutic purposes are discussed.

78

4.3 <u>Materials and Methods</u>

Chemicals and antibodies. Poly-L-lysine, o-phenylenediamine dihydrochloride (OPD), saponin, Brij 98, methyl-β-cyclodextrin, gluteraldehyde, paraformaldehyde, and 5-Bromo-4-chloro-3-indolyl-*β*-D-galactopyranoside (X-Gal) were purchased from Sigma Chemical (St. Louis, MO). Hydrogen peroxide 30%, Triton X-100, and polyoxyethylene 20-sorbitan monolaurate (Tween 20) were purchased from Fisher Scientific (Fair Lawn, NJ). Complete mini protease inhibitor cocktail tablets were purchased from Roche Diagnostics (Indianapolis, IN). Coomassie Plus-200 protein assay reagent was purchased from Pierce (Rockford, IL). Nonfat dry milk (blotting grade) was purchased from Bio-Rad Laboratories (Hercules, CA). Fumonisin B1 was purchased from Biomol International, LP (Plymouth Meeting, PA).

HIV-1 p24 gag mouse ascites monoclonal antibody #24-3 (from Dr. Michael H. Malim), HIV-1 p24 mouse monoclonal antibody 183-H12-5C (from Dr. Bruce Chesebro and Kathy Wehrly), and sheep antiserum to HIV-1 p24 (from Dr. Michael Phelan) were obtained through the AIDS Research and Reference Reagent Program, Division of AIDS, NIAID, NIH. Goat polyclonal antibody to HIV-1 p24 was purchased from Advanced Biotechnologies Incorporated (Columbia, MD). Rabbit polyclonal antibody against IL-2Rα was purchased from Santa Cruz Biotechnology, Inc (Santa Cruz, CA). Rabbit anti-folate receptor antisera was a kind gift from V.L. Stevens (Emory University School of Medicine, Atlanta, GA) [46]. Goat polyclonal anti-gp70 (79S834) was purchased from Quality Biotech (Camden, NJ). Mouse anti-gp70 antibodies were purified from the supernatant of the 83A25 hybridoma cell line [47] and mouse anti-Tac antibodies were purified from the supernatant of the 7G7 hybridoma cell line [48] following standard procedures [49]. Cy2-conjugated, Cy-3 conjugated, and horseradish

peroxidase (HRP)-conjugated antibodies, and normal donkey serum were purchased from Jackson Immunoresearch Laboratories, Inc. (West Grove, PA).

Cell culture. 293T/17 cells were maintained in Dulbecco's modified essential medium (DMEM) supplemented with 10% heat inactivated fetal bovine serum (FBS), 100 U/mL of penicillin, and 100 μg/mL streptomycin (HyClone Laboratories; Logan, UT). Plates coated with poly-L-lysine were incubated for 5 min in the 0.01% solution (150-300 kDa), washed once with deionized water, and dried.

Virus production. Lentiviruses pseudotyped with the amphotropic Env alone or with either FR-WT or Tac-CD16 were produced by transfecting 293T/17 cells, seeded (1×10^7 per well) the previous day on poly-L-lysine coated plates with Lipofectamine 2000 (Invitrogen; Carlsbad, CA) and 6 μg of the packaging construct pCMVΔR8.91 [50], 6 μg of the lentivirus vector pTYEFnlacZ (AIDS Research and Reference Reagent Program; Bethesda, MD), and 6 μg of the amphotropic envelope protein expression plasmid pFB4070ASALF [51] alone or with either 6 μg of the Tac-CD16 expression plasmid (kind gift of Harish Radhakrishna (School of Biology, Georgia Institute of Technology, Atlanta, GA [52]) or the folate receptor-α (FR-WT) expression plasmid (kind gift of V.L. Stevens [46]). The following day, producer cells may have been treated with 0.5 mM MβCD or 50 μM FB1. Viral supernatants were collected every 12 h from 48 to 60 h after transfection, filter sterilized (0.45 μm), and frozen (-80°C) for later use. Viruses were clarified and concentrated by ultracentrifugation through a 20% sucrose cushion at 35,000 rpm for 2 hours at 4^0C in a SW41 rotor.

Indirect immunofluorescence. To detect the presence of Gag and surface proteins, cells were seeded (1×10^5 per well) the previous day on poly-L-lysine coated 12-well plates containing coverslips (no. 1.5, 12 mm, Fisher Scientific; Suwanee, GA). Cells were then transfected with Polyfect (Qiagen, Valencia, CA) according to manufacturer's instructions. The next day cells were incubated with 4% paraformaldehyde (0.5 mL/well)

for 15 min and then blocked with PBS/sera (0.5 mL/well) (5% donkey sera in PBS) for 10 min. Cells were then incubated with primary antibody for 1 hour at room temperature in PBS/sera/0.2% saponin (1:500), washed 3 times with PBS, incubated with the secondary antibody for 1 hour at room temperature in PBS/sera/0.2% saponin (1:500), and then washed three times with PBS and once with distilled water. Cells may or may not have been labeled with 5 µg/mL A594-conjugated cholera toxin B subunit in PBS for 1 hour (Invitrogen) and washed three times. Coverslips were mounted on glass slides with gelvatol [53] at 4^0C. The next day cells were visualized by confocal microscopy at 63X. For each condition, eight cells were chosen at random and extent of colocalization was quantified by calculating the Pearson's overlap coefficient with ImageJ [54] and the Colocalisation Threshold plugin (Tony Collins, Wayne Rasband, and Kevin Baler). This calculation is based on the overlap of red and green pixels, with a high degree of overlap corresponding to a value of 1 and a low degree of overlap corresponding to a value of 0 [55]. Coefficients for eight separate cells were averaged and statistical significance was determined.

Immunoblotting. To detect p24, Tac-CD16, FR-WT, or amphotropic Env in virus samples and rafts, equal amounts of protein from each sample were combined 1:2 (v/v) with sample buffer containing 5% β-mercaptoethanol (both from Bio-Rad; Hercules, CA), vortexed, boiled for 5 min, separated by size by SDS-PAGE (4-20% Tris-HCl gel, Bio-Rad), and transferred to a PVDF membrane (0.2 µm, Bio-Rad). To probe for p24 in the membrane, mouse anti-p24 (24-3) was diluted 1:5000 in blocking buffer (5% nonfat milk in PBS with 0.1% Tween 20) and followed by incubation with HRP-conjugated donkey anti-mouse (diluted 1:400,000 in blocking buffer). Similarly, to probe for Tac-CD16, rabbit anti-IL-2Rα was diluted 1:1000 in blocking buffer followed by HRP-conjugated donkey anti-rabbit (1:400,000 in blocking buffer). To probe for FR-WT, rabbit anti-folate receptor antisera was diluted 1:2500 in blocking buffer followed by HRP-

conjugated donkey anti-rabbit (1:400,000 in blocking buffer). To probe for amphotropic Env, goat anti-gp70 antibody 79S834 was diluted 1:1000 in blocking buffer followed by HRP-conjugated donkey anti-goat (1:400,000 in blocking buffer). A chemiluminescent detection system was used for detection (Super Signal West Femto kit; Pierce). To quantitatively compare the amount of protein that was visualized as bands on the film, we used ImageJ to measure the band area and intensity and compared the product of the two values.

   Lipid raft isolation. To detect for proteins in lipid rafts, 293T/17 cells, seeded (1×10^7 per well) the previous day on poly-L-lysine coated plates with Lipofectamine 2000 and 6 μg of pCMVΔR8.91, 6 μg of the lentivirus vector pTYEFnlacZ, and 6 μg of pFB4070ASALF alone or with either 6 μg of the Tac-CD16 expression plasmid or the FR-WT expression plasmid. Cells were then pelleted with versene (PBS and 5 mM EDTA pH 7.5) and resuspended in 1 mL of ice-cold 0.5% Brij 98 in TNE buffer (25 mM Tris-base, 0.15 M sodium chloride, 5 M EDTA, pH 7.5). Lysates were dounce homogenized, adjusted to 40% sucrose by adding an equal volume of 80% sucrose in TNE buffer and placed in ultracentrifuge tubes. For whole raft isolation, samples were overlaid with 5 mL of ice-cold 30% sucrose in TNE followed by 4 mL of ice-cold 5% sucrose in TNE. For linear gradient raft isolation, samples were overlaid with 9 mL of a 5-30% continuous sucrose density gradient prepared with a SG series gradient maker (Hoefer Scientfici Instruments; San Francisco, CA). The samples were centrifuged at 30,000 rpm for 15 hours at 4^0C in an SW41 rotor (Beckman Coulter, Palo Alto, CA). For whole raft isolation, the proteins at the interface of the 5% and 38% sucrose solutions was isolated, mixed with ice-cold TNE buffer, and then centrifuged at 30,000 rpm for 1 hour at 4^0C in a SW41. The pelleted lipid raft fraction was resuspended in 100 μL of TNE buffer. For the linear gradient isolation, fractions of 1 mL were collected, and the density of each fraction was determined as mass/volume and reported as g/mL.

p24 ELISA. We used p24 ELISA to quantitatively compare the amount p24 viral supernatant and lipid rafts. ELISA plates (Nunc immuno Maxisorp 96-well plates, Nalgene Nunc International, Rochester, NY) were coated overnight at 37^0C with 1:800 dilution of mouse anti-p24 antibody 183-H12-5C (100 µL/well) in PBS. The next day, the antibody solution was removed and wells were washed twice (PBS, 0.05% Tween-20). Blocking buffer (PBS, 0.05% Tween-20, 5% non-fat milk) was added at 200 µL/well for 1 hour at 37^0C and removed. Samples were lysed in 2% Triton X-100 1:1 and added to the ELISA plate (100 µL/well), and incubated for 2 hours at 37^0C. Bound p24 was sandwiched by the addition of the sheep polyclonal anti-p24 antisera diluted 1:250 in blocking buffer, and incubated for 2 hours at 37^0C. The HRP-conjugated anti-sheep secondary antibody was diluted 1:1000 in blocking buffer and added to the ELISA plate (100 µL/well) for 1 hour at 37^0C. Plates were then developed for 20 min using a solution (100 µL/well) of 3 mg of OPD, 3 µL hydrogen peroxide, 7.5 mL substrate buffer (24 mM citric acid-monohydrate, 51 mM $Na_2HPO_4*7H_2O$, pH 5.0). 8N sulfuric acid (50 µL/well) was used to stop the reaction and the optical density at 490 nm was measured using an absorbance plate reader (non-specific background at 650 nm was subtracted). Values for each point are the average of at least triplicate wells.

Transduction. 293T cells were seeded in poly-L-lysine coated 12-well plates (1×10^5 cells per well) and incubated at 37°C. The next day, viral supernatant dilutions were incubated with cells for 48 h, after which the cells were fixed with gluteraldehyde and stained for β-galactosidase activity with X-Gal, and the number of *lacZ*+ colony-forming units (CFU) per milliliter was counted.

Statistics. Data are summarized as the mean ± the standard deviation for at least triplicate samples. Statistical analysis was performed using one-way analysis of variance for repeated measurements of the same variable. The Tukey multiple

comparison test was used to conduct pairwise comparisons between means. Differences at $p < 0.05$ were considered statistically significant.

4.4 Results

In order to determine whether lipid rafts compartmentalize host cell raft proteins, and whether protein incorporation into the lentiviral lipid bilayer is dependent upon colocalization with lentivirus-associated rafts, we studied the ability of two glycosylphosphatidylinositol (GPI) anchored proteins, folate receptor (FR-WT) and Tac-CD16 (i.e., the interleukin-2 receptor alpha chain fused with the cytoplasmic domain of the GPI-anchored CD16 protein [52]) to incorporate into lentivirus particles. GPI anchored proteins have been shown to associate with lipid rafts and lentivirus particles [56, 57], however not all GPI anchored proteins are incorporated into the lentiviral lipid bilayer [22, 58, 59]. As a first step, we examined whether Tac-CD16 and FR-WT displayed typical GPI anchored protein properties. We analyzed the amount of colocalization between the proteins and lipid rafts by transfecting $1x10^5$ 293T cells on glass coverslips with plasmids encoding for Tac-CD16 and FR-WT. Cells were also transfected with a plasmid encoding for HIV-1 Gag-Pol as an example of a protein that colocalizes with rafts [24]. The next day cells were fixed, permeabilized, and immunostained with a monoclonal antibody against Tac-CD16 or FR-WT followed by a Cy2-conjguated secondary antibody, and then stained for lipid rafts with A549-conjugated cholera toxin B subunit which binds to GM1 found in rafts (Figure 4.1A). Cells were visualized by confocal microscopy and the extent of colocalization between the GPI anchored protein and rafts was quantified by calculating the Pearson's overlap coefficient. We found a high degree of colocalization between lipid rafts and Tac-CD16, FR-WT, and Gag as shown by the overlapping of corresponding red (raft) and green

84
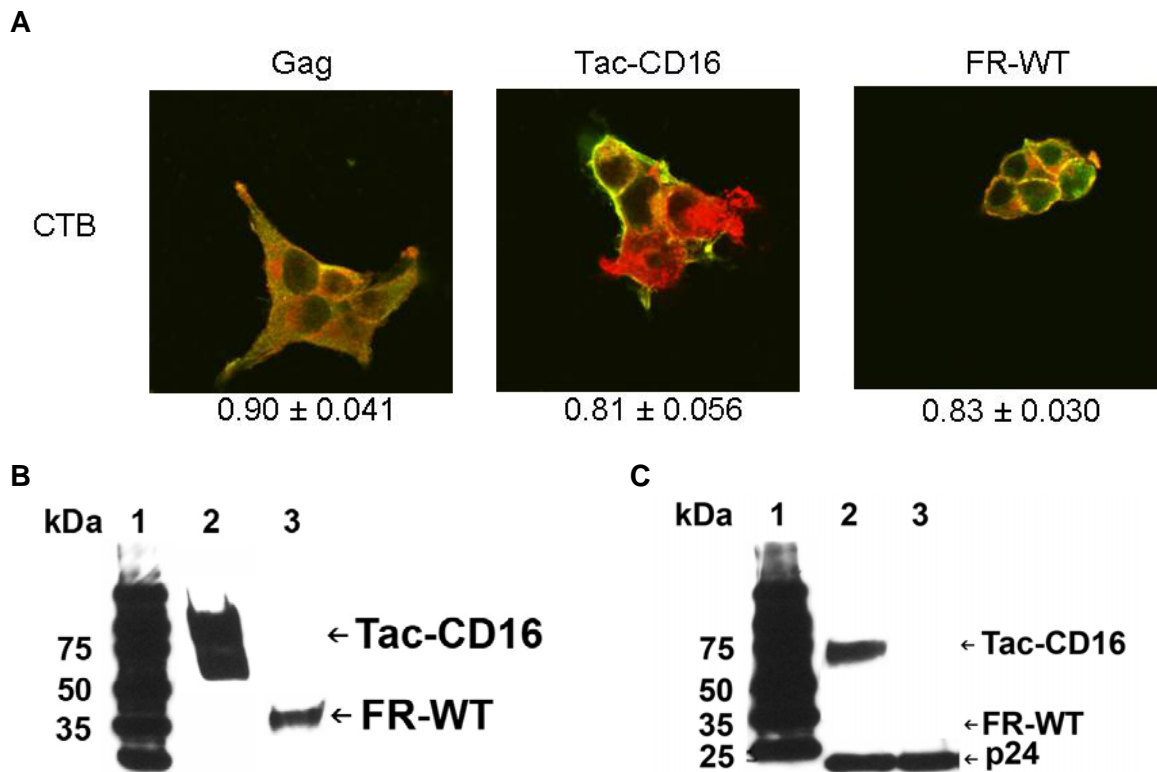
Figure 4.1. FR-WT and Tac-CD16 display typical GPI anchored protein properties however FR-WT is not incorporated into lentiviral particles. 293T cells were transiently transfected to express HIV-1 Gag-Pol (Gag), Tac-CD16, or FR-WT. Cells were fixed, permeabilized, and immunostained with a monoclonal antibody against Gag, Tac-CD16, or FR-WT followed by Cy2 conjugated secondary antibody. Cells were also stained for lipid rafts with A549-conjugated cholera toxin B subunit (CTB). Cells were visualized with confocal microscopy at 63X and overlays of CTB (red) with proteins (green) are shown. Eight cells were chosen at random and extent of colocalization was quantified with ImageJ (A). FR-WT and Tac-CD16 are in lipid rafts (B) but FR-WT is not in virus particles (C). 293T cells ($1x10^7$) were transfected with expression plasmids (8 μg each) for β-galactosidase, HIV-1 Gag-Pol, and either FR-WT or Tac-CD16. Detergent resistant domains were isolated by lysing cells with ice-cold Brij 98 (0.5% in TNE) and flotation through a discontinuous sucrose gradient. The lipid raft fraction was pelleted by centrifugation and the pellet was analyzed by Western blot for the presence of Tac-CD16 (B, Lane 2) or FR-WT (B, Lane 3). The virus supernatant was harvested and ultracentrifuged through a 20% sucrose cushion, and then resuspended in PBS to 100-fold their original concentration. Samples were resuspended in lysis buffer and analyzed by Western blot for the presence of Tac-CD16 (C, Lane 2), FR-WT (C, Lane 3), and p24 (C, Lanes 2-3).

(proteins) pixels producing a yellow color, and also shown by the high Pearson's coefficient number (> 0.80).

To confirm biochemically that Tac-CD16 and FR-WT resided in lipid rafts, and determine if they are incorporated into lentiviral particles, we transfected cells with expression plasmids for β-galactosidase, HIV-1 Gag-Pol, and either FR-WT or Tac-CD16. Detergent resistant domains were isolated by lysing cells with ice-cold Brij 98 (0.5% in TNE) and flotation through a discontinuous sucrose gradient. The lipid raft fraction was pelleted by centrifugation and the pellet was analyzed by Western blot for the presence of Tac-CD16 or FR-WT (Figure 4.1B). As expected, FR-WT and Tac-CD16 were both detected in the detergent resistant fraction. The virus supernatant of the transfected cells was then analyzed for protein content after it was harvested, ultracentrifuged through a 20% sucrose cushion, and then resuspended in PBS to 100-fold the original concentration. Samples were resuspended in lysis buffer and analyzed by Western blot for the presence of Tac-CD16, FR-WT, and the lentiviral Gag protein p24 (Figure 4.1C). Surprisingly, even though both are GPI anchored proteins, Tac-CD16 was incorporated into lentiviral particles while FR-WT was not.

To see whether FR-WT was not incorporated into lentiviruses because FR-WT was not colocalized virus proteins, we analyzed the amount of colocalization between FR-WT and lentiviral proteins, Gag and amphotropic Env, and compared it to Tac-CD16. 293T cells ($1x10^5$) on coverslips were transiently transfected to express HIV-1 Gag-Pol or amphotropic Env, and either Tac-CD16 or FR-WT. To determine whether Tac-CD16 and FR-WT were colocalized with each other, cells were also transfected with both Tac-CD16 and FR-WT. Cells were fixed, permeabilized, and immunostained with a mouse monoclonal antibody against Gag or Env, followed by a Cy2 conjugated secondary antibody. Corresponding cells were also stained with a monoclonal antibody against FR-WT or Tac-CD16 followed by a Cy3-conjugated secondary antibody. Cells were

visualized by confocal microscopy and the extent of colocalization was quantified by calculating the Pearson's overlap coefficient with ImageJ (Figure 4.2). As expected, Tac-CD16 and Gag were strongly colocalized (0.82 ± 0.046). Interestingly, even though FR-WT, Tac-CD16, and Gag were all found in lipid rafts, FR-WT was not highly colocalized with Gag (0.55 ± 0.070, p<0.05) or even Tac-CD16 (0.72 ± 0.20). Tac-CD16 was slightly more colocalized with the amphotropic Env than FR-WT (0.780 ± 0.079 and 0.72 ± 0.047), although the difference was not statistically significant. These results suggested that FR-WT may be localized to a different set of rafts than Tac-CD16, Gag, and Env.

In a typical raft isolation procedure, proteins are collected at the interface of the 5% and 30% sucrose solutions. To further characterize the location of GPI anchored proteins compared to virus proteins in lipid rafts, we analyzed the distribution of FR-WT, Tac-CD16, Gag, and amphotropic Env in a linear gradient of 5-30% sucrose. 293T cells (1×10^7) were transfected with expression plasmids for HIV-1 Gag-Pol or Env, and either FR-WT or Tac-CD16. Detergent resistant domains were isolated by flotation through a linear sucrose gradient after lysing cells with ice-cold Brij 98 (0.5% in TNE). Fractions were collected and analyzed by Western blot for the presence of Tac-CD16 and FR-WT (Figure 4.3A) and Env (Figure 4.3C). When co-expressed with Gag, Tac-CD16 was distributed as very strong bands in fractions 3-6, a strong band in fraction 2, and a weak band in fraction 7. However when co-expressed with Gag, the bands for FR-WT were present as average bands in fractions 4-5, and as weak bands in fraction 3 and 6. To characterize the distribution of Gag in the linear sucrose gradient, a p24 ELISA was performed on the fractions (Figure 4.3B). Generally as the fraction density increased, the concentration of p24 increased. Significant amounts of p24 was detected when Gag was co-expressed with Tac-CD16, however the amount detected when co-expressed with FR-WT was on average 5-fold less. Similar to Gag, the amphotropic Env bands

A

Tac-CD16   FR-WT   Tac-CD16 + FR-WT

Gag

0.82 ± 0.046 $0.55 \pm 0.070^{*}$ 0.72 ± 0.20

B

Tac-CD16 + Ampho   FR-WT + Ampho

0.78 ± 0.079 0.72 ± 0.047
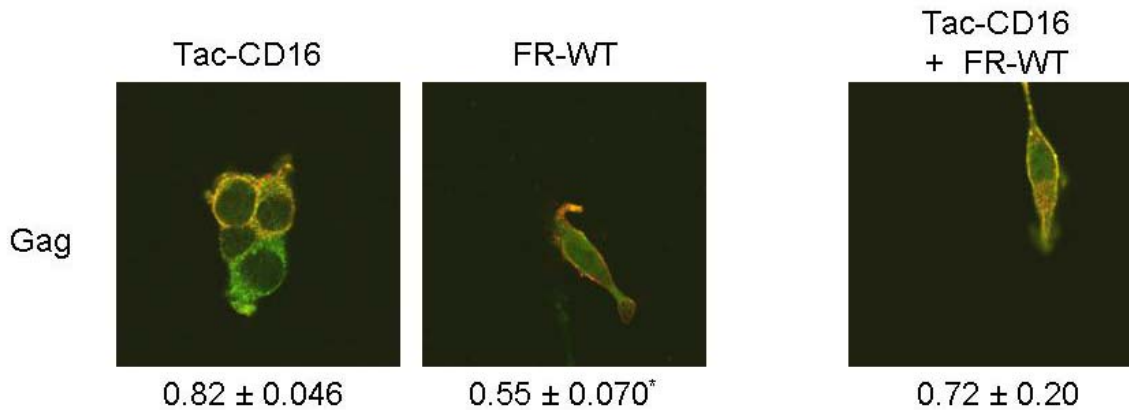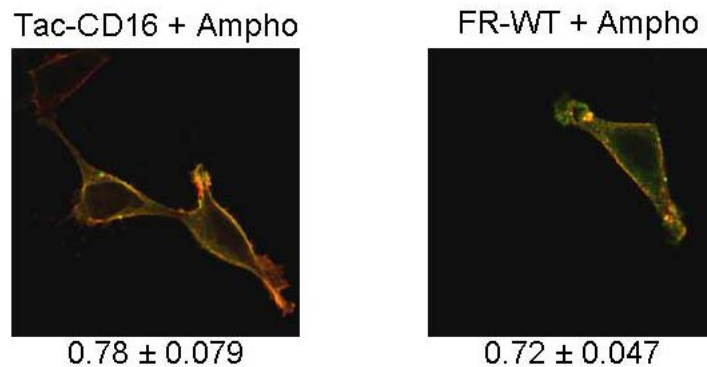
Figure 4.2. FR-WT is not colocalized with Gag or Env while Tac-CD16 is. 293T cells were transiently transfected to express HIV-1 Gag-Pol or amphotropic Env and either Tac-CD16 or FR-WT. Cells were also co-transfected with both Tac-CD16 and FR-WT. Cells were fixed, permeabilized, and immunostained with a monoclonal antibody against Gag (A) or Env (B), followed by Cy2 conjugated secondary antibody, and a monoclonal antibody against Tac-CD16 or FR-WT followed by Cy3 conjugated secondary antibody. Cells were visualized with confocal microscopy at 63X and overlays of red with green are shown. Eight cells were chosen at random and extent of colocalization was quantified with ImageJ. Statistically significant differences ($p < 0.05$) in colocalization values between Tac-CD16 colocalized with Gag and FR-WT colocalized Gag are denoted with *.

A

| 2 | 3 | 4 | 5 | 6 | 7 | 8 | 9 | 10 |

Tac-CD16

FR-WT

B

C

| 2 | 3 | 4 | 5 | 6 | 7 | 8 | 9 | 10 |

Ampho alone

Ampho +
Tac-CD16

Ampho +
FR-WT
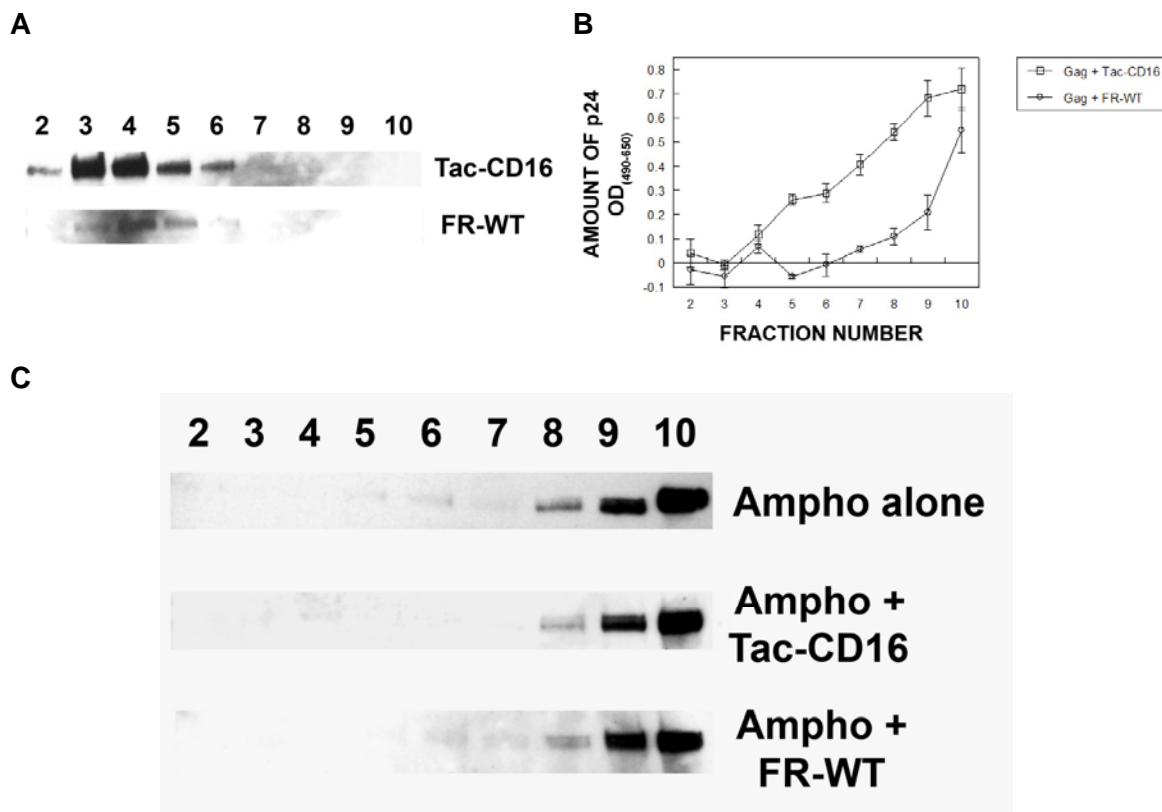
Figure 4.3. Tac-CD16 distribution in rafts overlap Gag while FR-WT does not, and Tac-CD16 reduces amount of Env in rafts while FR-WT does not. 293T cells (1×10^7) were transfected with expression plasmids for HIV-1 Gag-Pol, and either FR-WT or Tac-CD16 (A and B) or amphotropic Env alone or with either FR-WT or Tac-CD16 (C). Detergent resistant domains were isolated by lysing cells with ice-cold Brij 98 (0.5% in TNE) and flotation through a linear sucrose gradient. Fractions were collected and analyzed by Western blot for the presence of Tac-CD16 (A, top), FR-WT (A, bottom), or Env (C). Amount of p24 in the fractions from A was also quantified with p24 ELISA (B). The density of fractions 2-10 were 1.073, 1.076, 1.083, 1.091, 1.091, 1.097, 1.104, 1.130, 1.115 g/mL.

were intense in the denser fractions of 6-10, and were most intense in fractions 9 and 10. Interestingly, FR-WT had no effect on the distribution of amphotropic Env in fractions 6 and 7 compared to Env alone, whereas Tac-CD16 seemed to decrease the amount of amphotropic Env in raft fractions 6-8 compared to Env alone.

Since our data suggested FR-WT inhibited Gag localization to the less dense, FR-WT-containing rafts, we determined whether FR-WT would affect the budding, envelope incorporation, and titer of amphotropic pseudotyped lentivirus particles. 293T cells were transfected with expression plasmids for β-galactosidase, HIV-1 Gag-Pol, amphotropic Env alone or with either FR-WT or Tac-CD16. Whole cell lysates were isolated by lysing cells with ice-cold Brij 98 (0.5% in TNE), and whole raft fractions were isolated by flotation through a discontinuous sucrose gradient. The virus supernatant was harvested and ultracentrifuged through a 20% sucrose cushion, and then resuspended in PBS to 100-fold their original concentration. Whole cell lysates, whole raft fractions, and amount of virus produced was analyzed for p24 concentrations with a p24 ELISA (Figure 4.4, A, B, C, respectively). In the presence of Tac-CD16, the amount of p24 in whole cell lysates and whole raft isolates dropped 2.7-fold ($p<0.05$) and 2.5-fold ($p>0.05$), respectively, while the amount of virus produced increased 1.2-fold ($p>0.05$). In the presence of FR-WT, the amount of p24 in whole cell lysates increased 1.4-fold ($p<0.05$) while the amount of virus produced decreased 1.2-fold ($p>0.05$). Consistent with the previous data, the amount of p24 in rafts decreased 3.8-fold ($p<0.05$). Since the amount of FR-WT in whole cell lysates increased and rafts decreased while the amount of virus released into the supernatant decreased, these results suggested that not only did FR-WT reduce localization of Gag to rafts, it also reduced viral budding.

A

B

C
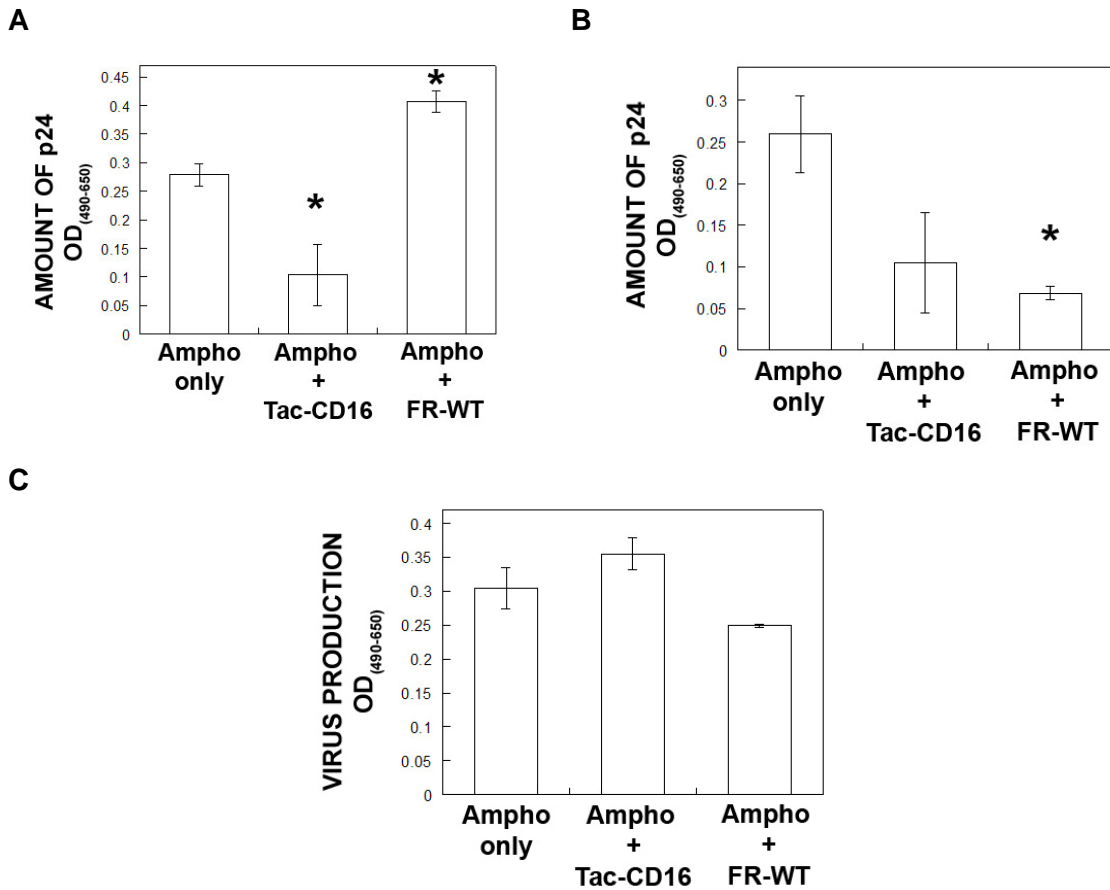
Figure 4.4. FR-WT inhibits Gag localization to rafts and lentiviral budding while Tac-CD16 does not. 293T cells (1×10^7) were transfected with expression plasmids (6 μg each) for β-galactosidase, HIV-1 Gag-Pol, amphotropic Env alone or with either FR-WT or Tac-CD16. Whole cell lysates were isolated by lysing cells with ice-cold Brij 98 (0.5% in TNE) and detergent resistant domains were isolated by flotation through a discontinuous sucrose gradient. The virus supernatant was harvested and ultracentrifuged through a 20% sucrose cushion, and then resuspended in PBS to 100-fold their original concentration. Whole cell lysates (A), whole raft fractions (B), or virus supernatant (C) were analyzed for p24 amounts with a p24 ELISA. * denotes statistically significant difference ($p<0.05$) in p24 amounts between whole cell lysates or rafts containing Ampho only or Ampho + GPI anchored protein.

The whole raft fractions and virus supernatants were then analyzed by Western blot for amount of Tac-CD16, FR-WT, and amphotropic Env (Figure 4.5, A, B, C, respectively). Densitometry analysis on the bands showed the amount of Tac-CD16 in virus and in lipid rafts decreased 7.9-fold and 1.3-fold, respectively, in the presence of the amphotropic envelope protein. Consistent with previous data, FR-WT was not detected in virus particles. However, the amount of FR-WT in lipid rafts decreased 1.2-fold when the amphotropic Env was co-transfected. There did not seem to be detectable differences in the amount of amphotropic Env in virus particles when co-transfected with either GPI anchored proteins, however the amount of Env in lipid rafts decreased 1.2-fold and 1.6-fold when Tac-CD16 and FR-WT were co-transfected, respectively. When the viral supernatant was used to transduce cells in the diluted titer assay (Figure 4.5D), the normalized titer of amphotropic Env + Tac-CD16 pseudotyped viruses decreased 1.9-fold while the normalized titer of amphotropic Env + FR-WT pseudotyped viruses was not statistically different from amphotropic Env pseudotyped viruses.

Our data suggested there are dense, lentivirus-associated rafts and less dense, non-lentivirus-associated rafts, and that residing in separate rafts may prevent raft proteins from interacting with each other. Lipid rafts are enriched in cholesterol, glycolipids, and sphingolipids, and cholesterol levels have been shown to affect the integrity of lipid rafts and also the trafficking of membrane proteins [9, 60]. We investigated whether a cholesterol extracting compound such as methyl-beta-cycodextrin (MβCD) or a cholesterol sequestering and sphingolipids synthesis inhibiting compound such as fumonisin B1 (FB1) would have an effect on raft integrity such that colocalization of proteins residing in different rafts can occur. We first determined whether MβCD or FB1 treatment would affect the colocalization GPI anchored proteins
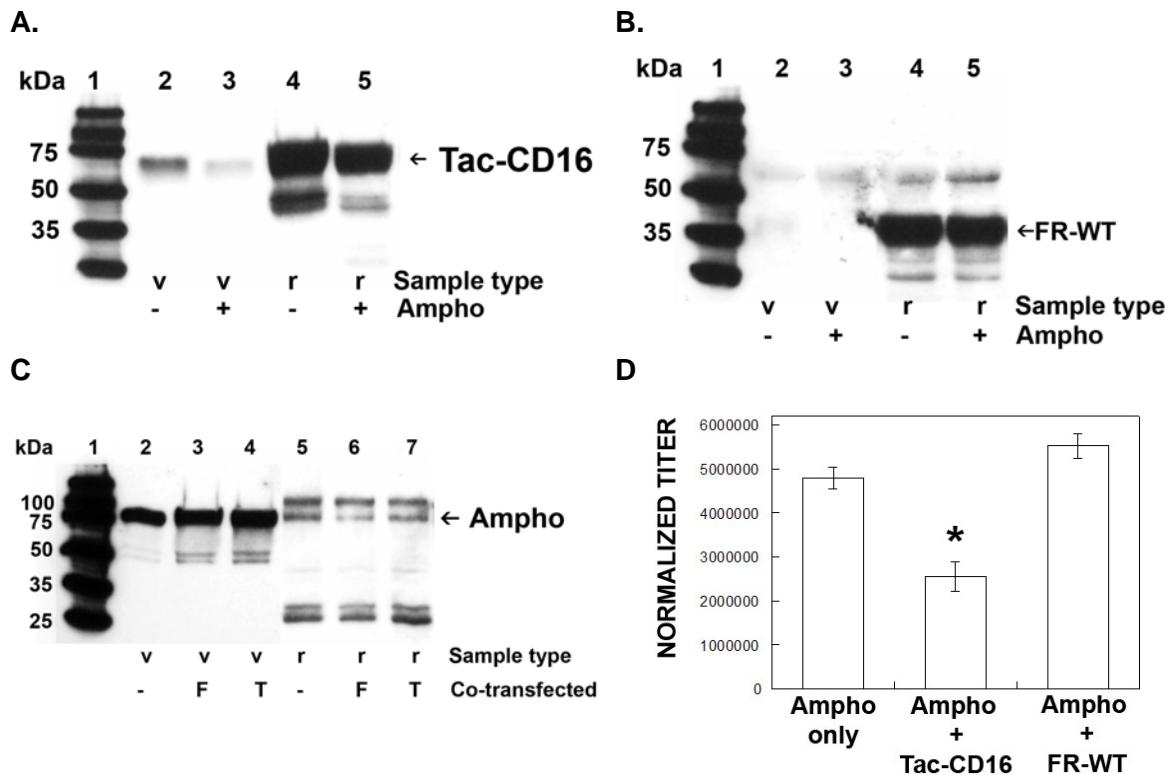
Figure 4.5.   FR-WT is not present in virus particles, does not alter amount of amphotropic Env in rafts or virus particles, and does not affect virus titer while Tac-CD16 does.   293T cells (1×10^7) were transfected with expression plasmids (6 µg each) for β-galactosidase, HIV-1 Gag-Pol, amphotropic Env alone (Ampho), Tac-CD16 alone, FR-WT alone, or amphotropic Env with either FR-WT (F) or Tac-CD16 (T).   The virus supernatant (v) was harvested, ultracentrifuged through a 20% sucrose cushion, resuspended in PBS to 100-fold their original concentration, and analyzed by Western blot after normalization for p24 (A and B Lanes 2-3, C Lanes 2-4).   Detergent resistant domains (r) were isolated by lysing cells with ice-cold Brij 98 (0.5% in TNE) and flotation through a discontinuous sucrose gradient.   The lipid raft fraction was pelleted by centrifugation and the pellet was analyzed by Western blot after normalization for protein content (A and B Lanes 4-5, C Lanes 5-7).   Blots were for the presence of Tac-CD16 (A), FR-WT (B), or Ampho (C).   In Part A, samples are as follows: Tac-CD16 alone (Lanes 2 and 4) or Tac-CD16 + Ampho (Lanes 3 and 5).   In Part B, samples are as follows: FR-WT alone (Lanes 2 and 4) or FR-WT + Ampho (Lanes 3 and 5).   In Part C, samples are as follows: Ampho alone (Lanes 2 and 5), Ampho + FR-WT (Lanes 3 and 6), Ampho + Tac-CD16 (Lanes 4 and 7).   Titer of viruses was analyzed with diluted titer assay (D).   Viruses were used to transduce target cells and transduced cells were incubated for 2 days at 37^0C until confluent, fixed, and stained for *lacZ* activity with X-Gal, colonies of *lacZ*+ cells were counted, and the titer normalized to p24 amounts. * denotes statistically significant differences ($p<0.05$) in normalized titer of viruses containing amphotropic Env only or amphotropic Env + Tac-CD16.

with virus proteins. 293T cells were transiently transfected to express HIV-1 Gag-Pol, β-galactosidase, amphotropic Env, and either Tac-CD16 or FR-WT. Cells were then cultured in the presence of 50 μM FB1 or 0.5 mM MβCD. Cells were fixed, permeabilized, and immunostained with a monoclonal antibody against amphotropic Env or Gag followed by Cy2 conjugated secondary antibody, and then a monoclonal antibody against Tac-CD16 or FR-WT followed by a Cy3 conjugated secondary antibody. Cells were then visualized by confocal microscopy and the extent of colocalization was quantified by calculating the Pearson's overlap coefficient with ImageJ (Figure 4.6). Treatment of cells with MβCD or FB1 did not statistically alter the amount of colocalization of Tac-CD16 with amphotropic Env or Gag. Treatment of cells with MβCD and FB1 had no statistical effect on amount of colocalization between amphotropic Env and FR-WT, however the amount of colocalization between FR-WT and Gag increased significantly ($p<0.05$).

To further determine the effects of MβCD and FB1 on raft integrity, we analyzed the distribution of GPI anchored protein and virus protein in rafts. 293T cells were transiently transfected to express HIV-1 Gag-Pol and either Tac-CD16 or FR-WT. Cells were then cultured in the presence of 50 μM FB1 or 0.5 mM MβCD. Detergent resistant domains were isolated by flotation through a linear sucrose gradient after lysing cells with ice-cold Brij 98 (0.5% in TNE). Fractions were collected and analyzed with Western blot for the presence of Tac-CD16 or FR-WT (Figure 4.7A). Treatment of cells with FB1 or MβCD shifted the Tac-CD16 distribution in lipid rafts slightly to less dense fractions (fractions 2-5 and 2-6, respectively) compared to untreated cells in Figure 4.3A. The treatment of cells with FB1 or MβCD greatly enhanced the amount of FR-WT in lipid raft fractions in both cases, as well as increased the distribution of FR-WT to more dense fractions (lanes 3-5, with weak bands in lanes 6 and 7) compared to untreated cells in Figure 4.3A. The amount of Gag in the fractions was also quantified with p24 ELISA
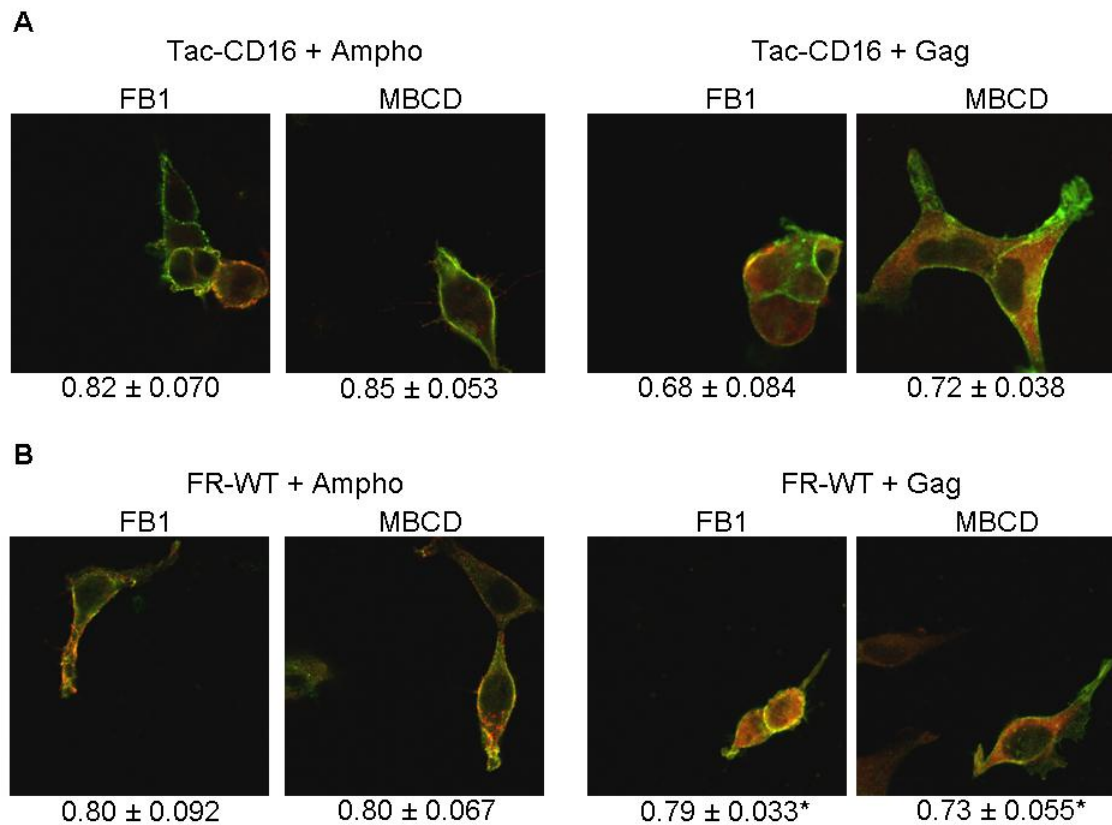
Figure 4.6. Treatment of cells with FB1 and MβCD increases colocalization of FR-WT with amphotropic Env and Gag. 293T cells were transiently transfected to express HIV-1 Gag-Pol (Gag), β-galactosidase, amphotropic Env (Ampho), and either Tac-CD16 or FR-WT. Cells were then cultured in the presence of 50 μM fumonisin B1 (FB1) or 0.5 mM (MβCD). Cells were fixed, permeabilized, and immunostained with a monoclonal antibody against Ampho or Gag followed by Cy2 conjugated secondary antibody, and then a monoclonal antibody against Tac-CD16 or FR-WT followed by a Cy3 conjugated secondary antibody. Cells were visualized with confocal microscopy at 63X and overlays of red with green are shown. Eight cells were chosen at random and extent of colocalization was quantified with ImageJ. * denotes statistically significant differences (p<0.05) in colocalization between FR-TW and Gag in untreated cells (Figure 4.2) and cells treated with FB1 or MβCD.
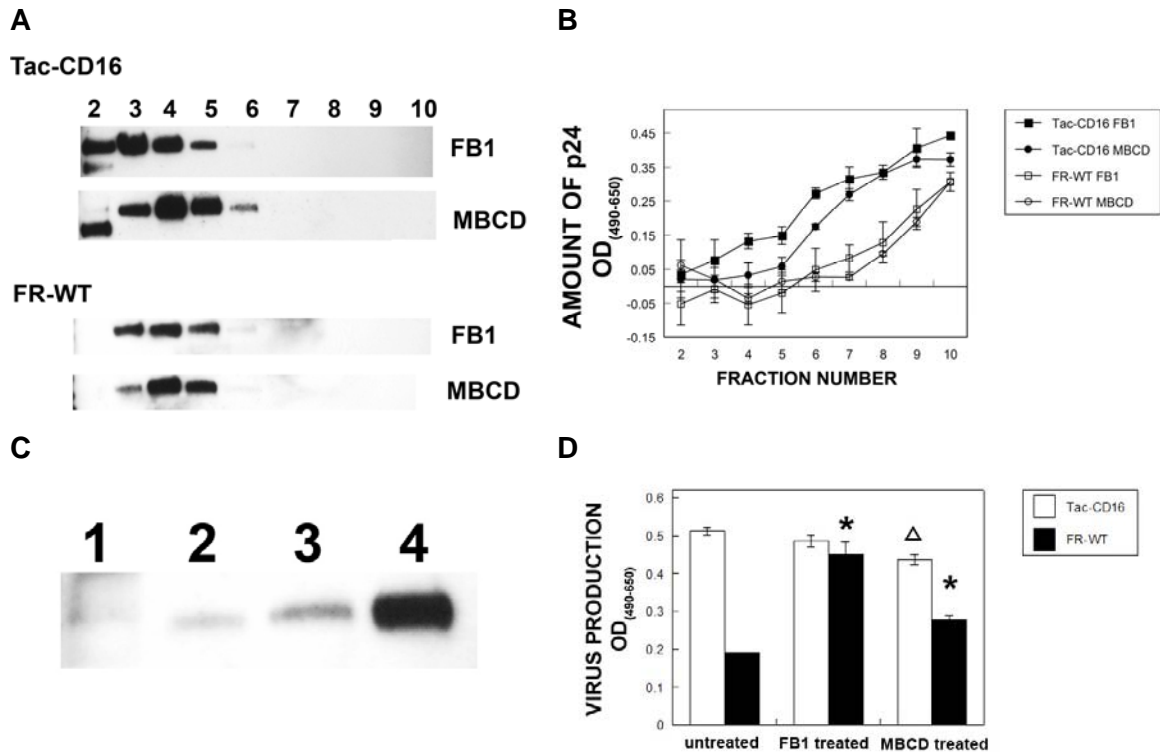
Figure 4.7. Treatment of cells with FB1 and MβCD disturbs lipid rafts and increases lentiviral budding and FR-WT incorporation into lentiviral particles. 293T cells were transiently transfected to express HIV-1 Gag-Pol (Gag) and either Tac-CD16 or FR-WT. Cells were then cultured in the presence of 50 μM fumonisin B1 (FB1) or 0.5 mM methyl-beta-cyclodextrin (MβCD). Detergent resistant domains were isolated by lysing cells with ice-cold Brij 98 (0.5% in TNE) and flotation through a discontinuous sucrose gradient (A). Fractions were collected and analyzed by Western blot for the presence of Tac-CD16 (A top) or FR-WT (A bottom). Amount of p24 was also quantified with p24 ELISA on the fractions (B). The density of fractions 2-10 were 1.060, 1.068, 1.076, 1.081, 1.086, 1.098, 1.110, 1.113, 1.118 g/mL. The virus supernatant was harvested and ultracentrifuged through a 20% sucrose cushion, and then resuspended in PBS to 100-fold their original concentration and analyzed by Western blot for FR-WT after normalization for p24 (C). Lanes are as follows 1) FR-WT LV untreated, 2) FR-WT LV with 50 μM FB1, 3) FR-WT LV with 0.5 mM MβCD, and 4) FR-WT in lipid raft as positive control. Virus supernatant was also analyzed for amount of p24 by p24 ELISA (D). Statistically significant differences ($p < 0.05$) in p24 amounts between (1) untreated FR-WT LV with treated FR-WT LV or (2) untreated Tac-CD16 LV with treated Tac-CD16 LV are denoted with * and Δ, respectively.

96

(Figure 4.7B). Similar to previous results, the overall amount of p24 was higher when co-transfected with Tac-CD16 than FR-WT, and amount of p24 increased as fraction density increased. However in MβCD and FB1 treated cells, the presence of Gag when co-transfected with FR-WT was detectable in less dense fractions (beginning in fractions 5 and 6) compared untreated cells in Figure 4.2C (where presence of Gag was detectable beginning in fraction 7). Also the amount of Gag in FR-WT co-transfected cells was only 2.6-fold and 3.5-fold less, respectively, with FB1 and MβCD treatment than cells co-transfected with Tac-CD16 (compared to 5-fold less in untreated cells from Figure 4.2C).

Since FB1 and MβCD treatment increased colocalization of FR-WT with Gag, we then examined whether FB1 or MβCD treatment would increase the amount of folate receptor incorporated into lentiviral particles. The virus supernatant from the above treated cells were harvested and ultracentrifuged through a 20% sucrose cushion, and then resuspended in PBS to 100-fold their original concentration and analyzed by Western blot for FR-WT after normalization for p24 (Figure 4.7C). FB1 and MβCD treatment of producer cells increased the amount of FR-WT in virus particles 2.9-fold and 11.6-fold, respectively, however the amount incorporated was still significantly less than Tac-CD16 or amphotropic Env. Virus supernatant was also analyzed for amount of virus produced by p24 ELISA (Figure 4.7D). FB1 and MβCD treatment decreased the amount of virus produced from Tac-CD16 cells 1.1-fold ($p>0.05$) and 1.2-fold ($p<0.05$), respectively. Interestingly, FB1 and MβCD increased the amount of virus produced from FR-WT transfected cells 2.4-fold ($p<0.05$) and 1.5-fold ($p<0.05$), respectively.

We then determined whether MβCD treatment would have an effect on Tac-CD16 and amphotropic Env incorporation into rafts and virus particles. 293T cells were transiently transfected to express HIV-1 Gag-Pol, β-galactosidase, amphotropic Env or Tac-CD16. Cells were then cultured in the presence or absence of 0.5 mM MβCD.

Detergent resistant domains were isolated by lysing cells with ice-cold Brij 98 (0.5% in

TNE), flotation through a discontinuous sucrose gradient, and pelleting the raft fraction.

The virus supernatant was harvested and ultracentrifuged through a 20% sucrose

cushion, and resuspended in PBS to 100-fold their original concentration. The lipid raft

fractions and virus supernatants were then analyzed by Western blotting for amount of

Tac-CD16 (Figure 4.8A) and amphotropic Env (Figure 4.8B). In Tac-CD16 transfected

cells, MβCD treatment decreased the amount of Tac-CD16 in virus particles 2.4-fold and

also decreased the amount in lipid rafts 1.1-fold. Interestingly, MβCD treatment also

decreased the amount of amphotropic Env in virus particles 1.3-fold and the amount in

rafts 1.9-fold.
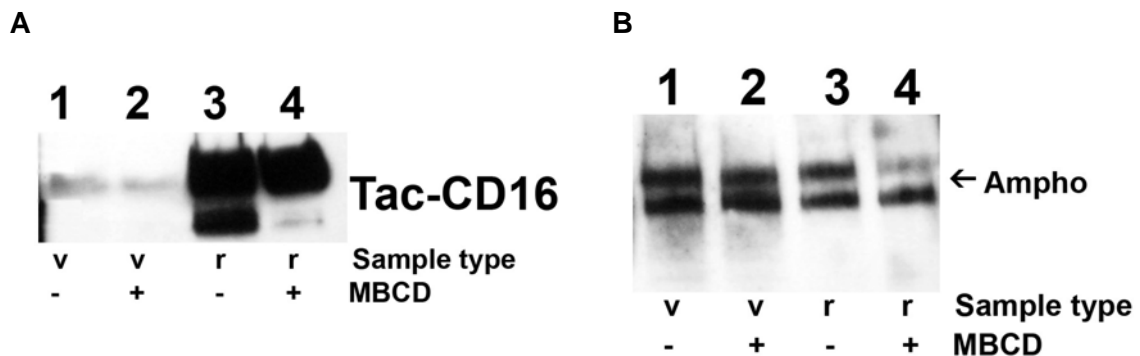
Figure 4.8. Treatment of cells with MβCD decreases amount of Tac-CD16 and amphotropic Env in raft and virus. 293T cells were transiently transfected to express HIV-1 Gag-Pol, β-galactosidase, and either amphotropic Env (Ampho) or Tac-CD16. Cells were then cultured in the presence or absence of 0.5 mM MβCD. Detergent resistant domains were isolated by lysing cells with ice-cold Brij 98 (0.5% in TNE) and flotation through a discontinuous sucrose gradient. The raft fraction (r) was pelleted and analyzed by Western blot after being normalized for protein content (A and Lanes 3-4). The virus supernatant (v) was harvested and ultracentrifuged through a 20% sucrose cushion, and then resuspended in PBS to 100-fold their original concentration and analyzed by Western blot after normalization for p24 (A and B, Lanes 1-2). Gels were immunoblotted for Tac-CD16 (A), or amphotropic Env (B).

Discussion

      Lipid rafts have been shown to be important for proper lentivirus assembly and budding. We hypothesized that lipid rafts compartmentalize host cell raft proteins, and protein incorporation into the lentiviral lipid bilayer is dependent upon colocalization with lentivirus-associated rafts. To test this hypothesis, we studied the ability of two glycosylphosphatidylinositol (GPI) anchored proteins, folate receptor (FR-WT) and Tac-CD16 (the interleukin-2 receptor alpha chain fused with the cytoplasmic domain of the GPI-anchored CD16 protein) to associate with viral proteins, Gag and amphotropic Env, in lipid rafts and lentivirus particles. We examined the distribution of the GPI anchored proteins and virus proteins in whole cells, lipid rafts, and viral supernatant. We found that Tac-CD16 and FR-WT exhibited the classic GPI anchored protein property of associating with lipid rafts, however Tac-CD16 colocalized with Gag and incorporated into lentiviral particles, while FR-WT did not colocalize with Gag and was not incorporated into virus particles. In raft fractions separated by a linear sucrose gradient, FR-WT generally colocalized to less dense rafts while Gag and Env were localized to more dense rafts. Tac-CD16 was also located to less dense rafts, but had a wider distribution in the linear gradient than FR-WT. Most significantly, we found that when we treated producer cells with fumonisin B1 (FB1) or methyl-beta-cyclodextrin (MβCD), the amount of colocalization between FR-WT and Gag increased, FR-WT had a wider distribution in the linear raft gradient, and FR-WT was incorporated 2.9 to 11.6-fold more into lentiviral particles, respectively. In contrast, the raft distribution of Tac-CD16 in the linear raft gradient decreased and the amount of Tac-CD16 in virus particles decreased 2.4-fold with MβCD treatment. Taken together, these results demonstrated lipid rafts segregate proteins, and for a protein to be incorporated into virus particles, it must be colocalized with lentivirus-associated rafts.

We also found folate receptor inhibited p24 localization to less dense rafts and proteins may compete with each other for space in lipid rafts. The amount of p24 detected in rafts when co-expressed with FR-WT was 5-fold less in linear gradients than when co-expressed with Tac-CD16. The presence of FR-WT inhibited Gag localization to rafts 3.8-fold ($p<0.05$) and virus release 1.2-fold ($p>0.05$), while the presence of Tac-CD16 decreased Gag localization to rafts 2.5-fold ($p>0.05$) and increased virus release 1.2-fold ($p<0.05$). However, amphotropic Env raft distribution in a linear gradient and titers of Env pseudotyped lentiviruses were not affected when producer cells were co-transfected with FR-WT, while Env raft distribution decreased and titers dropped 1.9-fold ($p<0.05$) when cells were co-transfected with Tac-CD16. In general, FB1 or MβCD treatment of producer cells disrupted rafts but did not abolish rafts such that previously sequestered raft proteins were localized to lentivirus-associated rafts. When cells were treated with FB1 or MβCD, the amount of p24 detected in rafts when co-expressed with FR-WT was only 2.6 to 3.5-fold less in linear gradients than when co-expressed with Tac-CD16. In addition, FB1 or MβCD treatment increased virus production in FR-WT transfected cells 2.4 and 3.5-fold (both $p<0.05$), respectively, while virus production from Tac-CD16 transfected cells decreased about 1.2-fold. Interestingly, MβCD treatment of producer cells decreased the amount of Tac-CD16 in rafts 1.1-fold and the amount in virus particles 2.4-fold, and also decreased the amount of Env in rafts 1.9-fold and the amount in virus particles 1.3-fold.

Our results demonstrating lipid rafts compartmentalize raft proteins on the cell surface is consistent with literature on the heterogeneity of lipid rafts. Previous work has shown the existence of distinct raft populations such as less dense and more dense rafts [61], Brij 98 or Triton X-100 isolated rafts [62], apical and basolateral rafts [63], and caveolae-positive and caveolae-negative rafts [64]. Indeed, raft markers such as Thy-1, Yes, and Lyn [62], Thy-1 and GM1 [65], and even GPI anchored proteins such as Thy-1

and prion protein [66], and folate receptor and PLAP [67], are located in different raft domains. Raft-raft separation by detergent solubility and density, perhaps because of differences in content and ordered structure of proteins and lipids [2, 68], presumably allows for further separation of raft proteins based on functional diversity. In this study, we chose to use the nonionic detergent Brij 98 at a concentration of 0.5%, since it has been shown to inhibit inter-mixing of raft proteins with each other and nonraft proteins [66], and populations of assembling, membrane-bound Gag (termed 'barges') was isolated using Brij 98, and not with Triton X-100 [68].

The localization of Gag and GPI anchored proteins on linear raft gradients showed rafts may separate raft proteins based on their ability to localize to low or high density rafts, and that lentivirus-associated rafts were localized to high density rafts. This is consistent with literature that indicates lentiviruses assemble and bud from specific locations in the cell, even though the precise location still remains controversial. In 293T, a common producer cell type that was also used in this study, Gag either is targeted directly to the plasma membrane [69, 70], or first to multivesicular bodies and then transported to the plasma membrane [71]. Besides lipid rafts in general [25, 30, 72, 73], tetraspanin-containing regions have also been implicated as assembly and budding sites [74-76], although rafts and tetraspanin-enriched domains have not yet been shown to be exclusive. One apparent reason for lentivirus assembly and budding to occur in rafts is to further concentrate lentiviral proteins for proper assembly. For proteins to be incorporated into lentivirus particles, they have to be localized to sites of assembly [77-79]. These assembly sites must be specific to specific rafts since raft markers such as flotillin [22] and the GPI anchored protein CD14 [58, 59] are not incorporated into virus particles. Indeed we and others have shown Gag is located in the more dense fractions [25], and in this study, we have shown proteins that were not in the dense fractions, like FR-WT, were not incorporated into virus particles.

Tac-CD16 and FR-WT may be used as probes to determine what affects virus assembly and incorporation into lentiviral particles. Our data showed FR-WT had no effect on the distribution of amphotropic Env in linear raft fractions compared to Env alone, whereas Tac-CD16 seemed to decrease the amount of amphotropic Env in raft fractions compared to Env alone. Env also decreased the amount of Tac-CD16 in rafts 1.3-fold while the amount of FR-WT in rafts decreased 1.2-fold compared to Tac-CD16 or FR-WT transfected alone. While the amount of Env did not decrease in virus particles with the presence of GPI anchored proteins, the amount of Tac-CD16 decreased in virus particles 7.9-fold. However titer of Env pseudotyped lentiviruses decreased 1.9-fold ($p<0.05$) when Tac-CD16 was expressed and was not significantly affected when FR-WT was expressed. Since amphotropic Env and Tac-CD16 overlapped in linear raft gradients while Env and FR-WT did not, these results suggested the composition of lentivirus-associated rafts may be altered by proteins and that Tac-CD16 and Env may compete with each other for space in lentivirus-associated rafts. Since the degree of packing in lipid rafts depends on types and amounts of proteins and lipids [80], there is presumably limited space in rafts. FR-WT probably had no effect on Env raft localization, virus incorporation, and titer since it was not localized with Env in lentivirus-associated rafts and not incorporated in virus particles. The reason the amount of amphotropic Env incorporated in virus particles was not affected by GPI anchored proteins may have been because Env was highly colocalized with Gag in the denser raft fractions. However since Tac-CD16 was slightly colocalized with the denser raft fractions, the presence of amphotropic Env may have had a greater detrimental effect on Tac-CD16 incorporation. Our data also showed that even though virus levels of amphotropic Env was not greatly decreased by the incorporation of Tac-CD16, titers were still significantly affected. The small decrease in Env incorporated may have resulted in lower transduction efficiency [81-83], although this seemed unlikely since the

amount of Env detected was so high. It is also possible Tac-CD16 may be interfering with Env binding or fusion, or increasing the amount of uncleaved Env incorporated in virus particles [84].

Interestingly, our results also indicated FR-WT may inhibit Gag localization to less dense rafts and inhibit, but not abolish, budding. We found the amount of p24 detected in rafts when co-expressed with FR-WT was about 5-fold less on a linear raft gradient than when co-expressed with Tac-CD16. Budding seemed to have decreased since the presence of FR-WT in producer cell inhibited release 1.2-fold (p>0.05) while the amount of Gag in whole cell lysates increased 1.4-fold (p<0.05). Since viruses still continued to be released, this suggested FR-WT may have caused Gag to be redistributed and bud from non-lipid rafts, yet still retain infectivity. However this may be unlikely since Gag oligomerization is dependent on rafts [85], and lentivirus and Env fusion depends on cholesterol levels [29, 86]. Alternatively, FR-WT may have strengthened compartmentalization of lentivirus-associated rafts, further restricting virus proteins to more dense raft fractions, and enabling viruses to still bud from the denser raft fractions while not affecting titer. It was also interesting that FB1 and MβCD treatment increased the amount of virus that budded from FR-WT transfected cells 2.4 and 1.5-fold, respectively. In Tac-CD16 transfected and MβCD treated cells, the amount of virus budding decreased 1.2-fold, similar to MβCD-treated HIV and MLV producer cells [24, 86]. However an increase in particle production after MβCD-treatment was also seen in Newcastle disease virus [87], influenza [88], Sendai virus [89], and VSV M protein transfected cells [24].

Our data showed we were disturbing and not abolishing raft integrity with 0.5 mM MBCD or 50 μM FB1 since Tac-CD16, FR-WT, amphotropic Env, and even Gag were still present in raft extractions. Previous studies that demonstrated MβCD permeabilized virus and disrupted rafts used 10 mM MβCD or higher concentrations [27, 29, 85]. In

addition, FB1 treatment may be affecting lipid raft integrity by reducing the amount of sphingolipids in the cell [90]. When MβCD or FB1 was added to producer cells, raft disturbance decreased the amount of proteins concentrated in the dense, lentivirus-associated rafts since total raft amounts of Tac-CD16 decreased 1.1-fold and amphotropic Env decreased 1.9-fold, and Tac-CD16 was present in fewer high density fractions. However, raft disruption increased the amount of colocalization and association of proteins sequestered to low density rafts, like FR-WT, with the more dense lentivirus-associated rafts such that a measurable amount of FR-WT was incorporated. Others have shown cholesterol depletion with MβCD does not disrupt Gag association with rafts [91] or Gag targeting to the cell membrane [85], however it does reduce the efficiency of Gag oligomerization [85]. Taken together, our data suggested raft disruptions allowed previously sequestered raft protein to inter-mix and may have caused previously concentrated raft proteins to decrease in concentration. Therefore, FB1 or MβCD treatment has more of a detrimental effect on virus incorporation of proteins already localized to lentivirus-associated rafts, and a positive effect on proteins that are not localized lentivirus-associated rafts.

In addition to affecting lipid rafts, cholesterol sequestration or depletion may be affecting the trafficking of FR-WT, the only known transport protein anchored to GPI moiety [92]. We do not know how Tac-CD16 trafficking is affected since the Tac protein is a cell surface protein not normally GPI anchored, and as such, has its own trafficking signals. MβCD and FB1 treatment noticeably increased the amount of FR-WT found in lipid rafts. Lipid rafts are often involved in the internalization of cell signaling molecules [9], and others have demonstrated cholesterol depletion resulted in increased protein concentrations at the plasma membrane because of either reduced endocytosis and degradation [60, 93], or increased trafficking to the cell surface [94]. FB1 treatment can also alter the distribution of proteins in the cells since it inhibits sphingolipids synthesis

and sphingolipids can affect vesicular trafficking of proteins to the apical surface [90, 95, 96]. Depletion of sphingolipids has been shown to enhance the rate of GPI anchored proteins trafficking to the plasma membrane from the recycling endosomes [97].

In conclusion, our results demonstrated lipid rafts segregate raft proteins, and for a protein to be incorporated into virus particles, it must be colocalized with lentivirus-associated rafts. Our data has demonstrated rafts may control the protein content of virus particles. Future studies should focus on manipulating rafts to alter protein incorporation into viruses and virus function, and also investigating the effects of cholesterol depletion on protein trafficking, and perturbing the lipid rafts on other types of viruses for the incorporation of other difficult-to-incorporate proteins.

4.5 <u>References</u>

1. Brown, D.A. and E. London, *Functions of lipid rafts in biological membranes.* Annu Rev Cell Dev Biol, 1998. **14**: p. 111-36.

2. Schuck, S., et al., *Resistance of cell membranes to different detergents.* Proc Natl Acad Sci U S A, 2003. **100**(10): p. 5795-800.

3. Brown, D.A. and E. London, *Structure and function of sphingolipid- and cholesterol-rich membrane rafts.* J Biol Chem, 2000. **275**(23): p. 17221-4.

4. Rodgers, W., B. Crise, and J.K. Rose, *Signals determining protein tyrosine kinase and glycosyl-phosphatidylinositol-anchored protein targeting to a glycolipid-enriched membrane fraction.* Mol Cell Biol, 1994. **14**(8): p. 5384-91.

5. van't Hof, W. and M.D. Resh, *Dual fatty acylation of p59(Fyn) is required for association with the T cell receptor zeta chain through phosphotyrosine-Src homology domain-2 interactions.* J Cell Biol, 1999. **145**(2): p. 377-89.

6. Shenoy-Scaria, A.M., et al., *Cysteine3 of Src family protein tyrosine kinase determines palmitoylation and localization in caveolae.* J Cell Biol, 1994. **126**(2): p. 353-63.

7. Lai, E.C., *Lipid rafts make for slippery platforms.* J Cell Biol, 2003. **162**(3): p. 365-70.

8. Jacobson, K. and C. Dietrich, *Looking at lipid rafts?* Trends Cell Biol, 1999. **9**(3): p. 87-91.

9. Simons, K. and D. Toomre, *Lipid rafts and signal transduction.* Nat Rev Mol Cell Biol, 2000. **1**(1): p. 31-9.

10. Helms, J.B. and C. Zurzolo, *Lipids as targeting signals: lipid rafts and intracellular trafficking.* Traffic, 2004. **5**(4): p. 247-54.

11. Field, K.A., D. Holowka, and B. Baird, *Fc epsilon RI-mediated recruitment of p53/56lyn to detergent-resistant membrane domains accompanies cellular signaling.* Proc Natl Acad Sci U S A, 1995. **92**(20): p. 9201-5.

12. Janes, P.W., et al., *The role of lipid rafts in T cell antigen receptor (TCR) signalling.* Semin Immunol, 2000. **12**(1): p. 23-34.

13. Krauss, K. and P. Altevogt, *Integrin leukocyte function-associated antigen-1-mediated cell binding can be activated by clustering of membrane rafts.* J Biol Chem, 1999. **274**(52): p. 36921-7.

14. Nichols, B.J., et al., *Rapid cycling of lipid raft markers between the cell surface and Golgi complex.* J Cell Biol, 2001. **153**(3): p. 529-41.

15. Nichols, B.J. and J. Lippincott-Schwartz, *Endocytosis without clathrin coats.* Trends Cell Biol, 2001. **11**(10): p. 406-12.

16. Laude, A.J. and I.A. Prior, *Plasma membrane microdomains: organization, function and trafficking.* Mol Membr Biol, 2004. **21**(3): p. 193-205.

17. Suomalainen, M., *Lipid rafts and assembly of enveloped viruses.* Traffic, 2002. **3**(10): p. 705-9.

18. Yang, C., C.P. Spies, and R.W. Compans, *The human and simian immunodeficiency virus envelope glycoprotein transmembrane subunits are palmitoylated.* Proc Natl Acad Sci U S A, 1995. **92**(21): p. 9871-5.

19. Zurcher, T., G. Luo, and P. Palese, *Mutations at palmitylation sites of the influenza virus hemagglutinin affect virus formation.* J Virol, 1994. **68**(9): p. 5748-54.

20. Bavari, S., et al., *Lipid raft microdomains: a gateway for compartmentalized trafficking of Ebola and Marburg viruses.* J Exp Med, 2002. **195**(5): p. 593-602.

21. Manie, S.N., et al., *Measles virus structural components are enriched into lipid raft microdomains: a potential cellular location for virus assembly.* J Virol, 2000. **74**(1): p. 305-11.

22. Brugger, B., et al., *The HIV lipidome: a raft with an unusual composition.* Proc Natl Acad Sci U S A, 2006. **103**(8): p. 2641-6.

23. Hermida-Matsumoto, L. and M.D. Resh, *Localization of human immunodeficiency virus type 1 Gag and Env at the plasma membrane by confocal imaging.* J Virol, 2000. **74**(18): p. 8670-9.

24.   Ono, A. and E.O. Freed, *Plasma membrane rafts play a critical role in HIV-1 assembly and release.* Proc Natl Acad Sci U S A, 2001. **98**(24): p. 13925-30.

25.   Bhattacharya, J., P.J. Peters, and P.R. Clapham, *Human immunodeficiency virus type 1 envelope glycoproteins that lack cytoplasmic domain cysteines: impact on association with membrane lipid rafts and incorporation onto budding virus particles.* J Virol, 2004. **78**(10): p. 5500-6.

26.   Lindwasser, O.W. and M.D. Resh, *Multimerization of human immunodeficiency virus type 1 Gag promotes its localization to barges, raft-like membrane microdomains.* J Virol, 2001. **75**(17): p. 7913-24.

27.   Graham, D.R., et al., *Cholesterol depletion of human immunodeficiency virus type 1 and simian immunodeficiency virus with beta-cyclodextrin inactivates and permeabilizes the virions: evidence for virion-associated lipid rafts.* J Virol, 2003. **77**(15): p. 8237-48.

28.   Campbell, S.M., S.M. Crowe, and J. Mak, *Virion-associated cholesterol is critical for the maintenance of HIV-1 structure and infectivity.* Aids, 2002. **16**(17): p. 2253-61.

29.   Guyader, M., et al., *Role for human immunodeficiency virus type 1 membrane cholesterol in viral internalization.* J Virol, 2002. **76**(20): p. 10356-64.

30.   Nguyen, D.H. and J.E. Hildreth, *Evidence for budding of human immunodeficiency virus type 1 selectively from glycolipid-enriched membrane lipid rafts.* J Virol, 2000. **74**(7): p. 3264-72.

31.   Orentas, R.J. and J.E. Hildreth, *Association of host cell surface adhesion receptors and other membrane proteins with HIV and SIV.* AIDS Res Hum Retroviruses, 1993. **9**(11): p. 1157-65.

32.   Cronin, J., X.Y. Zhang, and J. Reiser, *Altering the tropism of lentiviral vectors through pseudotyping.* Curr Gene Ther, 2005. **5**(4): p. 387-98.

33.   Giguere, J.F., et al., *Insertion of host-derived costimulatory molecules CD80 (B7.1) and CD86 (B7.2) into human immunodeficiency virus type 1 affects the virus life cycle.* J Virol, 2004. **78**(12): p. 6222-32.

34.   Thibault, S., et al., *Virus-associated host CD62L increases attachment of human immunodeficiency virus type 1 to endothelial cells and enhances trans infection of CD4+ T lymphocytes.* J Gen Virol, 2007. **88**(Pt 9): p. 2568-73.

35.   Verhoeyen, E., et al., *IL-7 surface-engineered lentiviral vectors promote survival and efficient gene transfer in resting primary T lymphocytes.* Blood, 2003. **101**(6): p. 2167-74.

36.   Breckpot, K., J.L. Aerts, and K. Thielemans, *Lentiviral vectors for cancer immunotherapy: transforming infectious particles into therapeutics.* Gene Ther, 2007. **14**(11): p. 847-62.

37. Chen, S.T., et al., *Generation of packaging cell lines for pseudotyped retroviral vectors of the G protein of vesicular stomatitis virus by using a modified tetracycline inducible system.* Proc Natl Acad Sci U S A, 1996. **93**(19): p. 10057-62.

38. Kavanaugh, M.P., et al., *Cell-surface receptors for gibbon ape leukemia virus and amphotropic murine retrovirus are inducible sodium-dependent phosphate symporters.* Proc Natl Acad Sci U S A, 1994. **91**(15): p. 7071-5.

39. Gummuluru, S., et al., *Binding of human immunodeficiency virus type 1 to immature dendritic cells can occur independently of DC-SIGN and mannose binding C-type lectin receptors via a cholesterol-dependent pathway.* J Virol, 2003. **77**(23): p. 12865-74.

40. Tardif, M.R. and M.J. Tremblay, *LFA-1 is a key determinant for preferential infection of memory CD4+ T cells by human immunodeficiency virus type 1.* J Virol, 2005. **79**(21): p. 13714-24.

41. Kueng, H.J., et al., *General strategy for decoration of enveloped viruses with functionally active lipid-modified cytokines.* J Virol, 2007. **81**(16): p. 8666-76.

42. Skountzou, I., et al., *Incorporation of glycosylphosphatidylinositol-anchored granulocyte- macrophage colony-stimulating factor or CD40 ligand enhances immunogenicity of chimeric simian immunodeficiency virus-like particles.* J Virol, 2007. **81**(3): p. 1083-94.

43. Kobinger, G.P., et al., *Filovirus-pseudotyped lentiviral vector can efficiently and stably transduce airway epithelia in vivo.* Nat Biotechnol, 2001. **19**(3): p. 225-30.

44. Pike, L.J., *Lipid rafts: heterogeneity on the high seas.* Biochem J, 2004. **378**(Pt 2): p. 281-92.

45. Jacobson, K., O.G. Mouritsen, and R.G. Anderson, *Lipid rafts: at a crossroad between cell biology and physics.* Nat Cell Biol, 2007. **9**(1): p. 7-14.

46. Doucette, M.M. and V.L. Stevens, *Folate receptor function is regulated in response to different cellular growth rates in cultured mammalian cells.* J Nutr, 2001. **131**(11): p. 2819-25.

47. Evans, L.H., et al., *A neutralizable epitope common to the envelope glycoproteins of ecotropic, polytropic, xenotropic, and amphotropic murine leukemia viruses.* J Virol, 1990. **64**(12): p. 6176-83.

48. Rubin, L.A., et al., *A monoclonal antibody 7G7/B6, binds to an epitope on the human interleukin-2 (IL-2) receptor that is distinct from that recognized by IL-2 or anti-Tac.* Hybridoma, 1985. **4**(2): p. 91-102.

49. Harlow, E. and D. Lane, *Storing and Purifying Antibodies*, in *Antibodies: A Laboratory Manual*. 1988, Cold Spring Harbor Laboratory Press: Cold Spring Harbor. p. 288-303.

50. Zufferey, R., et al., *Multiply attenuated lentiviral vector achieves efficient gene delivery in vivo.* Nat Biotechnol, 1997. **15**(9): p. 871-5.

51. Cosset, F.L., et al., *High-titer packaging cells producing recombinant retroviruses resistant to human serum.* J Virol, 1995. **69**(12): p. 7430-6.

52. Delahunty, M.D., et al., *Uncleaved signals for glycosylphosphatidylinositol anchoring cause retention of precursor proteins in the endoplasmic reticulum.* J Biol Chem, 1993. **268**(16): p. 12017-27.

53. Smith, R.F., *Microscopy and Photomicrography.* 2nd ed. 1994, Boca Raton: CRC Press. 162.

54. Rasband, W.S. *ImageJ.* [cited 2007 10-21]; Available from: http://rsb.info.nih.gov/ij/.

55. Abramoff, M., P. Magelhaes, and S. Ram, *Image processing with ImageJ.* Biophotonics International, 2004. **11**(7): p. 36-42.

56. Frank, I., et al., *Acquisition of host cell-surface-derived molecules by HIV-1.* Aids, 1996. **10**(14): p. 1611-20.

57. Ikezawa, H., *Glycosylphosphatidylinositol (GPI)-anchored proteins.* Biol Pharm Bull, 2002. **25**(4): p. 409-17.

58. Nguyen, D.G., et al., *Evidence that HIV budding in primary macrophages occurs through the exosome release pathway.* J Biol Chem, 2003. **278**(52): p. 52347-54.

59. Pelchen-Matthews, A., B. Kramer, and M. Marsh, *Infectious HIV-1 assembles in late endosomes in primary macrophages.* J Cell Biol, 2003. **162**(3): p. 443-55.

60. Kobayashi, T., A. Yamaji-Hasegawa, and E. Kiyokawa, *Lipid domains in the endocytic pathway.* Semin Cell Dev Biol, 2001. **12**(2): p. 173-82.

61. Halwani, R., et al., *Rapid localization of Gag/GagPol complexes to detergent-resistant membrane during the assembly of human immunodeficiency virus type 1.* J Virol, 2003. **77**(7): p. 3973-84.

62. Radeva, G. and F.J. Sharom, *Isolation and characterization of lipid rafts with different properties from RBL-2H3 (rat basophilic leukaemia) cells.* Biochem J, 2004. **380**(Pt 1): p. 219-30.

63. Brugger, B., et al., *The membrane domains occupied by glycosylphosphatidylinositol-anchored prion protein and Thy-1 differ in lipid composition.* J Biol Chem, 2004. **279**(9): p. 7530-6.

64. Schnitzer, J.E., et al., *Separation of caveolae from associated microdomains of GPI-anchored proteins.* Science, 1995. **269**(5229): p. 1435-9.

65. Wilson, B.S., et al., *Markers for detergent-resistant lipid rafts occupy distinct and dynamic domains in native membranes.* Mol Biol Cell, 2004. **15**(6): p. 2580-92.

66. Madore, N., et al., *Functionally different GPI proteins are organized in different domains on the neuronal surface.* Embo J, 1999. **18**(24): p. 6917-26.

67. Wang, J., et al., *Evidence for segregation of heterologous GPI-anchored proteins into separate lipid rafts within the plasma membrane.* J Membr Biol, 2002. **189**(1): p. 35-43.

68. Holm, K., et al., *Human immunodeficiency virus type 1 assembly and lipid rafts: Pr55(gag) associates with membrane domains that are largely resistant to Brij98 but sensitive to Triton X-100.* J Virol, 2003. **77**(8): p. 4805-17.

69. Finzi, A., et al., *Productive human immunodeficiency virus type 1 assembly takes place at the plasma membrane.* J Virol, 2007. **81**(14): p. 7476-90.

70. Jouvenet, N., et al., *Plasma membrane is the site of productive HIV-1 particle assembly.* PLoS Biol, 2006. **4**(12): p. e435.

71. Sherer, N.M., et al., *Visualization of retroviral replication in living cells reveals budding into multivesicular bodies.* Traffic, 2003. **4**(11): p. 785-801.

72. Campbell, S.M., S.M. Crowe, and J. Mak, *Lipid rafts and HIV-1: from viral entry to assembly of progeny virions.* J Clin Virol, 2001. **22**(3): p. 217-27.

73. Resh, M.D., *Intracellular trafficking of HIV-1 Gag: how Gag interacts with cell membranes and makes viral particles.* AIDS Rev, 2005. **7**(2): p. 84-91.

74. Nydegger, S., et al., *Mapping of tetraspanin-enriched microdomains that can function as gateways for HIV-1.* J Cell Biol, 2006. **173**(5): p. 795-807.

75. Jolly, C. and Q.J. Sattentau, *Human immunodeficiency virus type 1 assembly, budding, and cell-cell spread in T cells take place in tetraspanin-enriched plasma membrane domains.* J Virol, 2007. **81**(15): p. 7873-84.

76. Deneka, M., et al., *In macrophages, HIV-1 assembles into an intracellular plasma membrane domain containing the tetraspanins CD81, CD9, and CD53.* J Cell Biol, 2007. **177**(2): p. 329-41.

77. Sandrin, V. and F.L. Cosset, *Intracellular versus cell surface assembly of retroviral pseudotypes is determined by the cellular localization of the viral glycoprotein, its capacity to interact with Gag, and the expression of the Nef protein.* J Biol Chem, 2006. **281**(1): p. 528-42.

78. Sandrin, V., et al., *Intracellular trafficking of Gag and Env proteins and their interactions modulate pseudotyping of retroviruses.* J Virol, 2004. **78**(13): p. 7153-64.

79. Hammarstedt, M. and H. Garoff, *Passive and active inclusion of host proteins in human immunodeficiency virus type 1 gag particles during budding at the plasma membrane.* J Virol, 2004. **78**(11): p. 5686-97.

80. Bakht, O., P. Pathak, and E. London, *Effect of the Structure of Lipids Favoring Disordered Domain Formation on the Stability of Cholesterol-Containing Ordered Domains (Lipid Rafts): Identification of Multiple Raft-Stabilization Mechanisms.* Biophys J, 2007.

81. Bachrach, E., et al., *Effects of virion surface gp120 density on infection by HIV-1 and viral production by infected cells.* Virology, 2005. **332**(1): p. 418-29.

82. Logan, A.C., et al., *Factors influencing the titer and infectivity of lentiviral vectors.* Hum Gene Ther, 2004. **15**(10): p. 976-88.

83. Yuste, E., et al., *Modulation of Env content in virions of simian immunodeficiency virus: correlation with cell surface expression and virion infectivity.* J Virol, 2004. **78**(13): p. 6775-85.

84. Zavorotinskaya, T. and L.M. Albritton, *Failure To cleave murine leukemia virus envelope protein does not preclude its incorporation in virions and productive virus-receptor interaction.* J Virol, 1999. **73**(7): p. 5621-9.

85. Ono, A., A.A. Waheed, and E.O. Freed, *Depletion of cellular cholesterol inhibits membrane binding and higher-order multimerization of human immunodeficiency virus type 1 Gag.* Virology, 2007. **360**(1): p. 27-35.

86. Pickl, W.F., F.X. Pimentel-Muinos, and B. Seed, *Lipid rafts and pseudotyping.* J Virol, 2001. **75**(15): p. 7175-83.

87. Laliberte, J.P., et al., *Integrity of membrane lipid rafts is necessary for the ordered assembly and release of infectious Newcastle disease virus particles.* J Virol, 2006. **80**(21): p. 10652-62.

88. Barman, S. and D.P. Nayak, *Lipid raft disruption by cholesterol depletion enhances influenza A virus budding from MDCK cells.* J Virol, 2007.

89. Gosselin-Grenet, A.S., G. Mottet-Osman, and L. Roux, *From assembly to virus particle budding: pertinence of the detergent resistant membranes.* Virology, 2006. **344**(2): p. 296-303.

90. Simons, K. and E. Ikonen, *Functional rafts in cell membranes.* Nature, 1997. **387**(6633): p. 569-72.

91. Ding, L., et al., *Independent segregation of human immunodeficiency virus type 1 Gag protein complexes and lipid rafts.* J Virol, 2003. **77**(3): p. 1916-26.

92. Cross, G.A., *Glycolipid anchoring of plasma membrane proteins.* Annu Rev Cell Biol, 1990. **6**: p. 1-39.

93. Ikeda, M. and R. Longnecker, *Cholesterol is critical for Epstein-Barr virus latent membrane protein 2A trafficking and protein stability.* Virology, 2007. **360**(2): p. 461-8.

94.   Mayor, S., S. Sabharanjak, and F.R. Maxfield, *Cholesterol-dependent retention of GPI-anchored proteins in endosomes.* Embo J, 1998. **17**(16): p. 4626-38.

95.   Harder, T. and K. Simons, *Caveolae, DIGs, and the dynamics of sphingolipid-cholesterol microdomains.* Curr Opin Cell Biol, 1997. **9**(4): p. 534-42.

96.   Mays, R.W., et al., *Hierarchy of mechanisms involved in generating Na/K-ATPase polarity in MDCK epithelial cells.* J Cell Biol, 1995. **130**(5): p. 1105-15.

97.   Chatterjee, S., et al., *GPI anchoring leads to sphingolipid-dependent retention of endocytosed proteins in the recycling endosomal compartment.* Embo J, 2001. **20**(7): p. 1583-92.

CHAPTER 5

**IMPROVING INTERACTIONS WITH GAG INCREASES INCORPORATION OF
HUMAN PARAINFLUENZA TYPE 3 ENVELOPE PROTEINS**

5.1 <u>Abstract</u>

We have previously shown HPIV3 pseudotyped lentiviruses had titers too low to be useful for clinical gene transfer since the envelope proteins, HN and F, were not efficiently incorporated into lentivirus particles. We reasoned that incorporation was low because interactions between HN and F, or HN and F with lentiviral Gag were low. We found that HN and F were colocalized with each other, however HN and F were not as colocalized with Gag or lipid rafts as amphotropic Env. We then hypothesized that increasing interactions of HN and F with Gag would enhance their incorporation into lentiviral particles. To test this hypothesis, we used two main approaches: 1) we created HN and HIV Env fusion proteins that would actively interact with Gag, and 2) we disrupted the barriers that prevented HN and F from passively interacting with Gag. We found that when HN fusion proteins were created with portions of HIV gp41's cytoplasmic domain, HN-mpr and HN-LLP2, colocalization of the HN chimeras with Gag increased slightly from unmodified HN. The level of incorporation also increased 1.6-fold and 2.2-fold, respectively, however titers significantly decreased at least 25-fold. We then determined whether increased colocalization with Gag was sufficient for envelope protein incorporation. Previously we found small concentrations of methyl-beta-cyclodextrin (MβCD) disturbed lipid rafts such that raft proteins segregated by lipid rafts could inter-mix with lentivirus-associated rafts and become incorporated into virus particles. When lentiviruses pseudotyped with HPIV3 (HPIV3 LV) or amphotropic Env (Ampho LV) producer cells were treated with 0.5 mM MβCD for 54 hours after

transfection, titers of HPIV3 LV increased 6.4-fold while titers of Ampho LV decreased 3.6-fold. When we analyzed the amount of envelope incorporation from MβCD treated producer cells, we found the amount of amphotropic Env in virus particles decreased 3.0-fold while the amount of HN increased 1.4-fold. This data suggested that increasing interactions of HPIV3 envelope proteins with Gag through active and passive interactions enhanced HN and F incorporation into lentiviral particles.

5.2 <u>Introduction</u>

Lentivirus vectors have the potential to be useful tools for tissue engineering, prevention of disease, and for treatment of inherited diseases, infectious diseases, and cancer [1-4]. They offer attractive properties such as permanent integration, ability to transduce non-dividing cells, and ability to alter their tropism and target specific cells through replacement of the wild-type envelope protein [5]. However, pseudotyping lentiviruses can be very challenging. In the case of generating lentiviral vectors for respiratory diseases, many lung-tropic viruses including influenza, respiratory syncytial virus, Ross River virus, and Jaagsiekte sheep retrovirus [6-8], either do not pseudotype well, do not transduce polarized airway cells via their apical surfaces, or do not do so efficiently.

In addition to viral proteins, lentiviruses incorporate many host cell proteins during the lentivirus assembly process [9-11]. However, not all proteins are included as some are specifically excluded such as CD45, flotillin, and CD14 [12-16]. Generally, proteins are incorporated into virus particles if there are direct interactions between the cytoplasmic domain of the protein with Gag, the lentivirus core protein, or passive interactions with Gag [12, 16-18]. The only requirements for passive incorporation are to be present at the site of lentiviral budding and to have a cytoplasmic domain that is not sterically incompatible with virus assembly [19].

The assembly and budding of lentiviruses is driven by the oligomerization of Gag [20]. In cell lines such as 293T, Gag either is targeted directly to the plasma membrane [21, 22], or first to multivesicular bodies and then transported to the plasma membrane [23]. Gag has been shown to use lipid rafts, plasma membrane subdomains enriched in cholesterol, sphingolipids, and glycosphingolipids, as sites of assembly and budding [24]. Besides lipid rafts in general [15, 25-27], tetraspanin-containing regions have also been implicated as assembly and budding sites [28-30] although rafts and tetraspanin-enriched domains have not yet been shown to be exclusive.

Previously, we have shown envelope proteins F and HN from human parainfluenza virus type 3 (HPIV3), a lung-tropic virus, can pseudotype lentiviruses and that these viruses can infect polarized cells via their apical surfaces [31]. However titers of HPIV3 pseudotyped lentiviruses are low mainly because too few envelope proteins are incorporated [32]. In this study, we tested the hypothesis that increasing interactions with Gag will enhance HN and F incorporation into lentiviral particles. The implications of our findings for the generation of pseudotyped lentiviruses useful for clinical gene transfer are discussed.

5.3 <u>Materials and Methods</u>

Chemicals and antibodies. Poly-L-lysine, 1,5-Dimethyl-1,5-diazaundecamethylene polymethobromide (Polybrene), saponin, o-phenylenediamine dihydrochloride (OPD), methyl-β-cyclodextrin, gluteraldehyde, paraformaldehyde, and 5-Bromo-4-chloro-3-indolyl-β-D-galactopyranoside (X-Gal) were purchased from Sigma Chemical (St. Louis, MO). Complete mini protease inhibitor cocktail tablets were purchased from Roche Diagnostics (Indianapolis, IN). Hydrogen peroxide 30%, Triton X-100, and polyoxyethylene 20-sorbitan monolaurate (Tween 20) were purchased from Fisher Scientific (Fair Lawn, NJ). Coomassie Plus-200 protein assay reagent was

purchased from Pierce (Rockford, IL). Nonfat dry milk (blotting grade) was purchased from Bio-Rad Laboratories (Hercules, CA).

Goat polyclonal antibody to HIV-1 p24 was purchased from Advanced Biotechnologies Incorporated (Columbia, MD). Mouse ascites monoclonal antibody 66/4 and 170 against HPIV3-HN were generously provided by Judy Beeler (WHO Programme for Vaccine Development Reagent Bank for Respiratory Syncytial Virus and Parainfluenza Type 3). Mouse monoclonal antibody against HPIV3 HN was purchased from Fitzgerald Industries International, Inc. (Concord, MA). Mouse ascites monoclonal antibody c110 against HPIV3-F was generously provided by B.R. Murphy, Respiratory Viruses Section, NIAID, NIH (Bethesda, MD). Goat polyclonal anti-gp70 (79S834) was purchased from Quality Biotech (Camden, NJ). Mouse anti-gp70 antibodies were purified from the supernatant of the 83A25 hybridoma cell line [33] following standard procedures [34]. Cy2-conjugated, Cy-3 conjugated, and horseradish peroxidase (HRP)-conjugated antibodies, and normal donkey serum were purchased from Jackson Immunoresearch Laboratories, Inc. (West Grove, PA).

Cell culture. 293T/17 cells were maintained in Dulbecco's modified essential medium (DMEM) supplemented with 10% heat inactivated fetal bovine serum (FBS), 100 U/mL of penicillin, and 100 μg/mL streptomycin (HyClone Laboratories; Logan, UT). Vero cells were maintained in Minimum essential medium (Eagle) supplemented with 10% fetal bovine serum, 100 U/mL of penicillin, and 100 μg/mL streptomycin. Plates coated with poly-L-lysine were incubated for 5 min in the 0.01% solution (150-300 kDa), washed once with deionized water, and dried.

HN Chimeras. A pCAGGS derived expression plasmid (pCAGGS-HPIV3-HN-mpr) encoding for the 43 amino acid gp41 cytoplasmic domain appended to HPIV3-HN with the structure 5'- *Cla*I site - reversed gp41 cytoplasmic domain – HN envelope protein – *Nhe*I site – 3' was constructed as follows: (1) oligos encoding for the reversed

sequence of the 43 amino acids after the gp41 transmembrane domain and restriction sites *Nhe*I and *Xba*I were mixed in equal amounts in STE buffer, heated to 94^{0}C in a PCR machine for 5 min, and the temperature lowered by 15 degrees every 5 min until 4^{0}C. The oligo sequences are as follows: Gp41-mpr-top: CTAGCGTGTTACGAATTTCCAGAGACAGAGACAGAGAGGGAGGTGAAGAAGAAATA GGAGAACCCAGGGACCCCGGAAGGCCGATCCCACTCCACACCCAGTTTTCGTTAC CATCATATGGACAGAGGGTTAGAT, and gp41-mpr-bottom: CTAGATCTAACCCTCTGTCCATATGATGGTAACGAAAACTGGGTGTGGAGTGGGAT CGGCCTTCCGGGGTCCCTGGGTTCTCCTATTTCTTCTTCACCTCCCTCTCTGTCTCT GTCTCTGGAAATTCGTAACACG. Samples were run on a 2% agarose gel, extracted, digested, and ligated into the *Nhe*I and *Xba*I sites in pcDNA3.1+/Neo vector (Invitrogen). (2) The pcDNA3.1 gp41-mpr sequences were then PCR amplified with primers gp41mprHN-gFOR: TAGGCGATCGATATGGTGTTACGAATTTCCAGAGAC and gp41mprHN-hREVsewg: TGGTATGCTTCCAGTATTCCATTCTAACCCTCTGTCCATA. (3) The HN sequence from pCAGGS-HPIV3-HN was PCR amplified with primers gp41mprHN-gFORsewh: TATGGACAGAGGGTTAGAATGGAATACTGGAAGCATACCA and HN-REV: CATGGACGTCTCCAGCTCATTGCCAGC. (4) The PCR products of (2) and (3) were separated by agarose gel, extracted, and PCR amplified (75 ng each PCR product) with primers gp41mprHN-gFOR and HN-REV. The final PCR product was digested with *Cla*I and *Nhe*I and ligated back into the pCAGGS backbone. The sequence of pCAGGS-HPIV3-HN-mpr was verified by DNA sequencing.

Similarly, a pCAGGS derived expression plasmid (pCAGGS-HPIV3-HN-LLP2) encoding for the 31 amino acid alpha helix 2 of the gp41 cytoplasmic domain appended to HPIV3-HN with the structure 5'- *Cla*I site - reversed gp41 LLP2 cytoplasmic domain – HN envelope protein – *Nhe*I site – 3' was constructed as follows: (1) oligos encoding for the reversed sequence of the 31 amino acids of the alpha helix 2 domain from the

cytoplasmic tail and restriction sites *Nhe*I and *Xba*I were mixed in equal amounts in STE buffer, heated to 94^0C in a PCR machine for 5 min, and the temperature lowered by 15 degrees every 5 min until 4^0C. The oligo sequences are as follows: Gp41LLP2Rtop: CTAGCATCGATATGCTCGCCGAATGGGGGAGGCGCGGACTGCTTGAAGTGATTAG GACGGTAATTTTGCTCTTAGACAGATTGCGCCACTACAGCTTCCTCTGCCTGT and GP41LLP2Rbot:

CTAGACAGGCAGAGGAAGCTGTAGTGGCGCAATCTGTCTAAGAGCAAAATTACCGT CCTAATCACTTCAAGCAGTCCGCGCCTCCCCCATTCGGCGAGCATATCGATG.

Samples were run on a 2% agarose gel, extracted, digested, and ligated into the *Nhe*I and *Xba*I sites in pcDNA3.1+/Neo vector (Invitrogen). (2) The pcDNA3.1 gp41-mpr sequences were then PCR amplified with primers gp41LLP2R-gFOR: ATATAATCGATATGCTCGCCGAATGGGGGAG and gp41LLP2R-hREVsewg: TATGCTTCCAGTATTCCATCAGGCAGAGGAAGCTGTA. (3) The HN sequence from pCAGGS-HPIV3-HN was PCR amplified with primers gp41LLP2R-gFORsewh: CTACAGCTTCCTCTGCCTGATGGAATACTGGAAGCATAC and HN-REV: CATGGACGTCTCCAGCTCATTGCCAGC. (4) The PCR products of (2) and (3) were separated by agarose gel, extracted, and PCR amplified (75 ng each PCR product) with primers gp41LLP2R-gFOR and HN-REV. The final PCR product was digested with *Cla*I and *Nhe*I and ligated back into the pCAGGS backbone. The sequence of pCAGGS-HPIV3-HN-mpr was verified by DNA sequencing.

Virus production. Human parainfluenza virus type 3 (strain Wash/57/47885), obtained from the National Institute of Allergy and Infectious Disease (Bethesda, MD), was propagated on monolayers of Vero cells. Lentiviruses pseudotyped with the amphotropic or human parainfluenza virus type 3 envelope proteins were produced by transfecting 293T/17 cells, seeded (1×10^7 per well) the previous day on poly-L-lysine coated plates with Lipofectamine 2000 (Invitrogen; Carlsbad, CA) and 6 μg of the

packaging construct pCMVΔR8.91 [35], 6 μg of the lentivirus vector pTYEFnlacZ or pTYEFeGFP (AIDS Research and Reference Reagent Program; Bethesda, MD), and 6 μg of the amphotropic envelope protein expression plasmid pFB4070ASALF [36] or 6 μg each of the HPIV3 F and codon optimized HN envelope expression plasmids (i.e., pCAGGS-hPIV3-F and co-pCAGGS-hPIV3-HN, respectively). The following day, producer cells may have been treated with 0.5 mM MβCD. Viral supernatants were collected every 12 h from 48 to 60 h after transfection, filter sterilized (0.45 μm), and frozen (-80°C) for later use. Viruses were concentrated by incubation with 320 μg/mL polybrene for 30 min at 37^0C and centrifuging at 10,000 g for 30 min at room temperature [37]. For cholesterol measurement, the Amplex red cholesterol assay kit (Invitrogen) was used according to manufacturer's instructions. Codon-optimization of HPIV3-HN was performed by GENEART, Inc (Toronto, Canada). The cDNA was subcloned into the *Cla I* and *Sph I* sites of the pCAGGS.MCS expression vector [38] and the structure of the ligation sites was verified by DNA sequencing.

Metabolic labeling. To detect proteins in virus stocks and producer cells, cells were transfected as above with 6 μg each of pCMVΔR8.91, pTYEFnlacZ, pCAGGS-hPIV3-F, and either co-pCAGGS-hPIV3-HN, pCAGGS-hPIV3-HN-LLP2, or pCAGGS-hPIV3-HN-mpr for twenty-four hours. Cells were then incubated with methionine and cysteine-free DMEM for 15 min at 37°C and radiolabeled for 16 h at 37°C with 500 μCi of [35S]methionine-cysteine protein labeling mix (GE Healthcare; Piscataway, NJ). Virus samples were obtained by ultracentrifugation of the viral supernatants in a SW41Ti Beckman rotor (150,000 x g, 2 h, 4°C) through a 20% sucrose cushion after which the pellets were resuspended in RIPA buffer (50 mM Tris- HCl [pH 7.6], 150 mM NaCl, 0.5% Triton X-100, 0.5% sodium deoxycholate, 0.1% SDS, and protease inhibitors) for 30 min at 25°C. The proteins were separated by size by SDS-PAGE (4-15%), and then the gel dried (72°C for 45 min) and visualized by autoradiography (Bio-Max MR film; Amersham;

119

Piscataway, NJ). To quantitatively compare the amount of protein that was visualized as bands on the film, we used ImageJ to measure the band area and intensity and compared the product of the two values. We also compared the amount of radioactivity that was in the bands. We cut out the bands from the gels as slices, brought their volume to 3 mL with Ecoscint A scintillation cocktail (National Diagnostics, Atlanta, GA), and used a scintillation counter (Tricarb 2900TR; Perkin Elmer) to quantify the amount of ^{35}S in the samples.

Indirect immunofluorescence. To detect the presence of Gag and surface proteins, cells were seeded (1×10^5 per well) the previous day on poly-L-lysine coated 12-well plates containing coverslips (no. 1.5, 12 mm, Fisher Scientific; Suwanee, GA). Cells were then transfected with Polyfect (Qiagen, Valencia, CA) according to manufacturer's instructions. The next day cells were incubated with 4% paraformaldehyde (0.5 mL/well) for 15 min and then blocked with PBS/sera (0.5 mL/well) (5% donkey sera in PBS) for 10 min. Cells were then incubated with primary antibody for 1 hour at room temperature in PBS/sera/0.2% saponin (1:500), washed 3 times with PBS, incubated with the secondary antibody for 1 hour at room temperature in PBS/sera/0.2% saponin (1:500), and then washed three times with PBS and once with distilled water. Some cells were immunostained (1:250 in PBS/sera/0.2% saponin) with 488-conjugated anti-F (c110) or anti-HN (170) antibodies labeled with DyLight antibody labeling kit according to manufacturer's instructions (Rockford, IL). Cells also may or may not have been labeled with 5 µg/mL A594-conjugated cholera toxin B subunit in PBS for 1 hour (Invitrogen) and washed three times. Coverslips were mounted on glass slides with gelvatol [39] at 4^0C. The next day cells were visualized by confocal microscopy at 63X. For each condition, eight cells were chosen at random and extent of colocalization was quantified by calculating the Pearson's overlap coefficient with ImageJ [40]and the Colocalisation Threshold plugin (Tony Collins, Wayne Rasband, and Kevin Baler). This calculation is

120

based on the overlap of red and green pixels, with a high degree of overlap corresponding to a value of 1 and a low degree of overlap corresponding to a value of 0 [41]. Coefficients for eight separate cells were averaged and statistical significance was determined.

Immunoblotting and lipid raft isolation. To detect wild-type HN in raft samples, 293T/17 cells, seeded (1×10^7 per well) the previous day on poly-L-lysine coated plates, were infected with wild-type HPIV3 at an MOI of 1. Cells were then pelleted with versene (PBS and 5 mM EDTA pH 7.5) and resuspended in 1 mL of ice-cold 1% Triton X-10 in TNE buffer (25 mM Tris-base, 0.15 M sodium chloride, 5 M EDTA, pH 7.5). Lysates were dounce homogenized, adjusted to 40% sucrose by adding an equal volume of 80% sucrose in TNE buffer and placed in ultracentrifuge tubes. Samples were then overlaid with 5 mL of ice-cold 38% sucrose in TNE followed by 4 mL of ice-cold 5% sucrose in TNE and centrifuged at 30,000 rpm for 15 hours at 4^0C in an SW41 rotor (Beckman Coulter, Palo Alto, CA). The proteins at the interface of the 5% and 30% sucrose solutions was isolated, mixed with ice-cold TNE buffer, and then centrifuged at 30,000 rpm for 1 hour at 4^0C in a SW41. The pelleted lipid raft fraction was resuspended in 100 µL of TNE buffer. Equal amounts of protein from each sample were combined 1:2 (v/v) with sample buffer containing 5% β-mercaptoethanol (both from Bio-Rad; Hercules, CA), vortexed, boiled for 5 min, separated by size by SDS-PAGE (4-20% Tris-HCl gel, Bio-Rad), and transferred to a PVDF membrane (0.2 *µ*m, Bio-Rad). To probe for HN in the membrane, mouse monoclonal antibody against HN was diluted 1:1000 in blocking buffer (5% nonfat milk in PBS with 0.1% Tween 20) and bound IgG was detected by incubation with HRP-conjugated donkey anti-mouse (diluted 1:400,000 in blocking buffer), and detected with a chemiluminescent detection system (Super Signal West Femto kit; Pierce). To probe for amphotropic Env, amphotropic Env pseudotyped lentivirus was generated as before. Virus samples were obtained by

ultracentrifugation of the viral supernatants in a SW41Ti Beckman rotor (150,000 x g, 2 h, 4°C) through a 20% sucrose cushion after which the pellets were resuspended in RIPA buffer. The proteins were separated by size by SDS-PAGE (4-15%), transferred to a PVDF membrane, and blotted as described previously. For detection, goat anti-gp70 antibody 79S834 was diluted 1:1000 in blocking buffer followed by HRP-conjugated donkey anti-goat (1:400,000 in blocking buffer). To quantitatively compare the amount of protein that was visualized as bands on the film, we used ImageJ to measure the band area and intensity and compared the product of the two values.

p24 ELISA. We used p24 ELISA to quantitatively compare the amount p24 viral supernatant. ELISA plates (Nunc immuno Maxisorp 96-well plates, Nalgene Nunc International, Rochester, NY) were coated overnight at 37^0C with 1:800 dilution of mouse anti-p24 antibody 183-H12-5C (100 µL/well) in PBS. The next day, the antibody solution was removed and wells were washed twice (PBS, 0.05% Tween-20). Blocking buffer (PBS, 0.05% Tween-20, 5% non-fat milk) was added at 200 µL/well for 1 hour at 37^0C and removed. Samples were lysed in 2% Triton X-100 1:1 and added to the ELISA plate (100 µL/well), and incubated for 2 hours at 37^0C. Bound p24 was sandwiched by the addition of the sheep polyclonal anti-p24 antisera diluted 1:250 in blocking buffer, and incubated for 2 hours at 37^0C. The HRP-conjugated anti-sheep secondary antibody was diluted 1:1000 in blocking buffer and added to the ELISA plate (100 µL/well) for 1 hour at 37^0C. Plates were then developed for 20 min using a solution (100 µL/well) of 3 mg of OPD, 3 µL hydrogen peroxide, 7.5 mL substrate buffer (24 mM citric acid-monohydrate, 51 mM $Na_2HPO_4*7H_2O$, pH 5.0). 8N sulfuric acid (50 µL/well) was used to stop the reaction and the optical density at 490 nm was measured using an absorbance plate reader (non-specific background at 650 nm was subtracted). Values for each point are the average of at least triplicate wells.

Transduction. 293T cells were seeded in poly-L-lysine coated 12-well plates (1x10^5 cells per well) and incubated at 37°C. The next day, viral supernatant dilutions were incubated with cells for 48 h, after which the cells were fixed with gluteraldehyde and stained for β-galactosidase activity with X-Gal, and the number of *lacZ*+ colony-forming units (CFU) per milliliter was counted.

Statistics. Data are summarized as the mean ± the standard deviation for at least triplicate samples. Statistical analysis was performed using one-way analysis of variance for repeated measurements of the same variable. The Tukey multiple comparison test was used to conduct pairwise comparisons between means. Differences at *p* < 0.05 were considered statistically significant.

5.4 Results

We have previously shown that lentiviruses incorporated too few HPIV3 envelope proteins (HN and F) for high transduction efficiency [32]. We reasoned that incorporation was low because interactions between HN and F, or HN and F with lentiviral Gag were low. To determine whether HN and F could interact in producer 293T cells, we analyzed the amount of colocalization between the envelope proteins. We transfected 1x10^5 293T cells on glass coverslips with plasmids encoding for HPIV3-F and HPIV3-HN. The next day cells were fixed, permeabilized, and immunostained with a mouse monoclonal antibody against F (c110) followed by a Cy3-conjguated secondary antibody, and a mouse monoclonal antibody against HN (170) conjugated to A488 (Figure 5.1). Cells were visualized by confocal microscopy and the extent of colocalization between F and HN was quantified by calculating the Pearson's overlap coefficient. We found a high degree of colocalization between F and HN as shown by the overlapping of corresponding red and green pixels producing a yellow color, and also shown by the high Pearson's coefficient number (0.88 ± 0.031). This indicated HN and
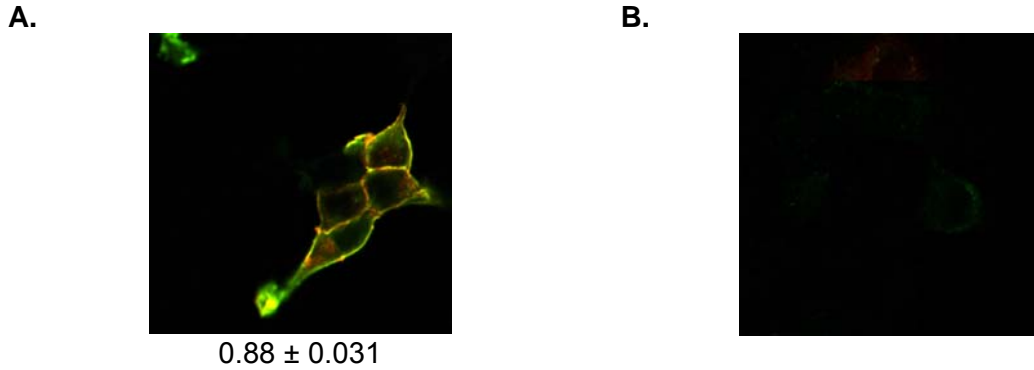
123

A.   **B.**

0.88 ± 0.031

Figure 5.1. HPIV3-F and HPIV3-HN colocalize with each other. 293T cells were transiently transfected to express HPIV3-F and HPIV3-HN (A). As a control, cells were not transfected (B). Cells were fixed, permeabilized, and immunostained with a mouse monoclonal antibody (c110) against F followed by donkey anti-mouse Cy3 conjugated secondary antibody, and then a mouse monoclonal antibody (170) against HN conjugated to A488. Cells were visualized with confocal microscopy at 63X and overlays of F (red) and HN (green) are shown. Eight cells were chosen at random and extent of colocalization between F and HN was quantified with ImageJ.

	Ampho	F	HN
Gag	0.87 ± 0.042	0.78 ± 0.13	0.67 ± 0.083*
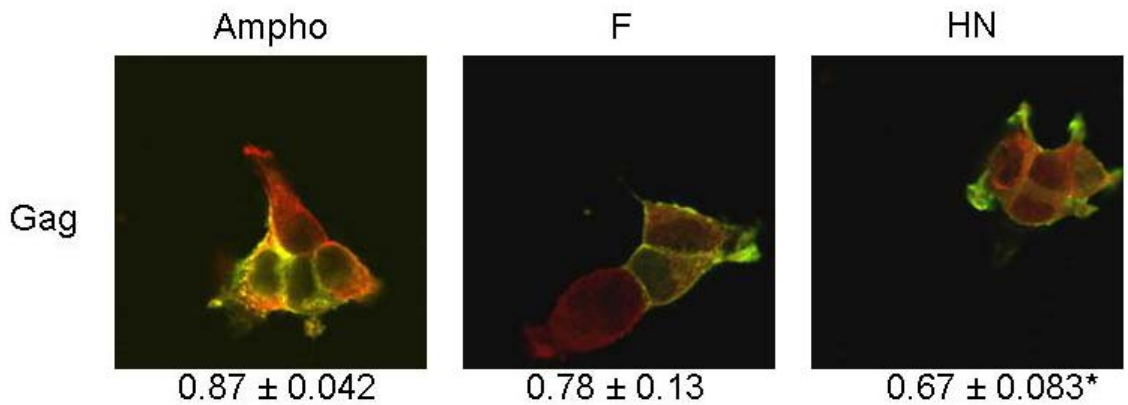
Figure 5.2. HPIV3-F and HPIV3-HN are not highly colocalized with Gag. 293T cells were transiently transfected to express HIV-1 Gag-Pol (Gag) and either amphotropic Env (Ampho) or HPIV3-F (F) and HPIV3-HN (HN). Cells were fixed, permeabilized, and immunostained with a mouse monoclonal antibody against Gag, followed by donkey anti-mouse Cy3 conjugated secondary antibody. Corresponding cells were also stained with a rat antibody against amphotropic Env (83A25) followed by donkey anti-rat Cy2 conjugated secondary antibody, or a mouse monoclonal antibody against HN (170) or F (b108) conjugated to A488. Cells were visualized with confocal microscopy at 63X and overlays of Gag (red) with Ampho, F, or HN (green) are shown. Eight cells were chosen at random and extent of colocalization was quantified with ImageJ. Statistically significant differences (P<0.05) in colocalization values between Ampho and F or HN colocalized with Gag are denoted with *.

F can interact with each other and can together be incorporated into a budding lentiviral particle since they are located in the same area.

To determine whether HN and F could interact with Gag in HPIV3-lentivirus producer cells, we analyzed the amount of colocalization between the proteins. 293T cells (1×10^5) on coverslips were transiently transfected to express HIV-1 Gag-Pol (Gag), HPIV3-F (F), and HPIV3-HN (HN). Cells were fixed, permeabilized, and immunostained with a mouse monoclonal antibody against Gag, followed by a Cy3 conjugated secondary antibody. Corresponding cells were also stained with a rat antibody against amphotropic Env followed by an anti-rat Cy2-conjugated secondary antibody, or a mouse monoclonal antibody against HN or F conjugated to A488. Cells were visualized by confocal microscopy and the extent of colocalization was quantified by calculating the Pearson's overlap coefficient with ImageJ (Figure 5.2). As a positive control, cells were also transfected and stained for Gag and the amphotropic Env, which is highly incorporated into lentiviral particles [42]. As expected, amphotropic Env was strongly colocalized with Gag (0.87 ± 0.042). Interestingly, F and HN were less colocalized with Gag (0.78 ± 0.13 ($p>0.05$) and 0.67 ± 0.083 ($p<0.05$), respectively) than amphotropic Env was, particularly HN. This strongly suggested the reason for low incorporation of HN and F was the lack of available interaction with Gag.

Since HN was the least colocalized with Gag, we constructed two chimeric HN proteins modified with sequences from the cytoplasmic domain of the HIV-1 glycoprotein gp41 to examine the effects of increasing interactions with Gag (Figure 5.3). The N-terminal cytoplasmic domain of HN was attached to the inverted 31 amino acid sequence of the gp41 helix2 (HN-LLP2) or the inverted sequence of the first 43 amino acids of the gp41 cytoplasmic tail (HN-mpr), which have both been shown to interact with HIV-1 matrix and the plasma membrane [43] [44-46]. To see if the chimeric HN proteins interacted more with Gag, 293T cells were transfected with plasmids expressing
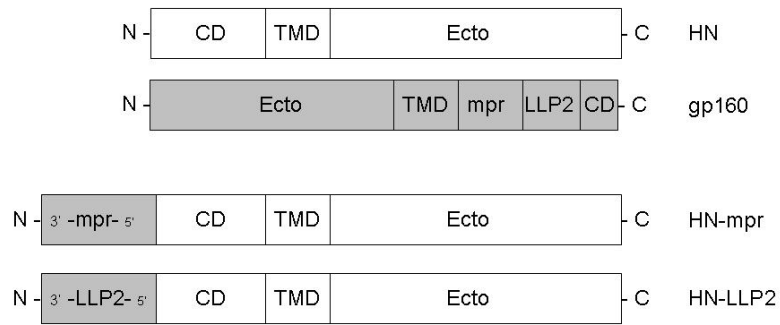
Figure 5.3. Schematic diagram of HN chimeras. Schematic diagrams of the structure of wild-type HIV gp160 envelope protein, wild-type HPIV3-HN envelope protein, and chimeras HN-mpr and HN-LLP2 are shown. The positions of some of the functional regions are indicated: CD, cytoplasmic domain; TMD, transmembrane domain; Ecto, ectodomain; mpr, transmembrane proximal region; LLP2, LLP2 region; N, N-terminus; C, C-terminus.
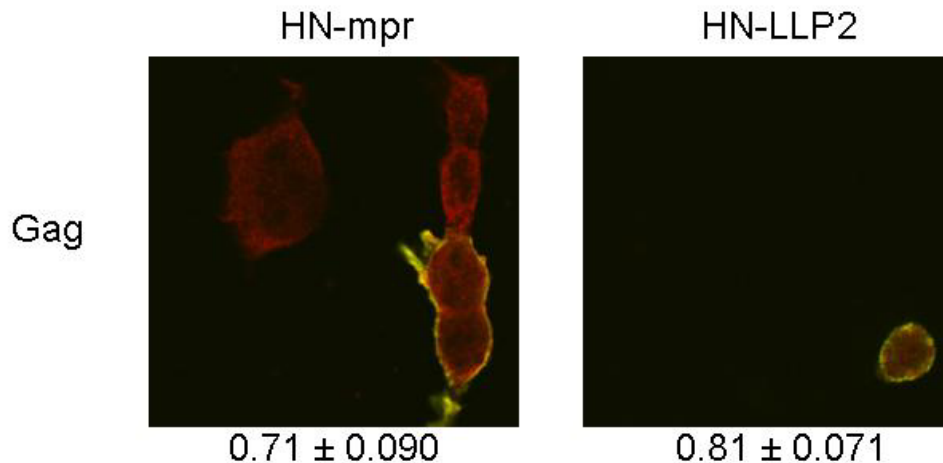
Figure 5.4. HN chimeras demonstrate increased colocalization with Gag. 293T cells were transiently transfected to express HIV-1 Gag-pol (Gag), HPIV3-F, and either HN-mpr or HN-LLP2. Cells were fixed, permeabilized, and immunostained with a mouse monoclonal antibody against Gag, followed by donkey anti-mouse Cy3 conjugated secondary antibody. Cells were also stained with a mouse monoclonal antibody against HN (170) conjugated to A488. Cells were visualized with confocal microscopy at 63X and overlays of Gag (red) with HN chimeras(green) are shown. Eight cells were chosen at random and extent of colocalization was quantified with ImageJ.

Gag-Pol and either HN-LLP2 or HN-mpr. The next day cells were fixed, permeabilized, and stained with a mouse monoclonal antibody against Gag, followed by an anti-mouse Cy3-conjugated secondary antibody, and also a monoclonal antibody against HN conjugated to A488. Cells were visualized by confocal microscopy and the extent of colocalization was quantified by calculating the Pearson's overlap coefficient with ImageJ (Figure 5.4). The amount of colocalization between the HN chimeras and Gag increased slightly (HN-LLP2 with Gag was 0.81 ± 0.071, p=0.06, and HN-mpr with Gag was 0.71 ± 0.09, p=0.21).

We next measured the amount of HN-LLP2 or HN-mpr incorporated into lentiviral particles.   293T cells (1×10^7) were transfected with expression plasmids for β-galactosidase, HIV-1 Gag-Pol, HPIV3-F, and either HPIV3-HN, HN-LLP2, or HN-mpr. The next day, cells were metabolically-labeled with 500 µCi [35S] methionine and cysteine for 18 h, after which culture supernatant were harvested, ultracentrifuged through a 20% sucrose cushion, and then resuspended in PBS to 100-fold their original concentration. Samples were then separated by size by SDS-PAGE, and then the gel dried and visualized by autoradiography (Figure 5.5). We found that incorporating sequences from the gp41 cytoplasmic tail increased the amount of the HN incorporated into lentiviral particles. To quantify the amount of HN in each sample, we excised the bands that contained HN from the gel, measured their radioactivity with a scintillation counter, and normalized the amount to radioactive p24. We found that HN-mpr was incorporated into lentiviral particles 1.6-fold more, and HN-LLP2 was incorporated 2.2-fold more than unmodified HN.

To determine whether the HN chimeras were functional in lentiviral particles, we generated viruses as before and used them to transduce target cells in a diluted titer assay. We also measured the amount of particles produced (Table 5.1). We found that producer cells transfected with the HN chimeras produced less virus particles, and those
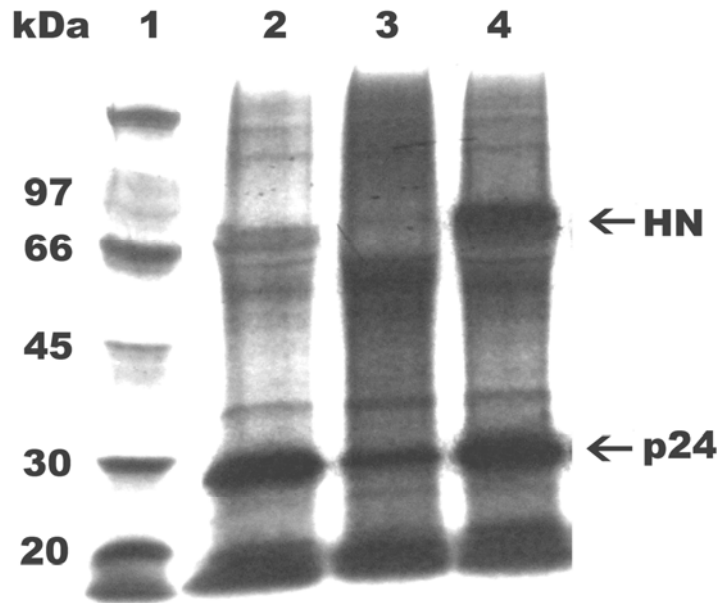
127

Figure 5.5. The number of envelope proteins incorporated by lentiviruses are higher with HN chimeras than normal HN. 293T cells (1×10^7) were transfected with expression plasmids (6 µg each) for β-galactosidase, HIV-1 Gag-Pol, HPIV3-F, and either HPIV3-HN (Lane 2), HN-LLP2 (Lane 3), or HN-mpr (Lane 4). The next day, cells were serum-starved for 15 min, metabolically-labeled with 500 µCi [35S] methionine and cysteine for 18 h, after which culture supernatant were harvested, ultracentrifuged through a 20% sucrose cushion, and then resuspended in PBS to 100-fold their original concentration. Samples were resuspended in lysis buffer, separated by size by SDS-PAGE, and then the gel dried and visualized by autoradiography.

Table 5.1. Lentivirus titers of HN chimeras and F.

Pseudotype	Titer (CFU/mL)[a]	p24 Amount (OD$_{490-650}$)[b]	Normalized Titer
HN+F LV	$2.7 (\pm 0.52) \times 10^3$	0.30 ± 0.028	$9.2 (\pm 2.0) \times 10^3$
HN-mpr + F LV	$8.3 (\pm 2.8) \times 10^1$	0.19 ± 0.005	$4.4 (\pm 1.5) \times 10^2$
HN-LLP2 + F LV	$5.0 (\pm 1.0) \times 10^0$	0.17 ± 0.012	$3.0 (\pm 0.63) \times 10^1$

Lentiviruses pseudotyped with HN and F (HN+F LV), HN-mpr and F (HN-mpr +F LV), or HN-LLP2 and F (HN-LLP2 + F LV) were used to transduce 293T cells. Titer of [a]lentiviral pseudotypes (CFU/mL) and [b]p24 levels (OD$_{490-650}$) represent the mean of experimental values +/- standard deviation. Normalized titer was obtained by normalizing titer to corresponding p24 amount.

128

virus particles were very inefficient at transducing cells. When titer was normalized by the amount of p24 produced, viruses containing HN-mpr was 20-fold less efficient than viruses containing normal HN, and viruses containing HN-LLP2 was 300-fold less efficient.

Because appending gp41 sequences to the HN chimeras may have altered the structure and subsequent binding and/or fusion activation function of HN, we investigated other less disruptive methods of increasing associations of Gag with HPIV3 envelope proteins. Since the above data suggested HN and F did not localize with Gag, we wanted to further characterize the location of HN in the cell. Gag has been shown to be localized to and bud out of lipid rafts in the cell [47]. To determine whether HN was localized to lipid rafts or merely present, we infected 293T cells with wild-type HPIV3 at an MOI of 1. Cells were then lysed with ice-cold Triton X-100 and subject to equilibrium flotation centrifugation. Detergent resistant membranes were isolated, pelleted, and analyzed by Western blot for the presence of HN (Figure 5.6). Wild-type infected HN did not appear to be enriched in lipid rafts although it was present in rafts.

In our previous chapter, Chapter 4, we showed lipid rafts segregated raft proteins, and for a protein to be incorporated into virus particles, it must be colocalized with lentivirus-associated rafts. We also showed we were able to disturb the integrity of lipid rafts with the cholesterol extracting compound, methyl-beta-cycodextrin (MβCD), such that raft proteins segregated away from lentivirus-associated rafts were associated with lentivirus proteins and incorporated into lentiviral particles. We investigated whether MβCD would increase the presence of HN or F with lipid rafts. 293T cells were plated on coverslips and transiently transfected to express HIV-1 Gag-Pol, HPIV3-F, and HPIV3-HN. As a control, some cells were transfected with Gag-Pol and amphotropic Env. Cells were then exposed to the presence or absence of 0.5 mM MβCD, and 24 hours later, fixed, permeabilized, and stained for lipid rafts with A549-conjugated cholera
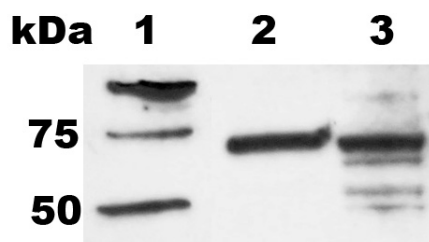
Figure 5.6. Wild-type HN are present but not concentrated in lipid rafts. Lipid rafts were isolated from 293T cells infected with wild-type HPIV3 at an MOI of 1. Cells were lysed with ice-cold Triton X-100 (1% in TNE) and subjected to equilibrium flotation centrifugation. The lipid raft fraction (Lane 2) was isolated and pelleted by ultracentrifugation and then analyzed by Western blot for the presence of HN. As a control, the whole cell lysate of the cells (Lane 3) was also analyzed for HN.
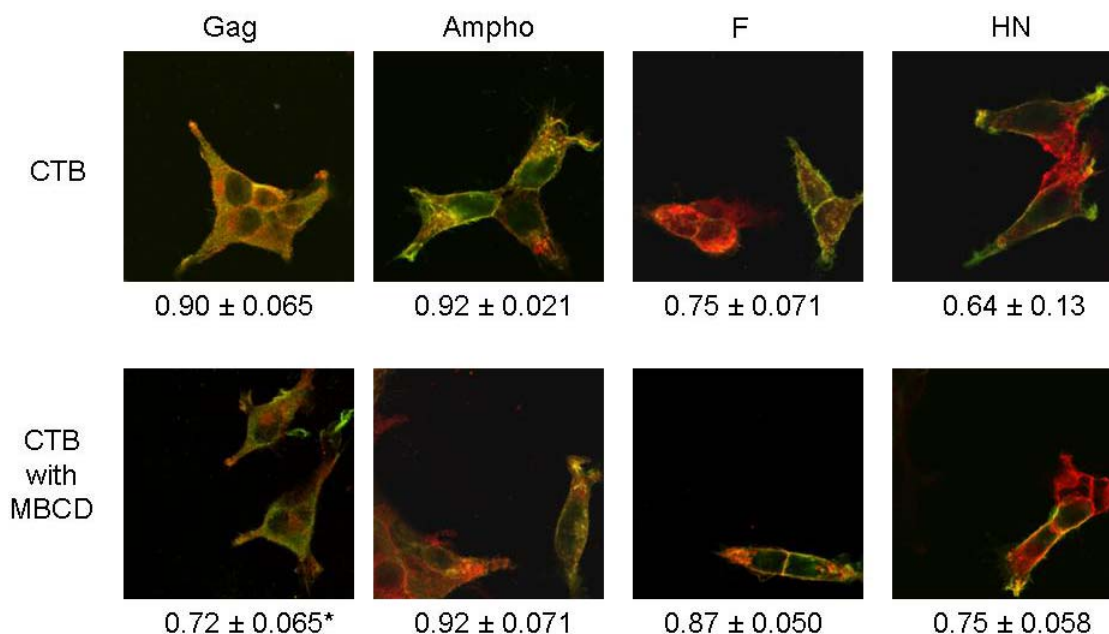
Figure 5.7. Lipid raft disruption with MβCD increases colocalization of F and HN with lipid raft marker. 293T cells were transiently transfected to express HIV-1 Gag-Pol (Gag), amphotropic Env (Ampho), or HPIV3-F (F) and HPIV3-HN (HN) in the presence (bottom row) or absence (top row) of 0.5 mM MβCD. Cells were fixed, permeabilized, and immunostained with a mouse monoclonal antibody against Gag followed by a donkey anti-mouse Cy2 conjugated secondary antibody, a rat antibody against amphotropic Env (83A25) followed by a donkey anti-rat Cy2 conjugated secondary antibody, or a mouse monoclonal antibody against HN (170) or F (b108) conjugated to A488. Cells were then incubated with 5 µg/mL A549 conjugated cholera toxin B subunit (CTB). Cells were visualized with confocal microscopy at 63X and overlays of CTB (red) with Gag, Ampho, F, or HN (green) are shown. Eight cells were chosen at random and extent of colocalization was quantified with ImageJ. Statistically significant differences (P<0.05) in colocalization values between Gag with CTB and Gag with CTB in the presence of MβCD are denoted with *.

130

toxin B subunit. Cells were also immunostained with a corresponding antibody against Gag followed by Cy2 secondary antibody, amphotropic Env followed by a Cy2 secondary antibody, or A488-conjugated F antibody, or A488-conjugated HN antibody. Cells were visualized by confocal microscopy and the extent of colocalization was quantified by calculating the Pearson's overlap coefficient with ImageJ (Figure 5.7). As expected, Amphotropic Env and Gag was highly colocalized with the lipid raft marker $(0.92 \pm 0.021$ and 0.90 ± 0.065, respectively) while F and HN were significantly not as colocalized with lipid raft marker $(0.75 \pm 0.071$ and 0.64 ± 0.13, respectively, $p<0.05$ for both). Treatment with MβCD significantly decreased the amount of Gag associated with the lipid raft marker (0.72 ± 0.065), while it increased the amount of F and HN associated with the raft marker, although not significantly $(0.87 \pm 0.050$ and 0.75 ± 0.058, respectively).

We next determined whether MβCD treatment affected the production of virus particles from producer cells and whether it had an impact on the amount of cholesterol in virus particles. 293T cells were transfected with expression plasmids for β-galactosidase, HIV-1 Gag-Pol, and either amphotropic Env or HPIV3-F and HPIV3-HN. Producer cells were then incubated in the presence or absence of 0.5 mM MβCD for 30 and 54 hours before viral supernatant was harvested, pelleted and resuspended in PBS, and analyzed for p24 content and cholesterol levels (Figure 5.8). In the presence of MβCD, the production of amphotropic pseudotyped lentiviruses increased 1.6-fold $(p<0.05)$ however the amount of HPIV3 pseudotyped lentiviruses produced did not significantly change. When analyzing cholesterol content however, the amount of cholesterol in amphotropic pseudotyped lentiviruses decreased 1.4-fold $(p>0.05)$ while the amount in HPIV3 pseudotyped lentiviruses increased 1.5-fold $(p>0.05)$.

Since 0.5 mM MβCD treatment did not appear to drastically alter the production or cholesterol content of viruses, we next determined the transduction efficiency of
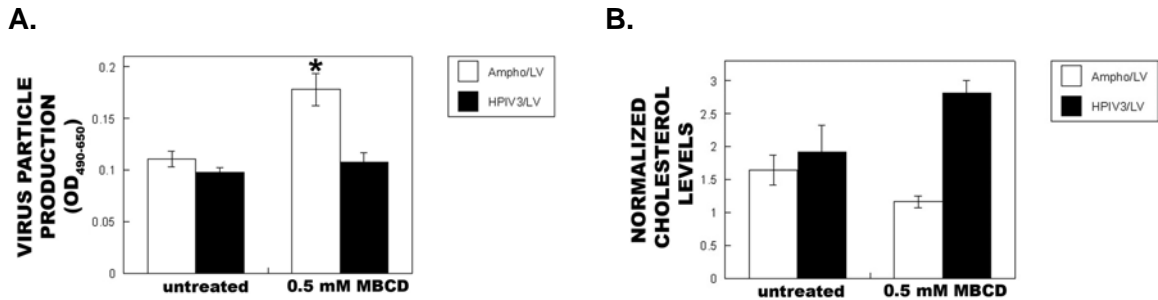
Figure 5.8. Virus production of pseudotyped lentiviruses increase with MβCD while cholesterol content in Ampho/LV decreases and HPIV3/LV increases. 293T cells (1x10^7) were transfected with expression plasmids (6 μg each) for β-galactosidase, HIV-1 Gag-Pol, and either amphotropic Env (white bars) or HPIV3-F and HPIV3-HN (black bars). The next day, cells were incubated in the presence or absence of 0.5 mM MβCD. Viral laden supernatant were harvested 30 and 54 hours after addition of MβCD, pelleted with 320 μg/mL polybrene and resuspended in PBS to the original volume. The concentration of 54-hour virus was determined with the p24 ELISA and the cholesterol content was determined with a cholesterol kit. * denotes statistically significant difference (P<0.05) in amphotropic lentivirus production in the presence or absence of MβCD treatment.

viruses produced from MβCD-treated cells (Figure 5.9). In the first 30 hours of MβCD treatment, the titer of amphotropic pseudotyped lentiviruses decreased 2.3-fold (p<0.05). After an additional 24 hours of treatment, the titer decreased 3.6-fold (p<0.05) compared to untreated producer cells. Interestingly, the first 30 hours of MβCD treatment did not alter the titer of HPIV3 pseudotyped lentiviruses, however 24 additional hours of MβCD treatment increased titer 6.4-fold (p<0.05) compared to untreated producer cells.

Finally we wanted to determine whether or not this effect on titers was due to the amount of envelope protein incorporated into viruses from MβCD-treated producer cells. 293T cells (1x10^7) were transfected with expression plasmids (6 μg each) for β-galactosidase, HIV-1 Gag-Pol, and either amphotropic Env or HPIV3-F and HPIV3-HN. The next day cells were incubated in the presence or absence of 0.5 mM MβCD. HPIV3 pseudotyped lentiviral producer cells were also serum-starved for 15 min, metabolically-
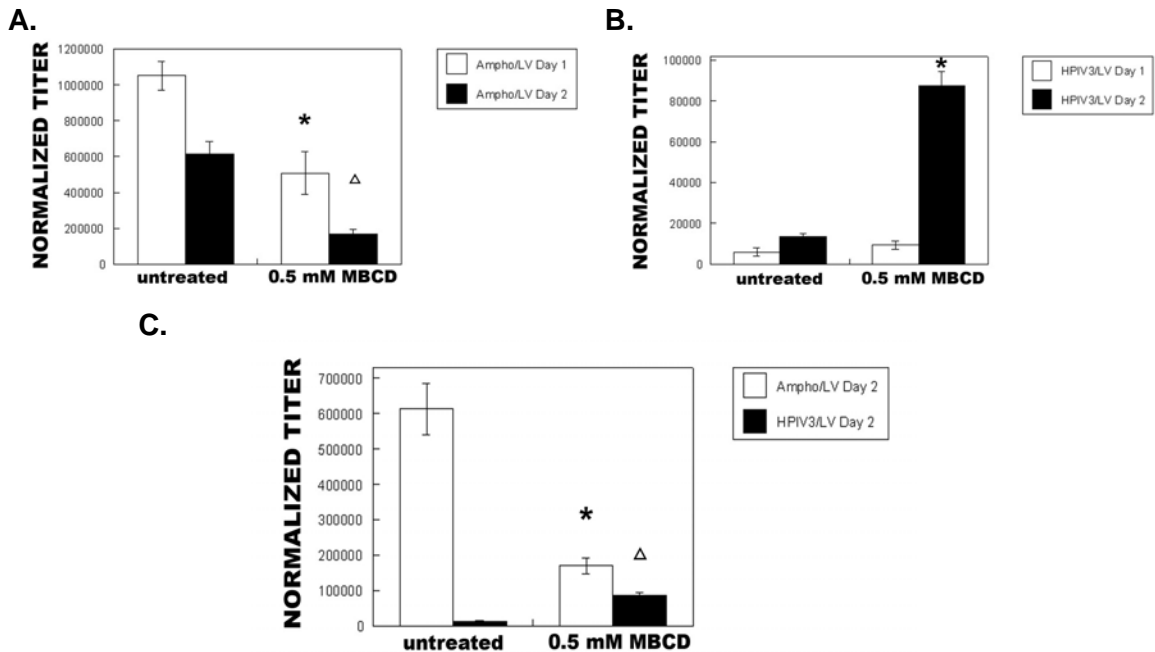
Figure 5.9. Amphotropic pseudotyped lentiviral titer decreases with MβCD treatment and HPIV3 pseudotyped lentiviral titer increases with MβCD treatment. 293T cells (1x10^7) were transfected with expression plasmids (6 µg each) for β-galactosidase, HIV-1 Gag-Pol, and either amphotropic Env (Part A, Part C white bars) or HPIV3-F and HPIV3-HN (Part B, Part C black bars). The next day, cells were incubated in the presence or absence of 0.5 mM MβCD. Viral laden supernatant were harvested 30 (Parts A and B, white bars) and 54 (Parts A and B, black bars, and Part C whole graph) hours after addition of MβCD, pelleted with 320 µg/mL polybrene and resuspended in PBS to the original volume. Viruses were used to transduce target cells in the diluted titer assay. The transduced cells were incubated for 2 days at 37^{0}C until confluent, fixed, and stained for *lacZ* activity with X-Gal, colonies of *lacZ*+ cells were counted, and the titer normalized to p24 amounts. * and Δ denote statistically significant differences (P<0.05) in normalized titer of viruses produced in the presence or absence of MβCD treatment.
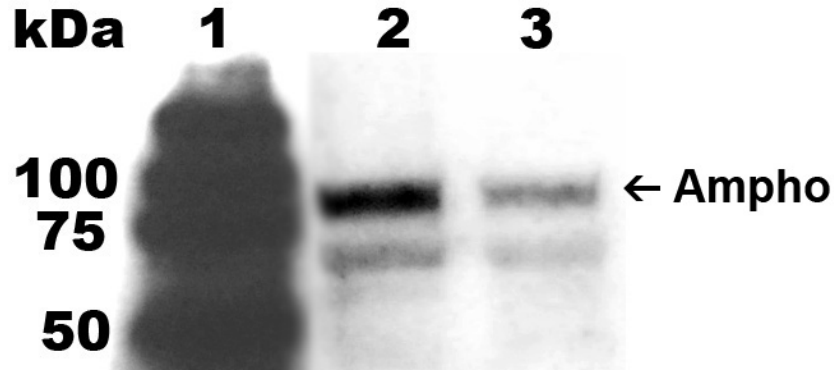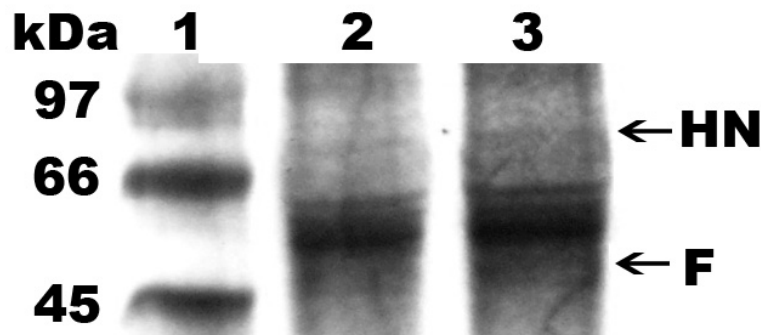
Figure 5.10. Amphotropic pseudotyped lentiviruses produced in the presence of MβCD contain fewer envelope proteins while HPIV3 pseudotyped lentiviruses incorporate more envelope proteins. 293T cells ($1x10^7$) were transfected with expression plasmids (6 µg each) for β-galactosidase, HIV-1 Gag-Pol, and either amphotropic Env (Ampho) (A), or HPIV3-F and HPIV3-HN (B). The next day, cells were incubated with 0.5 mM MβCD for 54 hours (Part A and B, Lane 3) and as a control cells were not treated (Part A and B, Lane 2). HPIV3 pseudotyped lentivirus producer cells were also serum-starved for 15 min, and metabolically-labeled with 500 µCi [35S] methionine and cysteine. Both pseudotyped viruses were harvested and ultracentrifuged through a 20% sucrose cushion, and then resuspended in PBS to 100-fold their original concentration. Samples were resuspended in lysis buffer and separated by size by SDS-PAGE. Amphotropic pseudotyped lentiviruses were analyzed by Western blot for the amphotropic envelope protein. The gel for HPIV3 pseudotyped lentiviruses was dried and visualized by autoradiography.

labeled with 500 µCi [35S] methionine and cysteine. Tissue culture supernatant were harvested for both viruses, ultracentrifuged through a 20% sucrose cushion, and then resuspended in PBS to 100-fold their original concentration. Amphotropic pseudotyped lentiviruses were analyzed by Western blot for the amphotropic envelope protein and the gel for HPIV3 pseudotyped lentiviruses was dried and visualized by autoradiography (Figure 5.10). When producer cells were treated with 0.5 mM MβCD, less amphotropic envelope protein was incorporated into lentiviral particles, however more HN and F proteins were incorporated.   Using ImageJ, we found the amount of amphotropic envelope protein in lentiviral particles produced from 0.5 mM-treated producer cells was 3-fold less than amphotropic pseudotyped viruses from untreated producer cells.   To quantify the amount of HN from virus particles, we excised the bands that contained HN from the gel, measured their radioactivity with a scintillation counter, and normalized the amount to radioactive p24. We found that 1.4-fold more HN was incorporated into lentiviral particles produced from cells treated with 0.5 mM MβCD than untreated producer cells.

5.5 <u>Discussion</u>

We have previously shown HPIV3 pseudotyped lentiviruses had titers too low to be useful for clinical gene transfer since the envelope proteins, HN and F, were not efficiently incorporated into lentivirus particles. We reasoned that incorporation was low because interactions between HN and F, or HN and F with lentiviral Gag were low. We found that HN and F were colocalized with each other, however HN and F were not as colocalized with Gag or lipid rafts as amphotropic Env. We then hypothesized that increasing interactions of HN and F with Gag would enhance their incorporation into lentiviral particles. To test this hypothesis, we used two main approaches: 1) we created HN and HIV Env fusion proteins that would actively interact with Gag, and 2) we

disrupted the barriers that prevented HN and F from passively interacting with Gag. We found that when HN fusion proteins were created with portions of HIV gp41's cytoplasmic domain, HN-mpr and HN-LLP2, colocalization of the HN chimeras with Gag increased slightly from unmodified HN. The level of incorporation also increased 1.6-fold and 2.2-fold, respectively, however titers significantly decreased at least 25-fold. We then determined whether increased colocalization with Gag was sufficient for envelope protein incorporation. Previously we found small concentrations of methyl-beta-cyclodextrin (MβCD) disturbed lipid rafts such that raft proteins segregated by lipid rafts could inter-mix with lentivirus-associated rafts and become incorporated into virus particles. When lentiviruses pseudotyped with HPIV3 (HPIV3 LV) or amphotropic Env (Ampho LV) producer cells were treated with 0.5 mM MβCD for 54 hours after transfection, titers of HPIV3 LV increased 6.4-fold while titers of Ampho LV decreased 3.6-fold. When we analyzed the amount of envelope incorporation from MβCD treated producer cells, we found the amount of amphotropic Env in virus particles decreased 3.0-fold while the amount of HN increased 1.4-fold. This data suggested that increasing interactions of HPIV3 envelope proteins with Gag through active and passive interactions enhanced HN and F incorporation into lentiviral particles.

Our observation that HN and F did not colocalize with Gag, was consistent with our previous results that low titer was due to low efficiency of envelope incorporation and not poor expression of the envelope proteins [32]. Whether or not a protein is incorporated into a lentivirus particle is largely dictated by whether or not a protein is colocalized with the virus when it assembles and buds from the cell [17, 18, 48]. Previous work suggested HPIV3 Env and lentiviruses do not share a common intracellular trafficking pathway [49, 50], and HPIV3 has not been shown associated with multivesicular bodies and recycling endosomes as Gag has [12, 51, 52].

We therefore attempted to increase interactions of F and HN with Gag. Most proteins present on the surface of lentiviruses are incorporated passively when they localize to the site of budding [9-11]. Lipid rafts have been implicated as sites of lentivirus budding and assembly [15, 25-27]. Previous work has suggested the possibility of HPIV3 F and HN interaction with lipid rafts, for example the closely-related Sendai virus has been shown to incorporate the lipid raft marker GM1 [48], and measles virus H and F glycoproteins associate with lipid rafts (30% and 10%, respectively) [53]. In addition, the neuraminidase glycoprotein from influenza, a Type II transmembrane glycoprotein similar to HPIV3 HN, also localizes to lipid rafts [54]. However our results demonstrated HN and F were somewhat colocalized with rafts, and that wild-type HPIV3 HN was associated but not concentrated in rafts. Since our previous chapter (Chapter 4) showed that raft proteins not heavily localized to lentivirus-associated rafts were incorporated when lipid rafts were disturbed, we attempted to increase passive interactions of HPIV3 HN and F with Gag by disturbing rafts. We used 0.5 mM MβCD to treat producer cells and found that not only did it increase colocalization of F and HN with lipid raft markers, production of virus particles increased 1.1-fold (p>0.05). Other papers have reported increases in budding of Newcastle disease virus [55], influenza [56], Sendai virus [57], and VSV M protein transfected cells [47] after MβCD treatment.

We also found MβCD treatment of producer cells increased titers of HPIV3 pseudotyped lentiviruses 6.4-fold, while titers of amphotropic Env pseudotyped viruses dropped 3.6-fold. The increase in HN incorporation was additional to the 2.0-fold increase after codon optimization of HN [32]. When viruses from MβCD treated cells were analyzed for envelope protein incorporation, lentiviruses incorporated 1.4-fold more HN than normal HN while the amount of amphotropic Env incorporated dropped 3.0-fold. These results are consistent with our previous chapter's results in which MβCD treatment decreased incorporation of proteins concentrated in lentivirus-associated rafts

like amphotropic Env, and increased incorporation of proteins segregated from lentivirus-associated rafts.   Besides disturbing lipid rafts, cholesterol depletion may have resulted in increased F and HN concentrations at the plasma membrane because of either reduced endocytosis and degradation [58, 59] or acceleration in export rates from internal endosomes [60]. However this is not likely since others have shown HPIV3 HN is predominantly found on the cell surface and is not internalized [61]. This increase in titer compared to the amount of HN incorporated still suggests the threshold for more HPIV3 envelope proteins incorporation has not yet been reached [62-64].   For amphotropic Env, the decrease in Env incorporation correlates to the decrease in titer. However in addition to decreasing the amount of Env incorporated, cholesterol depletion may be affecting Ampho LV titers by inhibiting Env's fusion ability [65, 66].

In addition to increasing passive interactions of HPIV3 envelope proteins with Gag, we determined the effect of increasing active interactions of HN with Gag with our HN chimeras. Our previous results [32] and others [67, 68] have demonstrated the efficiency of HN incorporation largely determined functional titer or fusion activity. In the creation of the chimeras, we chose to invert the cytoplasmic domain sequences of gp41 since gp41 is a type I transmembrane protein and HN is a Type II transmembrane protein. The 31 amino acid sequence of the gp41 alpha helix2 and the first 43 amino acids of the gp41 cytoplasmic tail have both been shown to interact with HIV-1 matrix and the plasma membrane, and are both critical for gp41 incorporation into lentivirus particles [43-46, 67].   Colocalization with Gag increased slightly with the chimeric proteins compared to unmodified HN.   However we found that lentiviruses incorporated the HN chimeras 1.6 to 2.2-fold more than unmodified HN, while titers dropped more than 25-fold. The significant decrease in titers while envelope incorporation increased may be due to impairment of the binding or fusion-initiation properties of HN, which has been shown to undergo structural changes for both to occur normally [69-72] .

138

In summary, we have found that increasing interactions of HPIV3 envelope proteins with Gag through active and passive interactions enhanced HN and F incorporation into lentiviral particles. Future studies should focus on investigating the effects of cholesterol depletion on F and HN trafficking, perturbing the lipid rafts on other types of viruses for the incorporation of other difficult-to-incorporate proteins, and optimizing the effects of raft perturbations for increased envelope incorporation and high titers.

5.6 <u>References</u>

1. Cronin, J., X.Y. Zhang, and J. Reiser, *Altering the tropism of lentiviral vectors through pseudotyping.* Curr Gene Ther, 2005. **5**(4): p. 387-98.

2. Verhoeyen, E., et al., *IL-7 surface-engineered lentiviral vectors promote survival and efficient gene transfer in resting primary T lymphocytes.* Blood, 2003. **101**(6): p. 2167-74.

3. Breckpot, K., J.L. Aerts, and K. Thielemans, *Lentiviral vectors for cancer immunotherapy: transforming infectious particles into therapeutics.* Gene Ther, 2007. **14**(11): p. 847-62.

4. Clements, M.O., et al., *Lentiviral manipulation of gene expression in human adult and embryonic stem cells.* Tissue Eng, 2006. **12**(7): p. 1741-51.

5. Naldini, L., et al., *In vivo gene delivery and stable transduction of nondividing cells by a lentiviral vector.* Science, 1996. **272**(5259): p. 263-7.

6. Kang, Y., et al., *In vivo gene transfer using a nonprimate lentiviral vector pseudotyped with Ross River Virus glycoproteins.* J Virol, 2002. **76**(18): p. 9378-88.

7. Kobinger, G.P., et al., *Filovirus-pseudotyped lentiviral vector can efficiently and stably transduce airway epithelia in vivo.* Nat Biotechnol, 2001. **19**(3): p. 225-30.

8. Sinn, P.L., et al., *Gene transfer to respiratory epithelia with lentivirus pseudotyped with Jaagsiekte sheep retrovirus envelope glycoprotein.* Hum Gene Ther, 2005. **16**(4): p. 479-88.

9. Hammarstedt, M. and H. Garoff, *Passive and active inclusion of host proteins in human immunodeficiency virus type 1 gag particles during budding at the plasma membrane.* J Virol, 2004. **78**(11): p. 5686-97.

10.   Cantin, R., S. Methot, and M.J. Tremblay, *Plunder and stowaways: incorporation of cellular proteins by enveloped viruses.* J Virol, 2005. **79**(11): p. 6577-87.

11.   Kolegraff, K., P. Bostik, and A.A. Ansari, *Characterization and role of lentivirus-associated host proteins.* Exp Biol Med (Maywood), 2006. **231**(3): p. 252-63.

12.   Nguyen, D.G., et al., *Evidence that HIV budding in primary macrophages occurs through the exosome release pathway.* J Biol Chem, 2003. **278**(52): p. 52347-54.

13.   Orentas, R.J. and J.E. Hildreth, *Association of host cell surface adhesion receptors and other membrane proteins with HIV and SIV.* AIDS Res Hum Retroviruses, 1993. **9**(11): p. 1157-65.

14.   Brugger, B., et al., *The HIV lipidome: a raft with an unusual composition.* Proc Natl Acad Sci U S A, 2006. **103**(8): p. 2641-6.

15.   Nguyen, D.H. and J.E. Hildreth, *Evidence for budding of human immunodeficiency virus type 1 selectively from glycolipid-enriched membrane lipid rafts.* J Virol, 2000. **74**(7): p. 3264-72.

16.   Pelchen-Matthews, A., B. Kramer, and M. Marsh, *Infectious HIV-1 assembles in late endosomes in primary macrophages.* J Cell Biol, 2003. **162**(3): p. 443-55.

17.   Sandrin, V. and F.L. Cosset, *Intracellular versus cell surface assembly of retroviral pseudotypes is determined by the cellular localization of the viral glycoprotein, its capacity to interact with Gag, and the expression of the Nef protein.* J Biol Chem, 2006. **281**(1): p. 528-42.

18.   Sandrin, V., et al., *Intracellular trafficking of Gag and Env proteins and their interactions modulate pseudotyping of retroviruses.* J Virol, 2004. **78**(13): p. 7153-64.

19.   Henriksson, P., et al., *Incorporation of wild-type and C-terminally truncated human epidermal growth factor receptor into human immunodeficiency virus-like particles: insight into the processes governing glycoprotein incorporation into retroviral particles.* J Virol, 1999. **73**(11): p. 9294-302.

20.   Lindwasser, O.W. and M.D. Resh, *Multimerization of human immunodeficiency virus type 1 Gag promotes its localization to barges, raft-like membrane microdomains.* J Virol, 2001. **75**(17): p. 7913-24.

21.   Finzi, A., et al., *Productive human immunodeficiency virus type 1 assembly takes place at the plasma membrane.* J Virol, 2007. **81**(14): p. 7476-90.

22.   Jouvenet, N., et al., *Plasma membrane is the site of productive HIV-1 particle assembly.* PLoS Biol, 2006. **4**(12): p. e435.

23.   Sherer, N.M., et al., *Visualization of retroviral replication in living cells reveals budding into multivesicular bodies.* Traffic, 2003. **4**(11): p. 785-801.

24. Yang, C., C.P. Spies, and R.W. Compans, *The human and simian immunodeficiency virus envelope glycoprotein transmembrane subunits are palmitoylated.* Proc Natl Acad Sci U S A, 1995. **92**(21): p. 9871-5.

25. Bhattacharya, J., P.J. Peters, and P.R. Clapham, *Human immunodeficiency virus type 1 envelope glycoproteins that lack cytoplasmic domain cysteines: impact on association with membrane lipid rafts and incorporation onto budding virus particles.* J Virol, 2004. **78**(10): p. 5500-6.

26. Resh, M.D., *Intracellular trafficking of HIV-1 Gag: how Gag interacts with cell membranes and makes viral particles.* AIDS Rev, 2005. **7**(2): p. 84-91.

27. Campbell, S.M., S.M. Crowe, and J. Mak, *Lipid rafts and HIV-1: from viral entry to assembly of progeny virions.* J Clin Virol, 2001. **22**(3): p. 217-27.

28. Nydegger, S., et al., *Mapping of tetraspanin-enriched microdomains that can function as gateways for HIV-1.* J Cell Biol, 2006. **173**(5): p. 795-807.

29. Jolly, C. and Q.J. Sattentau, *Human immunodeficiency virus type 1 assembly, budding, and cell-cell spread in T cells take place in tetraspanin-enriched plasma membrane domains.* J Virol, 2007. **81**(15): p. 7873-84.

30. Deneka, M., et al., *In macrophages, HIV-1 assembles into an intracellular plasma membrane domain containing the tetraspanins CD81, CD9, and CD53.* J Cell Biol, 2007. **177**(2): p. 329-41.

31. Jung, C., et al., *Lentiviral vectors pseudotyped with envelope glycoproteins derived from human parainfluenza virus type 3.* Biotechnol Prog, 2004. **20**(6): p. 1810-6.

32. Jung, C. and J.M. Doux, *Lentiviruses inefficiently incorporate human parainfluenza type 3 envelope proteins.* Biotechnol Bioeng, 2007.

33. Evans, L.H., et al., *A neutralizable epitope common to the envelope glycoproteins of ecotropic, polytropic, xenotropic, and amphotropic murine leukemia viruses.* J Virol, 1990. **64**(12): p. 6176-83.

34. Harlow, E. and D. Lane, *Storing and Purifying Antibodies*, in *Antibodies: A Laboratory Manual*. 1988, Cold Spring Harbor Laboratory Press: Cold Spring Harbor. p. 288-303.

35. Zufferey, R., et al., *Multiply attenuated lentiviral vector achieves efficient gene delivery in vivo.* Nat Biotechnol, 1997. **15**(9): p. 871-5.

36. Cosset, F.L., et al., *High-titer packaging cells producing recombinant retroviruses resistant to human serum.* J Virol, 1995. **69**(12): p. 7430-6.

37. Landazuri, N., M. Gupta, and J.M. Le Doux, *Rapid concentration and purification of retrovirus by flocculation with Polybrene.* J Biotechnol, 2006. **125**(4): p. 529-39.

38. Niwa, H., K. Yamamura, and J. Miyazaki, *Efficient selection for high-expression transfectants with a novel eukaryotic vector.* Gene, 1991. **108**(2): p. 193-99.

39. Smith, R.F., *Microscopy and Photomicrography*. 2nd ed. 1994, Boca Raton: CRC Press. 162.

40. Rasband, W.S. *ImageJ.* [cited 2007 10-21]; Available from: http://rsb.info.nih.gov/ij/.

41. Abramoff, M., P. Magelhaes, and S. Ram, *Image processing with ImageJ.* Biophotonics International, 2004. **11**(7): p. 36-42.

42. Spector, D.H., et al., *Human immunodeficiency virus pseudotypes with expanded cellular and species tropism.* J Virol, 1990. **64**(5): p. 2298-308.

43. Hourioux, C., et al., *Identification of the glycoprotein 41(TM) cytoplasmic tail domains of human immunodeficiency virus type 1 that interact with Pr55Gag particles.* AIDS Res Hum Retroviruses, 2000. **16**(12): p. 1141-7.

44. Murakami, T. and E.O. Freed, *Genetic evidence for an interaction between human immunodeficiency virus type 1 matrix and alpha-helix 2 of the gp41 cytoplasmic tail.* J Virol, 2000. **74**(8): p. 3548-54.

45. Piller, S.C., et al., *Mutational analysis of conserved domains within the cytoplasmic tail of gp41 from human immunodeficiency virus type 1: effects on glycoprotein incorporation and infectivity.* J Virol, 2000. **74**(24): p. 11717-23.

46. Freed, E.O. and M.A. Martin, *Domains of the human immunodeficiency virus type 1 matrix and gp41 cytoplasmic tail required for envelope incorporation into virions.* J Virol, 1996. **70**(1): p. 341-51.

47. Ono, A. and E.O. Freed, *Plasma membrane rafts play a critical role in HIV-1 assembly and release.* Proc Natl Acad Sci U S A, 2001. **98**(24): p. 13925-30.

48. Pickl, W.F., F.X. Pimentel-Muinos, and B. Seed, *Lipid rafts and pseudotyping.* J Virol, 2001. **75**(15): p. 7175-83.

49. Bose, S., A. Malur, and A.K. Banerjee, *Polarity of human parainfluenza virus type 3 infection in polarized human lung epithelial A549 cells: role of microfilament and microtubule.* J Virol, 2001. **75**(4): p. 1984-9.

50. Owens, R.J., et al., *Human immunodeficiency virus envelope protein determines the site of virus release in polarized epithelial cells.* Proc Natl Acad Sci U S A, 1991. **88**(9): p. 3987-91.

51. Nydegger, S., et al., *HIV-1 egress is gated through late endosomal membranes.* Traffic, 2003. **4**(12): p. 902-10.

52. Orenstein, J.M., et al., *Cytoplasmic assembly and accumulation of human immunodeficiency virus types 1 and 2 in recombinant human colony-stimulating*

factor-1-treated human monocytes: an ultrastructural study. J Virol, 1988. **62**(8): p. 2578-86.

53. Manie, S.N., et al., *Measles virus structural components are enriched into lipid raft microdomains: a potential cellular location for virus assembly.* J Virol, 2000. **74**(1): p. 305-11.

54. Barman, S. and D.P. Nayak, *Analysis of the transmembrane domain of influenza virus neuraminidase, a type II transmembrane glycoprotein, for apical sorting and raft association.* J Virol, 2000. **74**(14): p. 6538-45.

55. Laliberte, J.P., et al., *Integrity of membrane lipid rafts is necessary for the ordered assembly and release of infectious Newcastle disease virus particles.* J Virol, 2006. **80**(21): p. 10652-62.

56. Barman, S. and D.P. Nayak, *Lipid raft disruption by cholesterol depletion enhances influenza A virus budding from MDCK cells.* J Virol, 2007.

57. Gosselin-Grenet, A.S., G. Mottet-Osman, and L. Roux, *From assembly to virus particle budding: pertinence of the detergent resistant membranes.* Virology, 2006. **344**(2): p. 296-303.

58. Kobayashi, T., A. Yamaji-Hasegawa, and E. Kiyokawa, *Lipid domains in the endocytic pathway.* Semin Cell Dev Biol, 2001. **12**(2): p. 173-82.

59. Ikeda, M. and R. Longnecker, *Cholesterol is critical for Epstein-Barr virus latent membrane protein 2A trafficking and protein stability.* Virology, 2007. **360**(2): p. 461-8.

60. Mayor, S., S. Sabharanjak, and F.R. Maxfield, *Cholesterol-dependent retention of GPI-anchored proteins in endosomes.* Embo J, 1998. **17**(16): p. 4626-38.

61. Leser, G.P., K.J. Ector, and R.A. Lamb, *The paramyxovirus simian virus 5 hemagglutinin-neuraminidase glycoprotein, but not the fusion glycoprotein, is internalized via coated pits and enters the endocytic pathway.* Mol Biol Cell, 1996. **7**(1): p. 155-72.

62. Bachrach, E., et al., *Effects of virion surface gp120 density on infection by HIV-1 and viral production by infected cells.* Virology, 2005. **332**(1): p. 418-29.

63. Yuste, E., et al., *Virion envelope content, infectivity, and neutralization sensitivity of simian immunodeficiency virus.* J Virol, 2005. **79**(19): p. 12455-63.

64. Yuste, E., et al., *Modulation of Env content in virions of simian immunodeficiency virus: correlation with cell surface expression and virion infectivity.* J Virol, 2004. **78**(13): p. 6775-85.

65. Guyader, M., et al., *Role for human immunodeficiency virus type 1 membrane cholesterol in viral internalization.* J Virol, 2002. **76**(20): p. 10356-64.

66.   Zavorotinskaya, T. and L.M. Albritton, *Failure To cleave murine leukemia virus envelope protein does not preclude its incorporation in virions and productive virus-receptor interaction.* J Virol, 1999. **73**(7): p. 5621-9.

67.   Kobayashi, M., et al., *Pseudotyped lentivirus vectors derived from simian immunodeficiency virus SIVagm with envelope glycoproteins from paramyxovirus.* J Virol, 2003. **77**(4): p. 2607-14.

68.   Dutch, R.E., S.B. Joshi, and R.A. Lamb, *Membrane fusion promoted by increasing surface densities of the paramyxovirus F and HN proteins: comparison of fusion reactions mediated by simian virus 5 F, human parainfluenza virus type 3 F, and influenza virus HA.* J Virol, 1998. **72**(10): p. 7745-53.

69.   Hu, X.L., R. Ray, and R.W. Compans, *Functional interactions between the fusion protein and hemagglutinin-neuraminidase of human parainfluenza viruses.* J Virol, 1992. **66**(3): p. 1528-34.

70.   Bagai, S. and R.A. Lamb, *Quantitative measurement of paramyxovirus fusion: differences in requirements of glycoproteins between simian virus 5 and human parainfluenza virus 3 or Newcastle disease virus.* J Virol, 1995. **69**(11): p. 6712-9.

71.   Moscona, A. and R.W. Peluso, *Fusion properties of cells persistently infected with human parainfluenza virus type 3: participation of hemagglutinin-neuraminidase in membrane fusion.* J Virol, 1991. **65**(6): p. 2773-7.

72.   Tanaka, Y. and M.S. Galinski, *Human parainfluenza virus type 3: analysis of the cytoplasmic tail and transmembrane anchor of the hemagglutinin-neuraminidase protein in promoting cell fusion.* Virus Res, 1995. **36**(2-3): p. 131-49.

CHAPTER 6

CONCLUSIONS AND FUTURE CONSIDERATIONS

6.1 Summary of results

In chapter two we described the generation of lentiviruses pseudotyped with human parainfluenza type 3 envelope (HPIV3) glycoproteins. Lentivirus particles incorporated HPIV3 hemagglutinin-neuraminidase (HN) and fusion (F) proteins into their lipid bilayers and were able to transduce human kidney epithelial cells and polarized MDCK, HBE, and A549 cells via their apical surface. Neuraminidase, AZT, and anti-HPIV3 antisera blocked transduction, which is consistent with lentiviral-mediated transduction via sialated receptors for HPIV3. Our findings showed that HPIV3 pseudotyped lentiviruses can be formed and may have a number of useful properties for human gene transfer.

In chapter three we investigated the cause of low HPIV3 pseudotyped lentivirus titers. Transfected cells contained similar levels of HN and F cytosolic mRNA, but fewer cell-surface HN and F proteins (3.8 and 1.3-fold less, respectively), than cells infected with wild-type HPIV3. To increase expression of HN in transfected cells, we codon-optimized HN and used it to transfect lentivirus producer cells. Cell surface expression of HN, as well as the amount of HN incorporated into virus particles, increased 2 to 3-fold. Virus titers increased 1.2 to 6.4-fold, and the transduction efficiency of polarized MDCK cells via their apical surfaces increased 1.4-fold. Interestingly, even though codon optimization improved the expression levels of HN and virus titers, we found that HPIV3 pseudotyped viruses contained about 14-fold fewer envelope proteins than lentiviruses pseudotyped with the amphotropic envelope protein. Taken together, our findings suggested that titers were low, not because virus producer cells expressed

145

levels of HPIV3 envelope proteins that were too low, but because too few of these proteins were incorporated by lentiviruses for them to be able to efficiently transduce cells.

In chapter four we investigated the ability of two glycosylphosphatidylinositol (GPI) anchored proteins, folate receptor (FR-WT) and Tac-CD16 (CD25 or the interleukin-2 receptor alpha chain which has been modified with the GPI anchor motif from CD16) to associate with viral proteins, Gag and amphotropic Env, in lipid rafts and lentivirus particles. We found that Tac-CD16 and FR-WT exhibited the classic GPI anchored protein property of associating with lipid rafts, however Tac-CD16 colocalized with Gag and incorporated into lentiviral particles, while FR-WT did not colocalize with Gag and was not incorporated into virus particles. We found FR-WT generally colocalized to less dense rafts while Gag and Env were localized to more dense rafts. Tac-CD16 was widely distributed in both less dense and more dense rafts. Most significantly, we found that when we treated producer cells with fumonisin B1 (FB1) or methyl-beta-cyclodextrin (MβCD), the amount of colocalization between FR-WT and Gag increased, FR-WT was located to more dense rafts, and FR-WT was incorporated 2.9 to 11.6-fold more into lentiviral particles, respectively. In contrast, the raft distribution of Tac-CD16 decreased and the amount of Tac-CD16 in virus particles decreased 2.4-fold with MβCD treatment. Taken together, these results demonstrated lipid rafts segregate raft proteins, and for a protein to be incorporated into virus particles, it must be colocalized with lentivirus-associated rafts.

In chapter five we reasoned that incorporation of HPIV3 envelope proteins, HN and F, into lentiviral particles was low because interactions between HN and F, or HN and F with lentiviral Gag were low. We found that HN and F were colocalized with each other, however HN and F were not as colocalized with Gag or lipid rafts as amphotropic Env. We used two main approaches to increase interactions of the envelope proteins

146

with Gag: 1) we created HN and HIV Env fusion proteins that would actively interact with Gag, and 2) we disrupted the barriers that prevented HN and F from passively interacting with Gag. We found that the HN chimeras had increased colocalization with Gag compared to unmodified HN. The level of incorporation also increased 1.6-fold and 2.2-fold, respectively, however titers significantly decreased at least 25-fold. We then determined whether increased colocalization with Gag was sufficient for envelope protein incorporation. When lentiviruses pseudotyped with HPIV3 (HPIV3 LV) or amphotropic Env (Ampho LV) producer cells were treated with 0.5 mM MβCD for 54 hours after transfection to disturb lipid rafts, titers of HPIV3 LV increased 6.4-fold while titers of Ampho LV decreased 3.6-fold. When we analyzed the amount of envelope incorporation from MβCD treated producer cells, we found the amount of amphotropic Env in virus particles decreased 3.0-fold while the amount of HN increased 1.4-fold. This data suggested that increasing interactions of HPIV3 envelope proteins with Gag through active and passive interactions enhanced HN and F incorporation into lentiviral particles.

6.2 <u>Conclusions</u>

In conclusion, we determined:

1. Lentiviruses can be pseudotyped with the envelope proteins from HPIV3. The pseudotyped viruses can infect polarized cells via the apical surface.

2. Titers of HPIV3 pseudotyped lentiviruses are low because of low envelope incorporation levels.

3. Lipid rafts segregate raft proteins, and for a protein to be incorporated into virus particles, it must be colocalized with lentivirus-associated rafts.

4. Titers of HPIV3 pseudotyped lentiviruses can be improved by enhancing active and passive interactions of envelope proteins with Gag, leading to improved incorporation levels.

6.3 **Future Considerations**

The following are suggestions for future research:

1. Though we have improved incorporation of HPIV3 envelope proteins with lentivirus particles, titers are still at least 5 to 10-fold less than that of amphotropic Env pseudotyped lentiviruses. Future work should focus on improving HPIV3 pseudotyped lentivirus infection of polarized cells via the apical surface by improving envelope incorporation levels. For example, the F protein could also be codon optimized, the number of plasmids used to produce pseudotyped viruses could be reduced, and MβCD or FB1 treatment of producer cells could be optimized. Additional work should be performed in an attempt to improve the function of the HN fusion proteins since the HN fusion proteins had increased corporation levels, however titers were low. Other sequences for increased Gag interaction of localization could be used, for example, the alpha helix 1 region of the gp41 cytoplasmic tail, or sequences from Type II transmembrane proteins that colocalize with virus particles. Work should also be performed to determine how much incorporation can be achieved when HN fusion proteins are combined with MβCD or FB1 treatment.

2. MβCD and FB1 treatment improved lentiviral incorporation and titers of HPIV3. Future work should investigate whether or not treatment improves titers of other hard-to-pseudotype envelope proteins such as influenza and respiratory syncytial virus for the generation of pseudotyped

viruses for lung gene transfer. Additionally, the effect of MβCD and FB1 treatment on envelope incorporation by retroviruses and SIV should also be explored.

3. We have shown lipid rafts can regulate the proteins incorporated into virus particles and disruption of rafts can alter the protein composition of viruses. Future work should investigate how to manipulate lipid rafts for protein incorporation into and exclusion from virus particles. For example, non-raft and raft-segregated proteins can be altered or rafts can be disrupted for colocalization with lentivirus-associated rafts.

4. We have shown cell proteins, such as the GPI anchored proteins, can affect lentivirus assembly, budding, and envelope incorporation. These results have important implications for the addition of accessory molecules that can alter the targeting and signaling of virus particles. The addition of accessory molecules may have to be optimized so as not to affect virus infection, since we show Tac-CD16 may limit the number of envelope proteins in rafts and affect virus infection. Additionally, work should be performed to determine whether other cellular proteins can facilitate lentivirus assembly and budding and targeting.

5. We have also shown FR-WT inhibited lentivirus localization to lipid rafts, although budding and transduction efficiency was not affected, and variants of folate receptor were not incorporated into virus particles. Future work should focus on determining the sequence for inhibition and exploiting this inhibition perhaps for anti-viral purposes.

6. Future work should also investigate the effects of MβCD and FB1 treatment on protein expression of envelope proteins and GPI anchored

proteins. Specifically, it should be determined whether or not treatment increases surface localization or merely redistributes cell surface proteins.

7. Future work should further analyze the effects of MβCD and FB1 treatment on cholesterol levels in lipid rafts and in virus particles, and whether or not this affects envelope protein function of binding and fusion.

APPENDIX A

ADDITIONAL DATA

A.1 HPIV3-F Characteristics

F internalization rates. The cytoplasmic tail of HPIV3-F contains a YXXR sequence, which possibly indicates an internalization motif. We hypothesized lentiviruses may not contain much F protein if it is rapidly internalized. We therefore used site-directed mutagenesis to change the tyrosine to an alanine (F-Y518A). We then compared internalization rates between normal F and F-Y518A by transfecting cells grown on coverslips and then incubating for 48 hours. Media was then replaced with cold media for 30 min on ice before cells were incubated with a monoclonal antibody against F at 4^0C. Coverslips were then transferred to pre-warmed media and incubated at 37^0C for 0, 30 min, 1 hr, and 2 hr. After each timepoint, cells were chilled on ice in cold PBS for 30 min. Cells were then washed, labeled with A549-conjugated concanavalin A to stain for the cell surface, washed, fixed, and then incubated with Cy2-conjugated secondary antibody before being washed and mounted on slides with gelvatol. Cells were visualized by confocal microscopy and extent of colocalization between F and cell surface was quantified with ImageJ. No significant difference in internalization level between F and F-Y518A was detected, and F was stably present on the cell surface. This indicates the F YXXR sequence is not an internalization motif and F is not rapidly internalized.

F RNA localization. In addition to determining whether HPIV3-F RNA was spliced in Chapter 3, we analyzed whether F RNA exported from the nucleus of transfected cells. Cytoplasmic and nuclear RNA were isolated from fractionated cells, reverse transcribed, and then amplified by real-time PCR (Figure A.1). High levels of F

RNA were detected in the nucleus and cytoplasm of transfected cells, regardless whether cells were transfected only with the expression plasmid for F, or multiply transfected to express F, Gag-Pol, and the lentiviral transgene β-galactosidase. A small amount of F RNA was detected in the nuclear fraction of wild-type HPIV3 infected cells due to limitations with the experimental procedure which did not completely prevent contamination of the nuclear fraction with cytoplasmic mRNA. These results indicate that F mRNA was efficiently exported from the nucleus to the cytoplasm in transfected cells.
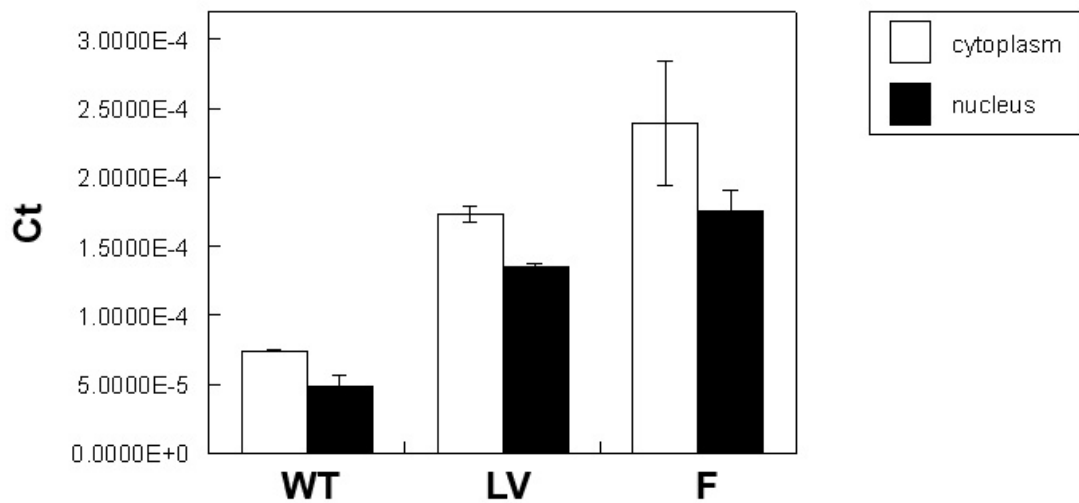
Figure A.1. Transfected F RNA is exported to the cytoplasm of cells. 293T/17 cells ($2x10^6$) were transfected with 1 μg of an expression plasmid for HPIV3-F (F), 1 μg each of expression plasmids for HPIV3-F, HPIV3-HN, β-galactosidase, and lentiviral Gag-Pol (LV), or infected with wild-type HPIV3 (WT) at an MOI of 1. Two days later, RNA from the cytoplasmic and nuclear fractions were isolated using the RNeasy kit per the manufacturer's instructions. Portions (1 μg) of the cytoplasmic and nuclear RNA fractions were reverse-transcribed using OligodT primers and then quantified by real-time PCR using F-specific primers. Bars show the mean level ± standard deviation of triplicate wells.

A.2 <u>**Pseudotyping Other Retroviruses and Attempts in Increasing HPIV3/LV Titers**</u>

Pseudotyping HPIV3 with SIV and RV. We determined whether other retroviruses could pseudotype HPIV3 envelope proteins and produce titers similar to retroviruses pseudotyped with amphotropic Env. The first retrovirus we tried was MLV-derived. The stable retrovirus producing cell line TelCeb6 was transfected with either the amphotropic Env or F and HN. Virus was harvested every 12 hours and used to transduce 293T in the diluted titer assay. The titer of amphotropic Env pseudotyped retroviruses was $(4.2 \pm .038) \times 10^6$ CFU/mL while the titer of HPIV3 pseudotyped retroviruses was 0.

The next retrovirus we tried was simian immunodeficiency virus (SIV). 293T cells were plated and transfected with plasmids encoding SIV Gag, SIV GFP reporter gene, SIV helper plasmid, and either the amphotropic Env or HN and F. Virus was harvested every 12 hours and used to transduce 293T in the diluted titer assay. The titer of amphotropic Env pseudotyped SIV was $(3.62 \pm .053) \times 10^6$ CFU/mL while the titer of HPIV3 pseudotyped SIV was $(4.9 \pm .78) \times 10^2$ CFU/mL

Together these results demonstrated HPIV3 envelope proteins are not easily pseudotyped by retroviruses or SIV since the titer difference between amphotropic Env and HPIV3 envelope proteins is 10^6-fold for retroviruses, 10^4-fold for SIV, and 10^2-fold for HIV.

Varying DNA amounts of HN and F. Besides optimizing the amount of DNA and Lipofectamine 2000 for HPIV3/LV production, we varied the DNA amount of F and HN to each other to determine whether titers would improve. However the 1:1 ratio of F and HN resulted in the highest titers.

Stable cell line. We attempted to create a stable HPIV3-F or HPIV3-HN or lacZ cell line to reduce the amount of plasmid required for creation of the HPIV3/LV pseudotype (currently 4 plasmid transfection system). We transfected 293T with 3.6 µg

F or codon optimized HN or Z and 0.4 µg pSV2-his. Two days later we incubated cells in histidine-free MEM + FBS + 10 mM L-histidinol. Cells were cultured until the cells that were not transfected were dead. We selected 8 colonies of each F, HN, or lacZ-transfected cells and tested for F and HN expression by performing flow cytometry and lacZ expression by performing an ONPG. We then selected the best-expressing clone of each F and HN, however when compared to transiently transfected HPIV3/LV producer cells, the amount of F and HN expressed by the clones were half that of the 4-plasmid transfected cells. We then transfected the clones with normal amounts of 3 plasmids and either 0 µg or half the amount of plasmid normally used of the corresponding clone, and tested for the amount of virus produced and the transduction efficiency (Table A.1.) We found that the clones produced less virus particles than transiently transfected producer cells. We also found the virus transduction efficiency produced from the clones were almost nonexistent compared to virus from transiently transfected cells. However when half the amount of corresponding clone plasmid was transfected, the transduction efficiency of the virus from the HN clone was similar to that of transiently transfected cells, while the virus from the F clone was 1.6-fold lower. These results indicate the stable F and HN clones did not produce enough F and HN required for virus assembly and subsequent infection.

A.3 Lentiviral Incorporation of Other FR and Tac Mutants

We determined whether mutations of FR and Tac would affect the incorporation of FR and Tac into lentiviral particles. First we determined whether FR mutants FR-S67P and FR-MCP8 were in lipid rafts and whether or not they were incorporated into lentiviral particles. FR-S67P is similar to that of FR-WT except it is more localized to the surface of cells while FR-MCP8 has the GPI anchor of FR-WT replaced with the transmembrane region of membrane protein cofactor. To determine biochemically if FR-

154

Table A.1. p24 production and titer of virus produced from stable cell lines

Treatment	Virus production $(OD_{490-650})^a$	Titer $(CFU/mL)^b$
lacZ clone + 0 µg lacZ	0.226 ± 0.011	0
HPIV3-F clone + 0 µg F	0.135 ± 0.034	40 ± 10
HPIV3-F clone + ½ µg F	0.297 ± 0.013	2000 ± 100
HPIV3-HN clone + 0 µg HN	0.166 ± 0.027	10 ± 4
HPIV3-HN clone + ½ µg HN	0.178 ± 0.015	2900 ± 145
Transiently transfected HPIV3/LV	0.412 ± 0.042	3100 ± 155

Lentiviruses produced from stable lacZ, HN, or F clones were used to transduce 293T cells. ^{a}Virus production $(OD_{490-650})$ and ^{b}titer (CFU/mL) represent the mean of experimental values +/- standard deviation.

S67P and FR-MCP8 reside in lipid rafts, and if they are incorporated into lentiviral particles, we transfected cells with expression plasmids for β-galactosidase, HIV-1 Gag-Pol, and either FR-S67P or FR-MCP8. Detergent resistant domains were isolated by lysing cells with ice-cold Brij 98 (0.5% in TNE) and performing equilibrium flotation centrifugation. The lipid raft fraction was pelleted by centrifugation and the pellet was analyzed by Western blot for the presence of the folate proteins (Figure A.2). As expected, FR-S67P was detected in lipid rafts while FR-MPC8, lacking the GPI anchor, was not. The virus supernatant of the transfected cells was then analyzed for protein content after it was harvested, ultracentrifuged through a 20% sucrose cushion, and then resuspended in PBS to 100-fold their original concentration. Samples were normalized by p24, resuspended in lysis buffer, and analyzed by Western blot for the presence of
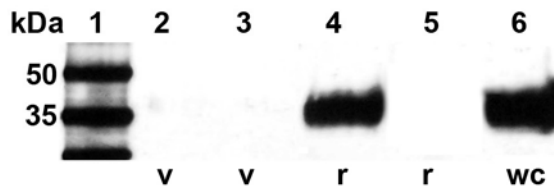
kDa	1	2	3	4	5	6
50						
35						
	v	v	r	r	wc	

Figure A.2. FR mutants FR-S67P and FR-MCP8 do not incorporate into lentiviral particles. 293T cells ($1x10^7$) were transfected with expression plasmids (6 µg each) for β-galactosidase, HIV-1 Gag-Pol, and either FR-S67P or FR-MCP8. The virus supernatant (v) was harvested, ultracentrifuged through a 20% sucrose cushion, resuspended in PBS to 100-fold their original concentration, and analyzed by Western blot after normalization for p24 (Lanes 2-3). Detergent resistant domains (r) were isolated by lysing cells with ice-cold Brij 98 (0.5% in TNE) and performing equilibrium flotation centrifugation. The lipid raft fraction was pelleted by centrifugation and the pellet was analyzed by Western blot after normalization for protein content (Lanes 4-5). Whole cell lysates for FR-MCP8 were also analyzed by Western Blot (Lane 6). Blots were for the presence of FR mutants and samples are as follows: FR-S67P (Lanes 2 and 4) or FR-MCP8 (Lanes 3, 5, 6).

folate receptor (Figure A.2). Both FR-S67P and FR-MCP8 were not detected in virus particles.

We then analyzed the raft localization and virus incorporation of two Tac-CD16 related proteins, normal Tac and Tac-DKQTLL, which has the rapid internalization sequence DKQTLL appended to the end of Tac. To determine biochemically if Tac and Tac-DKQTLL reside in lipid rafts, and if they are incorporated into lentiviral particles, we transfected cells with expression plasmids for β-galactosidase, HIV-1 Gag-Pol, and either Tac or Tac-DKQTLL. Detergent resistant domains were isolated by lysing cells with ice-cold Brij 98 (0.5% in TNE) and performing equilibrium flotation centrifugation. The lipid raft fraction was pelleted by centrifugation and the pellet was analyzed by Western blot for the presence of the Tac proteins (Figure A.3). As expected, Tac was somewhat localized to rafts and very little Tac-DKQTLL was localized to rafts. The virus supernatant of the transfected cells was then analyzed for protein content after it was

harvested, ultracentrifuged through a 20% sucrose cushion, and then resuspended in PBS to 100-fold their original concentration. Samples were normalized by p24, resuspended in lysis buffer, and analyzed by Western blot for the presence of the Tac proteins (Figure A.3). Both Tac and Tac-DKQTLL were detected in virus particles.

We next determined whether FR-WT was not incorporated into lentiviral particles because of the GPI anchor. We therefore swapped the GPI signal sequence of FR-WT and Tac-CD16 by PCR sewing and verified the sequence, creating FR-CD16 which is the folate receptor with the GPI anchor sequence from Tac-CD16, and Tac-FR which is Tac with the GPI anchor sequence from FR-WT. To determine biochemically if FR-CD16 and Tac-FR reside in lipid rafts, and if they are incorporated into lentiviral particles, we transfected cells with expression plasmids for β-galactosidase, HIV-1 Gag-Pol, and either FR-WT, FR-CD16, Tac-CD16, or Tac-FR. Detergent resistant domains
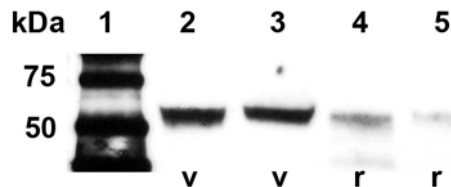

Figure A.3. Tac and Tac-DKQTLL incorporate into viral particles. 293T cells ($1x10^7$) were transfected with expression plasmids (6 µg each) for β-galactosidase, HIV-1 Gag-Pol, and either Tac or Tac-DKQTLL. The virus supernatant (v) was harvested, ultracentrifuged through a 20% sucrose cushion, resuspended in PBS to 100-fold their original concentration, and analyzed by Western blot after normalization for p24 (Lanes 2-3). Detergent resistant domains (r) were isolated by lysing cells with ice-cold Brij 98 (0.5% in TNE) and performing equilibrium flotation centrifugation. The lipid raft fraction was pelleted by centrifugation and the pellet was analyzed by Western blot after normalization for protein content (Lanes 4-5). Blots were for the presence of Tac mutants and samples are as follows: Tac (Lanes 2 and 4) or Tac-DKQTLL (Lanes 3 and 5).

were isolated by lysing cells with ice-cold Brij 98 (0.5% in TNE) and performing

equilibrium flotation centrifugation. The lipid raft fraction was pelleted by centrifugation

and the pellet was analyzed by Western blot for the presence of the folate proteins

(Figure A.4A) or Tac proteins (Figure A.4B). As expected, both FR-CD16 and Tac-FR

were detected in lipid rafts. The virus supernatant of the transfected cells was then

analyzed for protein content after it was harvested, ultracentrifuged through a 20%

sucrose cushion, and then resuspended in PBS to 100-fold their original concentration.

Samples were normalized by p24, resuspended in lysis buffer, and analyzed by Western

blot for the presence of folate proteins (Figure A.4A) or Tac proteins (Figure A.4B).

Surprisingly, FR-CD16 was not found in virus particles and Tac-FR was found in virus

particles. Taken together, these results demonstrate folate receptor is inhibitory to virus
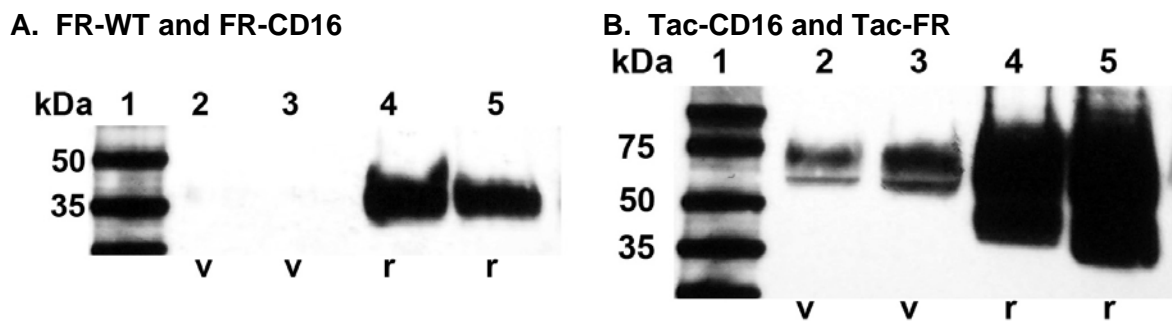
incorporation.

Figure A.4. FR-CD16 is not incorporated into lentiviral particles while Tac-FR is. 293T cells (1×10^7) were transfected with expression plasmids (6 µg each) for β-galactosidase, HIV-1 Gag-Pol, and either FR-CD16 or Tac-FR. The virus supernatant (v) was harvested, ultracentrifuged through a 20% sucrose cushion, resuspended in PBS to 100-fold their original concentration, and analyzed by Western blot after normalization for p24 (A and B Lanes 2-3). Detergent resistant domains (r) were isolated by lysing cells with ice-cold Brij 98 (0.5% in TNE) and performing equilibrium flotation centrifugation. The lipid raft fraction was pelleted by centrifugation and the pellet was analyzed by Western blot after normalization for protein content (A and B Lanes 4-5). Blots were for the presence of FR (A) or Tac (B). In Part A, samples are as follows: FR-WT (Lanes 2 and 4) or FR-CD16 (Lanes 3 and 5). In Part B, samples are as follows: Tac-CD16 (Lanes 2 and 4) or Tac-FR (Lanes 3 and 5).

EXPERIMENTAL PROTOCOLS

B.1. CsCl Purification of Plasmid DNA

1. Grow a 30 mL culture to an OD_{600} = 0.6 (late log phase)

2. Inoculate 500 mL LB with 25 mL of the culture. Incubate for 14.5-18.5 hours at 37^0 with shaking (if growing with 34 mg/ml chloramphenicol in ETOH, add 2.5 ml 2.5 hours after culture is started).

3. Harvest by centrifugation at 4000 rpm for 15 min at 4^0C in Sorvall GS3 rotor. Discard and drain away all the supernatant.

4. Resuspend the pellet in 100 mL of ice-cold STE (0.1 M NaCl, 10 mM Tris-Cl (pH 8), 1 mM EDTA (pH 8)) to wash the cells

5. Centrifuge again at 4000 rpm for 15 min at 4^0C in the GS3

6. Resuspend the washed pellet in 18 mL of Solution 1 (50 mM glucose/dextrose, 25 mM Tris-Cl (pH 8), 10 mM EDTA (pH 8), make 100 mL, autoclave for 15 min and store at 4^0C)

7. Add 2 mL of freshly prepared solution of lysozyme (10 mg/mL in 10 mM Tris-Cl (important! pH=8)).

8. Carefully add 40 mL of freshly prepared Solution 2 (0.2 N NaOH, 1% SDS). Mix by inversion and store at room temperature for 5-10 minutes. Add carefully.

9. Add 20 mL of ice-cold Solution 3 (60 mL 5M potassium acetate, 11.5 mL glacial acetic acid, 28.5 mL water). Mix well by inversion. Store on ice for 10 minutes

10. Centrifuge at 4000 rpm for 15 minutes at 4^0C in Sorvall GS3. (make sure there is pellet)

11. Filter the supernatant through 4 layers of cheesecloth into a 250 mL centrifuge bottle. Add 0.6 volume of isopropanol, mix well, and store for 10 minutes at room temperature.

12. Centrifuge at least 6000 rpm for 30 minutes at room temperature in Sorvall GS3

13. Decant supernatant carefully and drain away supernatant (turn upside down). Either resuspend in 70% ethanol at room temperature, centrifuge, drain, and then evaporate off ethanol, or just rinse with 3 mL ethanol and evaporate off.

14. Dissolve the pellet of nucleic acid in 3 mL of TE (pH 8) (10 mM Tris acid (pH=7.4), 1 mM EDTA, filter sterilized)

15. For every mL of DNA solution, add exactly 1 g CsCl. All the salt should be dissolved (warm to 30^0C if necessary)

16. Add 0.08 mL of ethidium bromide solution (10 mg/ml in water) for every 1 mL of DNA/CsCl solution. Mix immediately

17. Centrifuge the solution at 3300 g for 5 min at room temperature

18. Use Pasteur pipette to transfer the clear red solution under/over the scum into a tube (Beckman quick-seal or equivalent). Fill remainder of tube with filtered TE/CsCl/Ethidium Bromide in correct concentrations. Make sure tubes weigh the same

19. Use tube sealer to seal tube. Turn on for 4 min. Place seal former on each tube neck and press down firmly on tube knob, until it has moved about 2/3 of the way to the tube shoulder. Immediately lift one end of the rack slightly and move it one tube position to the right and press the heat sink gently until the seal former sits on the tube shoulder (do not go into the shoulder). Keep the heat sink on for a couple of seconds. Remove the seal former from tube. For centrifugation in the Ti70 rotor, remember to use the red hat on top of the tubes.

20. Centrifuge at 55,000 rpm for 24 hours at 20^0C.

21. Bring 18 and 21 gauge needles, UV light (long wavelength), ring stand, diapers, waste bottles, syringes, 15 mL centrifuge tubes to dark room. The 21 gauge needle is to make hole at top and the 18 gauge needle is to collect the bands. Upper band is nicked or chromosomal DNA and lower band is closed plasmid DNA. Stick needle at top to allow air to enter. Insert needle (beveled side up) so needle is under lowest band and make sure to sweep.   Repeat steps 18-21.

22. Add an equal volume of 1-butanol saturated with water or (top layer)

23. Mix the two phases by vortexing

24. Centrifuge the mixture at 1500 rpm for 3 min at room temp

25. Transfer the lower, aqueous phase to a clean tube with Pasteur pipette

26. Repeat steps 21-24 until all the pink color is gone from both phases

27. Remove the CsCl from the DNA solution by adding
     a. 3 volumes of water
     b. enough 3M sodium acetate (pH 5.2) to make final solution 0.3 M keeping in mind letter c
     c. 2 volumes of A +B with 100% ethanol
     d. 0.3 M (3v + v + NaAc) * 3 = 3M * NaAc

28. Put solutions in fridge for 30 min.

29. Centrifuge at 15,000 g for 30 min at 4^0C in clear tubes.

30. Add room-temperature 70% ethanol. Invert tube several times and spin again.

31. Dissolve the precipitated DNA in 1 mL of TE

32. Measure OD_{260} and store DNA at -20^0C. Now STERILE

B.2. Virus Production and Concentration

1. The day before: Plate 293T in DMEM+FBS so they will be very confluent at the time of transfection. See Table A1. Make sure to coat plate with Poly-l-lysine for 5 min, rinse with sterile water, and be completely dry before plating.

2. Dilute DNA with DMEM (no antibiotics or serum). For lentiviruses, equal amounts of gag (R8.91), env, and reporter gene work. Mix gently. Total volume should be 0.5 mL.

3. Mix Lipofectamine 2000 (Lipo) gently before use and then dilute the appropriate amount in DMEM. Mix gently and make sure to go to step 4 before 5 minutes is up.

4. Combine diluted DNA with diluted Lipo. Mix gently and incubate for 20 minutes at room temperature.

5. Replace media on cells with enough DMEM to coat the dish/wells.

6. Add DNA-Lipo mixture to a well. Mix gently by rocking plate back and forth. But remember not to rock too hard since 293T will come off.

7. 4-6 hours later, aspirate and add plating volume of DMEM+FBS+PS. DNA-Lipo complexes become unstable after 4-6 hours.

8. Incubate cells at 37^0. Change media 24 hours after transfection and first harvest is 36 hours. Harvest every 12 hours, with 48 -60 hour harvests being the best. Remember to filter with .45µm filter before storing at -80.

9. Virus can be concentrated by ultracentrifugation: at least 35,000 rpm in sw41 beckman rotor for 2 hours, 4 ^0C through a 2 ml 20% sucrose cushion, or overnight by low-speed centrifugation: 4^0C, 6000g, 12-16 hours, or by incubation with 320 µg/mL polybrene for 30 minutes and centrifuging at 10000g for 30 min.

Table B1. Transfection amounts

Culture vessel	293T cell density	Total amount of DNA and dilution in DMEM	Lipo and dilution in DMEM
96 well	6.3 e4	0.2 µg in 25 µL	.6 µL in 25 µL
12 well	9.4 e5	1.6 µg in 100 µL	4.8 µL in 100 µL
6 well	2.3 e6	4 µg in 250 µL	12 µL in 250 µL
60 mm	4.7 e6	8 µg in 0.5 ml	24 µL in 0.5 ml
10 cm	1.27 e7	24 µg in 1.5 ml	72 µL in 1.5 ml

B.3. Radiolabeling

1. Transfect 293T in 10cm dish according to above instructions.

2. 24 hours later, starve cells for 15 min in starved DMEM (17-204-CI) + 10 % HI-FBS (or 2.5%)

3. Bring to the hood: trash, pipettes, tray and liner, and paper towel under the tray.

4. Add S35 radiolabel (in tissue culture room 4^0C clear box) to each 10 cm at 10uCi/mL

    a. Calculate activity and record on the form. Make sure to include source #
        i. If on 1/1/03 -> 2.5 mCi, 90 days later is 0.49 * 2.5 = 1.225 mCi
        ii. 97 days later is the 7-day factor * the 90 day activity =   0.946 * 1.225 mCi= 1.16 mCi

    b. Write down waste: 2/3 of activity to solids, 1/3 of activity to liquids. Do not mix solids of different radionucleotides. Write down volume used (necessary when calculating volume to add per amount of activity). Note there is 175 µL of radiolabel solution. Activity and date is on the packing slip.

5. Incubate for 16-18 hours on top of tray with liner

6. Ultracentrifuge virus. Remember sucrose cushion. Resuspend in IP buffer (20mM sodium phosphate, 500 mM NaCl, 0.1% SDS, 1% NP40).

7. Run Biorad gel for 150V for 50 min

    a. 10 µL sample buffer + 10 µL 14C (blue bottle in -20) -> heat 100 deg C for 5 min and load all

    b. 15 µL sample + 30 µL buffer -> heat 100 deg C for 5 min and load 45 µL

8. Fix gel with 25 mL fixative with glycerol for 30 min with shaker (10% acetic acid, 40% methanol, 3% glycerol, 47% water)

9. Amplify 25 mL amplifier (Amersham) for 30 min on shaker

10. Incubate for 5 min in water. Then cut off thick (bottom) edge very carefully

11. Mount and dry without heat for 15 hrs

    a. Submerge sheet of cellophane and lay on top. Hang edges over all four sides and remove all air bubbles.

    b. Cut piece of biorad filter paper (165-0921) larger than gel and wet it. Put gel on top of filter paper and lay on cellophane. Remove bubbles and add lots of water to surface of filter paper and around edges of gels and fill in wells of gels.

    c. Cut saran wrap same as cellophane, wet it in water and drape over gel from one side. No bubbles at all.

d. Wet second sheet of cellophane and lay it over plastic wrap, hanging edges on all sides. No bubbles

e. Place metal square over cellophane and center over bottom frame and clamp (latch side up)

f. Slide into shelves of GelAir dryier and turn it ON (no heat)

g. Next day, cut peel of cellophane top layer and plastic wrap

12. Preflash film and expose to gel for 3-5 days in -80^{0}C (order should be screen, film, then facing gel)

13. Let cassette warm to room temp before developing

14. For scintillation counting, cut out bands and put into scintillation tubes. Make sure gel side is facing up and add 3 mL scintillation cocktail. Wait 15 min and then measure activity on the scintillation counter in 1D (protocol 3).

B.4. Immunoprecipitation

1. Ultracentrifuge virus to pellet.

2. Resuspend viral pellet in 200 μL IP buffer minus amount using for 5 μg antibody.

3. Preclear virus to agarose-coupled Protein A or G beads by adding virus to 20 μL beads. Rotate 30 min at 4^{0}C. Centrifuge and keep the supernatant (has virus)

4. Add the 5 μg antibody to virus (0.2 mL total). General rule is 1-2 μL per mL of virus, or 50 μg protein for 1-5 μg antibody. Incubate overnight at 4^{0}C with rotation. Can add 0.02% sodium azide as a preservative

5. Add beads to Antibody+virus and incubate for 2 hours at room temp with rotation. General rule is 50 μL of beads per 5 μg of antibody.

6. Wash by centrifuging 2-3 min, aspirating supernatant, and adding 0.5 mL wash solution (use IP buffer). Repeat 6X.

7. If ELISA:
   Elute with elution buffer (0.1M glycine-HCl pH 2.5): 50 μL for 5 min and spin down. Repeat, pooling. Then add 10 μL 1M Tris pH=8 to the 100 μL tube.

   Lyse virus with ELISA lysing buffer for 30 min at room temp. Centrifuge for 2-3 min and collect supernatant to run in ELISA or WB.

   If WB:
   Wash with 0.5 mL DI water. Incubate virus-antibody-bead complex for 5 min at 95^{0}C with 25 μL of WB sample buffer. Centrifuge the sample and collect the supernatant. Repeat, pooling supernatant for a total of 50 μL.

8. For cell lysates, make sure to wash cells in cold PBS, lyse them with chilled IP buffer and protease inhibitors for 30 min on ice, and then centrifuge at 10000g for 10-15 min and keep the supernatant.

B.5. Lipid Raft Isolation
1. Transfect cells. The next day, detach cells with versene (PBS, 5 mM EDTA), add equal volume of media, and pellet cells at 800 rpm.

2. Aspirate supernatant. Resuspend cells in 1 mL cold 1% Triton-X (or Brij 98) in TNE buffer (10X TNE = 3.03 g Tris base, 8.77g NaCl, 10 mL 0.5 M EDTA)

3. Dounce homogenize at least 20X

4. Quickly add 900 µL of homogenate to ultracentrifuge tube containing 900 µL cold 80% sucrose in TNE and mix solutions

5. Aliquot the rest of the homogenate to microcentrifuge tube and store in -20^{0}C as a whole-cell lysate

6. Carefully layer 5 mL of cold 38% sucrose in TNE

7. Then carefully layer 4 mL 5% cold sucrose/TNE on top of that and balance

8. Ultracentrifuge at 30000 rpm in SW41 rotor 4^{0}C for at least 12 hours (preferably 15).

9. There should be a fluffy white band at the 38%-5% interface. This is your lipid raft fraction. Carefully (using Pasteur pipette), suck up all the white stuff and put it into a new ultracentrifuge tube.

10. Fill the rest of the tube with cold TNE and mix solutions to make sure you cannot see 2 separate densities.

11. Ultracentrifuge for 1 hour at 30k, 4^{0}C in SW41 rotor.

12. Aspirate out supernatant. There should be a faint white pellet at bottom. Resuspend pellet in 100 µL room temp TNE.

13. For linear sucrose gradient, steps 1-4 are the same. Create a linear gradient using 4 mL 38% cold sucrose/TNE and 4 mL 5% cold sucrose/TNE and have it pour directly into ultracentrifuge tube. Ultracentrifuge same as step 8, and then collect 1 mL fractions from the bottom.

B.6. p24 ELISA
1. Coat a Nunc Maxisorp microtiter plate with p24 monoclonal antibody (183-H12-5C) by adding 100 µL of 1:800 dilution in PBS. Incubate at 37^{0}C overnight

2. Wash the plate 2X with Washing buffer (PBS, 0.2% Tween-20), 100 µL into each well.

3. Block non-specific sites by adding 200 µL of Blocking Buffer (PBS, 5% nonfat milk, 0.05% Tween-20) per well and incubating for 1 hour at 37^{0}C.

4. Wash 4X with Washing buffer

5. Lyse virus samples by 1:1 dilution into Lysing Buffer (PBS, 2% Triton X-100). Leave at room temperature for 30 minutes.

6. Add 100 µL of antigen-containing solution per well and incubate for 2 hr at 37^{0}C.

7. Wash 4X with Washing Buffer

8. Add 100 µL per well of sheep polyclonal anti-p24 antisera diluted 1:250 in Blocking Buffer. Incubate for 2 hrs at 37^{0}C

9. Wash the plate 4X with Washing Buffer

10. Add 100 µL of HRP-conjugated donkey-antisheep polyclonal serum diluted 1:1000 in Blocking Buffer to each well and incubate for 1 hr at 37^{0}C.

11. Wash the plate 4X with Washing Buffer

12. Add 100 µL of freshly prepared OPD developer solution (7.5 mL substrate buffer [1L water, 4.6g citric acid anhydrous, 7.3g Na$_2$HPO$_2$], 3 mg OPD tablet, 3 µL 1% hydrogen peroxide) per well and incubate for 20 minutes

13. Stop development reaction by adding 50 µL of 8 N sulfuric acid to each well

14. Read absorbance in plate reader (OD490-650).

B.7. Indirect Immunofluorescence
1. To make coverslips, buy 12 mm 1.5 circle (fisher 12-545-81). Put into beaker and put enough 0.1M HCl to at least cover. Boil for 30 min at slow boil. Quench with distlled water (10X the volume of acid). Pour down sign and take to hood where you rinse with sterile water. Put into jar with 70% isopropanol

2. Flame coverslips and transfer coverslip to the well of a 12 well dish.

3. Put 1 mL of cells into each well and rotate to evenly distribute cells (about 30k-50k cells/well)

4. Treat as required for experimental protocol

5. Remove medium and fix cells with 4% paraformaldehyde (0.5 g powder in 20 mL water, heat to 55^{0}C and shake, add NaOH until dissolves, cool to room temp, and add 2.5 mL 10X PBS and bring it up to 25 mL with water. pH = 7.0. store for 10 days or less)

6. Incubate for 10 minutes at room temperature

7. Remove fix and add 1 mL of 5% serum in PBS for 15 min. In general, use the serum of the secondary antibody.

8. Dilute primary into PBS/serum. If you want to permeabilize membrane, add 0.2% saponin (20 µL 10% saponin in water to 980 µL PBS/serum)

9. Place a piece of parafilm in the bottom of a 150 mm Petri dish labeled with numbers corresponding to a 12 well dish.

10. Add 30 µL of appropriate diluted antibody solution to each spot on the parafilm.

11. Pick up individual coverslips with tweezers and wick excess fluid on paper towel.

12. Invert coverslip onto antibody drop (cell side down). Cover dish and incubate in bench drawer for 1 hr.

13. Aspirate 12 well and add 1 mL PBS to wash. Place coverslip back into well cell side up (use 2 tweezers). Wash 3 times for 5 min each. Make sure coverslip is sitting in the PBS (push down with tweezers).

14. Dilute fluorescently-labeled secondary antibody in PBS/serum with or without 0.2% saponin. Spin for 10 min in cold centrifuge

15. Invert coverslip onto 30 µL drops of antibody on new parafilm and incubate in drawer for 1 hr

16. Wash coverslips 3 times for 5 min each on shaker with 1 mL PBS

17. Aspirate wash with 1 mL DI water.

18. With glass pipette, drop 1 drop of gelvatol onto glass slide and let dry overnight at 4^0C in the dark.

19. For colocalization, after images are taken, convert images to JPG files. Open with NIH ImageJ. Highlight the cell and run the Colocalisation Threshold plugin (Tony Collins, Wayne Rasband, and Kevin Baler). Rtotal is the Pearson's overlap coefficient. Copy and past values into Excel. Process 8 cells.

B.8. Diluted Titer Assay
1. Plate cells such that they are nonconfluent

2. Transduce cells with virus

3. 2-3 days later (when cells are confluent, aspirate off media

4. Fix in 0.5% glutaraldehyde in PBS for 10 minutes

5. Wash dishes 2-3x with 1 mM $MgCl_2$ in PBS for 10 min each time

6. Add Xgal solution (0.5 mL 20X KC [25 mL PBS, 0.82g $K_3Fe9(CN)_6$, 1.05g $K_4FE(CN)_6*3H_2O$], 10 µL 1M MgCl2, 0.25 mL Xgal [40 mg/mL in DMSO], brought to 10 mL in PBS) to dishes

7. Incubate at 37^0C overnight

8. Wash dishes with water

9. Let air dry then count

B.9. Cell-based ELISA
1. Plate 20,000 HeLa cells per well in a 96 well and transfect with Polyfect according to instructions.

2. The next day wash cells once with PBS

3. Fixed cells for 10 min with 4% paraformaldehye and block for 15 min with PBS/sera

4. Incubate cells with 1:800 antibody in PBS/sera for 1 hour at room temperature.

5. Wash four times with PBS

6. Incubate with 1:500 HRP-conjugated secondary antibody for 1 h at room temperature.

7. Wash four times with PBS

8. Add 100 µL of freshly prepared OPD developer solution and watch incubation

9. Stop development reaction by adding 50 µL of 8 N sulfuric acid to each well

10. Read absorbance in plate reader (OD490-650).

B.10. Western Blotting
1. Perform a protein assay according to manufacturer's instructions.

2. Dilute 1 part sample in 2 parts sample buffer (5% mercaptoethanol and 95% Laemmli sample buffer – both on shelf by gel machine). (ie 15 µL sample and 30 µL sample buffer)

3. Prepare marker by taking 5 µL ECL dualview and adding 5 µL sample buffer with 10% mercaptoethanol instead of 5%I.

4. Vortex samples and weight marker, and spin down. Heat for 5 minutes at 100^0C

5. After setting up the gel, make 350 mL 1X Running buffer (10X in 4^0C fridge: 15 g Tris base, 72 g glycine, 5g SDS into 500 mL). Fill inner chamber and use the rest for the outer chamber

6. Put 30-50 µL of sample in each gel lane. Load all of the weight marker.

7. Run at 150 volts for 50 minutes

8. Cold everything is, better the transfer

9. Have at least 350 mL transfer buffer – stored in cold room (700 mL methanol, 2800 mL ddh20, 10.68 g Tris, 50.4 g glycine)

10. Pry gel out of gel caster. Take the plate it sticks to and invert it into cold transfer buffer. Incubate for 15 min

11. Take filter paper and use it as a guide to cut PVDF membrane smaller than the filter paper. Also cut a corner in the PVDF membrane

12. Wet membrane in 100% methanol in green bucket

13. Soak everything going into sandwich in transfer buffer (2 pieces of filter paper, 2 sponges, 1 membrane). Membrane should go on bottom so it will not float up and dry.

14. Put sandwich together and stick into machine. Note which side of gel faces the edge of the PVDF membrane. Sandwich order is light side: pad: filter paper: membrane: gel: filter paper: pad. When laying membrane on top of gel, take Pasteur pipette and roll it over the membrane to get rid of bubbles

15. Slide sandwich into transfer tank. The light side faces the red circuit

16. Add ice block (in -20) and fill transfer tank with cold transfer buffer. Put in stir bar and turn on

17. Run for 100 volts for 1 hr

18. Blocking is done overnight at 4^0C or 1 hour at room temperature (5% milk, 0.05% tween in PBS). 5-10 mL. Remember to close lid and seal with parafilm if leaving on shaker overnight

19. Pour blocking solution out. Add primary antibody to 5-10 mL blocking solution. Incubate overnight at 4^0C or 1 hr at room temperature

20. Wash 6x with PBS/0.05% tween. 5 minutes each wash

21. Put secondary into blocking solution (about 1:400,000) and add 1:40,000 S protein. Incubate 1 hr at room temperature.

22. Swtich dark room developer on AND HIT RUN.

23. Wash 6x with PBS/tween

24. Take saran wrap and put membrane so that the protein side is up. Prepare Pierce's Super Signal West Femto 1:1. Make 1 mL for each membrane. Remember to do this quickly since it is light sensitive.

25. Drop the mixture onto the membrane and tilt so that it covers whole membrane. Develop for 5 min.

26. Fold saran wrap over membrane and press out bubbles. Tape down membrane in cassette

27. Go to dark room with film, cassette, membrane, marker, timer. Place film on top and expose about 5 min or longer.

28. Slide film into developer.

29. For determining band density, use ImageJ to measure the area of the band and intensity (Analyze > Set Measurements> make sure area and mean gray value is checked. Then go to Analyze>Measure.) Remember unless image colors are inverted, darker colors will be a smaller number. Multiply values together. Make sure to do an initial test by diluting antibody and measuring to ensure values are linear.